Analysis of the termodynamic profile of the atmosphere

by Agostino Manzato

OSMER - ARPA Friuli Venezia Giulia

Seminar made in “Istituto Cavanis” Venice on 7 November 2017

Outline

1. Basic thermodynamic variables in presence of water.
2. Atmosphere static and potential (in)stability.
3. Sounding diagrams: skew-T and Thetaplot.
4. Some sounding-derived indices and their properties.
5. Forecasting with sounding-derived indices: examples & problems

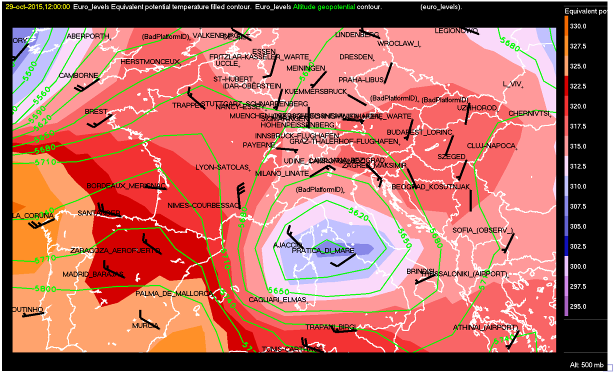

Europe at 500 hPa as seen by RDS alone (WND barbs, Z lines, Θ_e filled)

Section 1

Basic thermodynamic variables in presence of water

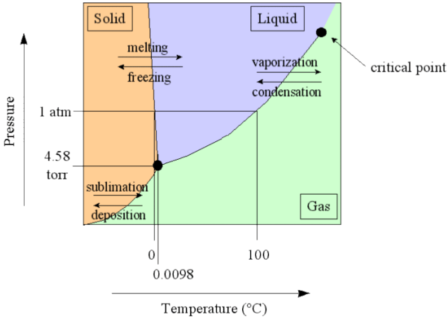

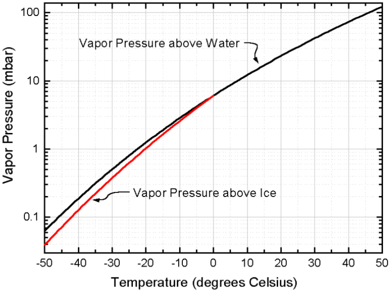

Source: http://www.its.caltech.edu/~atomic/snowcrystals/ice/ice.htm

Dry air and water vapor mixture

- Air is a mixture made by a *variable* part (0-4%) of H_2O (mass 18) in thermal equilibrium with a *fixed* proportion of other gases: 78% N_2 (mass 28), 21% of O_2 (mass 32), 0.9% of Ar, 0.03% of CO_2,. . .

Dry air and water vapor mixture

- Air is a mixture made by a *variable* part (0-4%) of H_2O (mass 18) in thermal equilibrium with a *fixed* proportion of other gases: 78% N_2 (mass 28), 21% of O_2 (mass 32), 0.9% of Ar, 0.03% of CO_2,...
- For this reason *meteorologists* define "air" as a mix of 2 ideal gases:
  1) DRY AIR: $\mathbf{p_d} = \rho_\mathbf{d}\mathbf{R_d}\mathbf{T}$, with $R_d = 286.99$ J/(kg K);
  2) VAPOR: $\mathbf{e} = \rho_\mathbf{v}\mathbf{R_v}\mathbf{T}$, with $R_v = R_d/0.62198 = 461.4$ J/(kg K).

Dry air and water vapor mixture

- Air is a mixture made by a *variable* part (0-4%) of H_2O (mass 18) in thermal equilibrium with a *fixed* proportion of other gases: 78% N_2 (mass 28), 21% of O_2 (mass 32), 0.9% of Ar, 0.03% of CO_2,...
- For this reason *meteorologists* define "air" as a mix of 2 ideal gases:
  1) DRY AIR: $\mathbf{p_d} = \rho_\mathbf{d} \mathbf{R_d T}$, with $R_d = 286.99$ J/(kg K);
  2) VAPOR: $\mathbf{e} = \rho_\mathbf{v} \mathbf{R_v T}$, with $R_v = R_d/0.62198 = 461.4$ J/(kg K).
- Air *pressure* is $\mathbf{p} = \mathbf{p_d} + \mathbf{e}$; air *density* is $\rho = \rho_\mathbf{d} + \rho_\mathbf{v} = \rho_\mathbf{d}(\mathbf{1} + \mathbf{q})$, where $\mathbf{q} = \rho_\mathbf{v}/\rho_\mathbf{d} = \mathbf{0.622}\frac{\mathbf{e}}{\mathbf{p-e}}$ is the water vapor *mixing ratio*. One can define *virtual temperature* $T_v \cong T(1 + 0.6q)$ so that $\mathbf{p} = \rho \mathbf{R_d T_v}$.

Dry air and water vapor mixture

- Air is a mixture made by a *variable* part (0-4%) of H_2O (mass 18) in thermal equilibrium with a *fixed* proportion of other gases: 78% N_2 (mass 28), 21% of O_2 (mass 32), 0.9% of Ar, 0.03% of CO_2,...
- For this reason *meteorologists* define "air" as a mix of 2 ideal gases:
  1) DRY AIR: $\mathbf{p_d} = \rho_\mathbf{d} \mathbf{R_d T}$, with $R_d = 286.99$ J/(kg K);
  2) VAPOR: $\mathbf{e} = \rho_\mathbf{v} \mathbf{R_v T}$, with $R_v = R_d/0.62198 = 461.4$ J/(kg K).
- Air *pressure* is $\mathbf{p} = \mathbf{p_d} + \mathbf{e}$; air *density* is $\rho = \rho_\mathbf{d} + \rho_\mathbf{v} = \rho_\mathbf{d}(\mathbf{1}+\mathbf{q})$, where $\mathbf{q} = \rho_\mathbf{v}/\rho_\mathbf{d} = \mathbf{0.622}\frac{\mathbf{e}}{\mathbf{p-e}}$ is the water vapor *mixing ratio*. One can define *virtual temperature* $T_v \cong T(1+0.6q)$ so that $\mathbf{p} = \rho \mathbf{R_d T_v}$.
- The maximum quantity of water vapor (before condensation) depends only by the *temperature*, via the *saturation vapor pressure*, simplified by: $\mathbf{e_{sat}(T)} = \mathbf{6.11} \cdot \mathrm{e}^{\frac{\mathbf{19.8 \cdot T}}{\mathbf{T+273}}}$. *Relative humidity* is $\mathbf{RH} = \mathbf{100} \cdot \frac{\mathbf{e}}{\mathbf{e_{sat}(T)}}$.

Dry air and water vapor mixture

- Air is a mixture made by a *variable* part (0-4%) of H_2O (mass 18) in thermal equilibrium with a *fixed* proportion of other gases: 78% N_2 (mass 28), 21% of O_2 (mass 32), 0.9% of Ar, 0.03% of CO_2,...
- For this reason *meteorologists* define "air" as a mix of 2 ideal gases:
  1) DRY AIR: $\mathbf{p_d} = \rho_\mathbf{d} \mathbf{R_d} \mathbf{T}$, with $R_d = 286.99$ J/(kg K);
  2) VAPOR: $\mathbf{e} = \rho_\mathbf{v} \mathbf{R_v} \mathbf{T}$, with $R_v = R_d/0.62198 = 461.4$ J/(kg K).
- Air *pressure* is $\mathbf{p} = \mathbf{p_d} + \mathbf{e}$; air *density* is $\rho = \rho_\mathbf{d} + \rho_\mathbf{v} = \rho_\mathbf{d}(\mathbf{1} + \mathbf{q})$, where $\mathbf{q} = \rho_\mathbf{v}/\rho_\mathbf{d} = \mathbf{0.622}\frac{\mathbf{e}}{\mathbf{p-e}}$ is the water vapor *mixing ratio*. One can define *virtual temperature* $T_v \cong T(1 + 0.6q)$ so that $\mathbf{p} = \rho \mathbf{R_d} \mathbf{T_v}$.
- The maximum quantity of water vapor (before condensation) depends only by the *temperature*, via the *saturation vapor pressure*, simplified by: $\mathbf{e_{sat}(T)} = \mathbf{6.11} \cdot \mathrm{e}^{\frac{\mathbf{19.8 \cdot T}}{\mathbf{T+273}}}$. *Relative humidity* is $\mathbf{RH} = \mathbf{100} \cdot \frac{\mathbf{e}}{\mathbf{e_{sat}(T)}}$.
- In NE Italy q varies between a minimum of 1 g/kg to a maximum of about **22 g/kg**. Note also that H_2O is *lighter* than dry air (molecular mass of 18 vs. 29): the more moist air is, the less dense it becomes.

Saturation diagram: the point of view of water

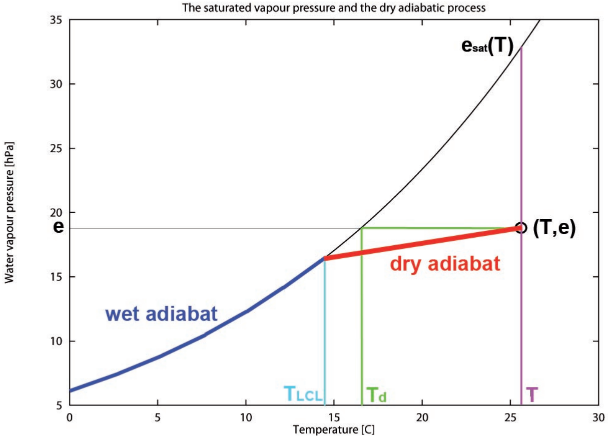

The *dew–point temperature*, $\mathbf{T_d}$, is defined implicitly on the $e_{sat}(T)$ curve as the temperature when air will become saturated along a hypothetical process that conserve its initial partial pressure e, so that $\mathbf{e} = \mathbf{e_{sat}}(\mathbf{T_d})$.

Saturation diagram: the point of view of water

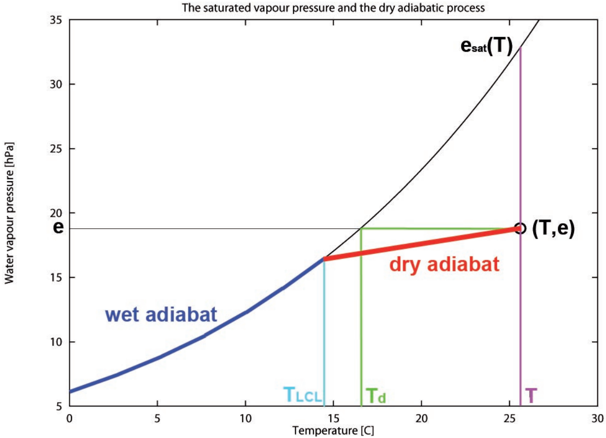

The *dew–point temperature*, $\mathbf{T_d}$, is defined implicitly on the $e_{sat}(T)$ curve as the temperature when air will become saturated along a hypothetical process that conserve its initial partial pressure e, so that $\mathbf{e} = \mathbf{e_{sat}}(\mathbf{T_d})$.

When air is lifted adiabatically, it follows a **dry** adiabat until saturation occurs at the *Lifted Condensation Level temperature*, T_{LCL}, then it follows a **wet** adiabat.

In conclusion, air is a gas mixture defined by 4 variables: p, T, ρ plus a variable for moisture, like q or RH or T_d or dew-point depressure $(T - T_d)$...

The point of view of the air parcel

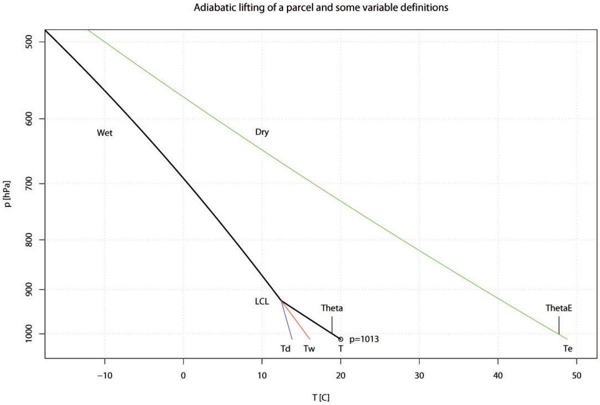

When the air parcel is lifted adiabatically it follows a dry adiabat until LCL. If from LCL the parcel *sinks* down pseudo-adiabatically along a wet adiabat (adding moisture to remain saturated) then it reaches the initial level at the *wet–bulb temperature*, $\mathbf{T_w}$.

The point of view of the air parcel

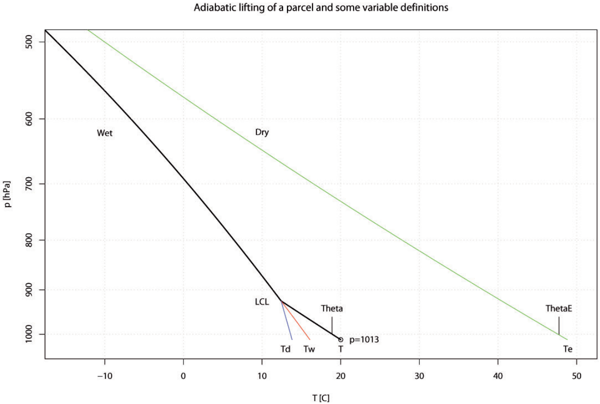

When the air parcel is lifted adiabatically it follows a dry adiabat until LCL. If from LCL the parcel *sinks* down pseudo-adiabatically along a wet adiabat (adding moisture to remain saturated) then it reaches the initial level at the *wet–bulb temperature*, $\mathbf{T_w}$.

However, if from LCL it is *lifted* along a wet pseudo-adiabat until all moisture is condensed and removed ($q = 0$) and then it sinks down at the initial level through a dry adiabat, it will reach the *equivalent temperature*, $\mathbf{T_e}$. "Equivalent" because it considers the warming due to the latent heat of condensation released by all the initial vapor.

Referring everything to a standard level

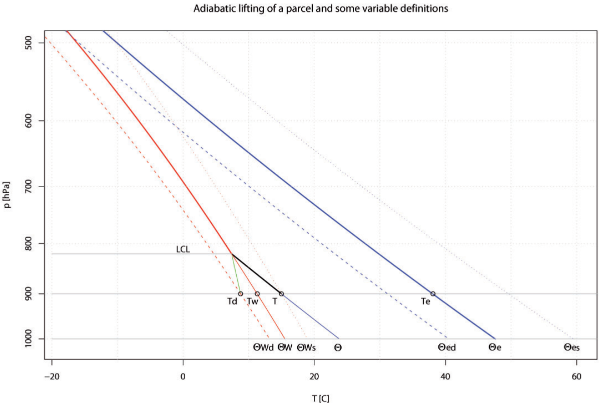

To make things more comparable, temperatures can be referred to the *standard* level (1000 hPa). Bringing the parcel at 1000 hPa along a dry adiabat defines the *potential temperature*, **Θ**.

The dry adiabat used to define T_e intersects the 1000 hPa level at the *equivalent potential temperature*, $\mathbf{\Theta_e}$.

Referring everything to a standard level

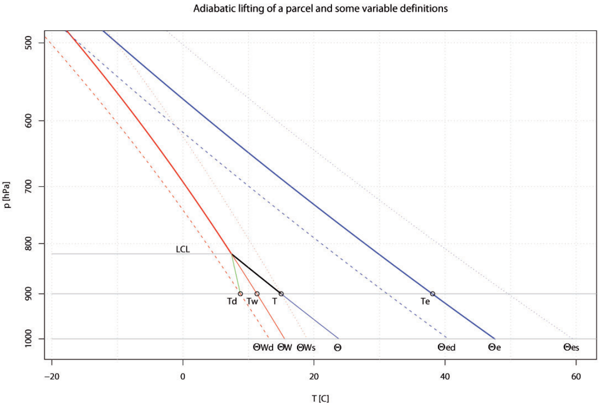

To make things more comparable, temperatures can be referred to the *standard* level (1000 hPa). Bringing the parcel at 1000 hPa along a dry adiabat defines the *potential temperature*, $\boldsymbol{\Theta}$.

The dry adiabat used to define T_e intersects the 1000 hPa level at the *equivalent potential temperature*, $\boldsymbol{\Theta_e}$.

Adding moisture till saturation at the initial level $[q = q_{sat} = 0.622\, e_{sat}(T)/(p - e_{sat}(T))]$ and doing the same process done for Θ_e defines the *saturated equivalent potential temperature*, $\boldsymbol{\Theta_{es}}$.

Referring everything to a standard level

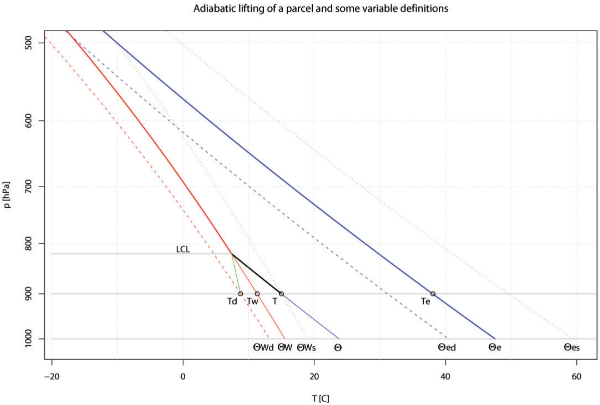

To make things more comparable, temperatures can be referred to the *standard* level (1000 hPa). Bringing the parcel at 1000 hPa along a dry adiabat defines the *potential temperature*, **Θ**.

The dry adiabat used to define T_e intersects the 1000 hPa level at the *equivalent potential temperature*, $\mathbf{\Theta_e}$.

Adding moisture till saturation at the initial level $[q = q_{sat} = 0.622\, e_{sat}(T)/(p - e_{sat}(T))]$ and doing the same process done for Θ_e defines the *saturated equivalent potential temperature*, $\mathbf{\Theta_{es}}$. Cooling the initial air until saturation conserving e (i.e. starting saturated from T_d) and doing the same process defines the *dew-point equivalent potential temperature*, $\mathbf{\Theta_{ed}}$.

3 transformations: potential, equivalent and wet-bulb

- Temperatures at the air parcel level: T_d, T_w and T.

3 transformations: potential, equivalent and wet-bulb

- Temperatures at the air parcel level: T_d, T_w and T.
- Bringing air to the 1000 hPa level:
  - using a dry adiabatic process (potential transformation): Θ (or $\Theta_v \dots$).

3 transformations: potential, equivalent and wet-bulb

- Temperatures at the air parcel level: T_d, T_w and T.
- Bringing air to the 1000 hPa level:
  - using a dry adiabatic process (potential transformation): Θ (or $\Theta_v \dots$).
  - using a saturated pseudo-adiabatic lifting until $q = 0$, followed by a dry adiabatic sinking (equivalent transformation): $\Theta_{ed} = \Theta_e(p, T_d, q)$, $\Theta_e(p, T, q)$ and $\Theta_{es} = \Theta_e[p, T, q_{sat}(T)]$ (note that Θ_{es} depends only by p and T!), where (Bolton 1980):

$$\Theta_e(p, T, q) = T \cdot \left(\frac{1000}{p}\right)^{0.2854\,(1-0.28q)} \cdot \mathrm{e}^{q(1+0.81q)\left(\frac{3376}{T_{LCL}} - 2.54\right)} \tag{1}$$

$$T_{LCL}(T, e) = \frac{2840}{3.5 \cdot \ln(T) - \ln(e) - 4.805} + 55 \tag{2}$$

3 transformations: potential, equivalent and wet-bulb

- Temperatures at the air parcel level: T_d, T_w and T.
- Bringing air to the 1000 hPa level:
  - using a dry adiabatic process (potential transformation): Θ (or $\Theta_v \dots$).
  - using a saturated pseudo-adiabatic lifting until $q = 0$, followed by a dry adiabatic sinking (equivalent transformation): $\Theta_{ed} = \Theta_e(p, T_d, q)$, $\Theta_e(p, T, q)$ and $\Theta_{es} = \Theta_e[p, T, q_{sat}(T)]$ (note that Θ_{es} depends only by p and T!), where (Bolton 1980):

$$\Theta_e(p, T, q) = T \cdot \left(\frac{1000}{p}\right)^{0.2854\,(1-0.28q)} \cdot \mathrm{e}^{q(1+0.81q)\left(\frac{3376}{T_{LCL}} - 2.54\right)} \tag{1}$$

$$T_{LCL}(T, e) = \frac{2840}{3.5 \cdot \ln(T) - \ln(e) - 4.805} + 55 \tag{2}$$

  - using a saturated pseudo-adiabat sinking one find the wet-bulb potential temperatures (wet-bulb transformation): Θ_{wd}, Θ_w and Θ_{ws}, used mainly by French people.

3 transformations: potential, equivalent and wet-bulb

- Temperatures at the air parcel level: T_d, T_w and T.
- Bringing air to the 1000 hPa level:
  - using a dry adiabatic process (potential transformation): Θ (or $\Theta_v \ldots$).
  - using a saturated pseudo-adiabatic lifting until $q = 0$, followed by a dry adiabatic sinking (equivalent transformation):
    $\Theta_{ed} = \Theta_e(p, T_d, q)$, $\Theta_e(p, T, q)$ and $\Theta_{es} = \Theta_e[p, T, q_{sat}(T)]$
    (note that Θ_{es} depends only by p and T!), where (Bolton 1980):

$$\Theta_e(p, T, q) = T \cdot \left(\frac{1000}{p}\right)^{0.2854\,(1-0.28q)} \cdot \mathrm{e}^{q(1+0.81q)\left(\frac{3376}{T_{LCL}} - 2.54\right)} \tag{1}$$

$$T_{LCL}(T, e) = \frac{2840}{3.5 \cdot \ln(T) - \ln(e) - 4.805} + 55 \tag{2}$$

  - using a saturated pseudo-adiabat sinking one find the wet-bulb potential temperatures (wet-bulb transformation): Θ_{wd}, Θ_w and Θ_{ws}, used mainly by French people.

There are 3 correspondences:

$$T_d \leftrightarrow \Theta_{ed} \leftrightarrow \Theta_{wd},$$
$$T_w \leftrightarrow \Theta_e \leftrightarrow \Theta_w,$$
$$T \leftrightarrow \Theta_{es} \leftrightarrow \Theta_{ws}.$$

Dry, moist and pseudo-saturated adiabatic processes

- Dry adiabatic: air is considered dry (neglecting the vapor enthalpy)

$$\text{No saturation } (q = q_0 = constant) \text{ and } c_p \cong c_{pd} = 7/2R_d \text{ (dry air is biatomic)} \tag{3}$$

$$\text{Invariant : } \Theta(T,p) = (T) \cdot \left(\frac{1000}{p}\right)^{R_d/c_{pd}} = (T) \cdot \left(\frac{1000}{p}\right)^{2/7}, \; T \text{ in [K]} \tag{4}$$

$$\text{LapseRate : } -\frac{\mathrm{d}\,T}{\mathrm{d}\,z} = \mathbf{\Gamma_d} = \frac{\mathbf{g}}{\mathbf{c_{pd}}} \cong 9.76\,\mathrm{K/km} \tag{5}$$

Dry, moist and pseudo-saturated adiabatic processes

- Dry adiabatic: air is considered dry (neglecting the vapor enthalpy)

$$\text{No saturation } (q = q_0 = constant) \text{ and } c_p \cong c_{pd} = 7/2R_d \text{ (dry air is biatomic)} \tag{3}$$

$$\text{Invariant}: \Theta(T, p) = (T) \cdot \left(\frac{1000}{p}\right)^{R_d/c_{pd}} = (T) \cdot \left(\frac{1000}{p}\right)^{2/7}, \; T \text{ in [K]} \tag{4}$$

$$\text{LapseRate}: \; -\frac{\mathrm{d}\,T}{\mathrm{d}\,z} = \mathbf{\Gamma_d} = \frac{\mathbf{g}}{\mathbf{c_{pd}}} \cong 9.76\,\mathrm{K/km} \tag{5}$$

- Moist adiabatic: air never saturated but vapor is considered

$$\text{No saturation } (q = q_0 = constant) \text{ and } mc_p = m_d c_{pd} + m_v c_{pv} = m_d 7/2R_d + m_v 4R_v \text{ (vapor is triatomic)} \tag{6}$$

$$\text{Invariant}: \Theta_{Paluch}(T, p, q_0) = (T) \cdot \left(\frac{1000}{p}\right)^{(R_d+R_v q_0)/(c_{pd}+c_{pv} q_0)} = (T) \cdot \left(\frac{1000}{p}\right)^{\frac{2}{7}\frac{1+R_v/R_d q_0}{1+\frac{8}{7}R_v/R_d q_0}} \tag{7}$$

The moist adiabat (Paluch 1979) approximates the dry adiabat as much as $8/7 \cong 1$, that is why it is often neglected.

Dry, moist and pseudo-saturated adiabatic processes

- Dry adiabatic: air is considered dry (neglecting the vapor enthalpy)

$$\text{No saturation } (q = q_0 = constant) \text{ and } c_p \cong c_{pd} = 7/2R_d \text{ (dry air is biatomic)} \tag{3}$$

$$\text{Invariant}: \Theta(T,p) = (T)\cdot\left(\frac{1000}{p}\right)^{R_d/c_{pd}} = (T)\cdot\left(\frac{1000}{p}\right)^{2/7}, \ T \text{ in [K]} \tag{4}$$

$$\text{LapseRate}: -\frac{\mathrm{d}\,T}{\mathrm{d}\,z} = \mathbf{\Gamma_d} = \frac{\mathbf{g}}{\mathbf{c_{pd}}} \cong 9.76\,\text{K/km} \tag{5}$$

- Moist adiabatic: air never saturated but vapor is considered

$$\text{No saturation } (q = q_0 = constant) \text{ and } mc_p = m_d c_{pd} + m_v c_{pv} = m_d 7/2R_d + m_v 4R_v \text{ (vapor is triatomic)} \tag{6}$$

$$\text{Invariant}: \Theta_{Paluch}(T,p,q_0) = (T)\cdot\left(\frac{1000}{p}\right)^{(R_d+R_v q_0)/(c_{pd}+c_{pv} q_0)} = (T)\cdot\left(\frac{1000}{p}\right)^{\frac{2}{7}\frac{1+R_v/R_d q_0}{1+\frac{8}{7}R_v/R_d q_0}} \tag{7}$$

The moist adiabat (Paluch 1979) approximates the dry adiabat as much as $8/7 \cong 1$, that is why it is often neglected.

- Saturated (or wet) pseudo-adiabatic: air is always saturated and condensate *falls out* of the lifted parcel

$$\text{saturation } q = q_{sat}(p,T), \text{ and } c_{p\,liq} \cong 0 \text{ and} c_{p\,ice} \cong 0 \tag{8}$$

$$\text{Invariant}: \Theta_e(T,p,q) = \text{ equation(1)} \tag{9}$$

$$\text{LapseRate}: -\frac{\mathrm{d}\,T}{\mathrm{d}\,z} = \mathbf{\Gamma_s(p,q)} \cong 5 \div 8\,\text{K/km (low troposphere} \div 500\,\text{hPa)} \tag{10}$$

The last is called "pseudo" because it is not reversible (rainfall).

Section 2

Atmosphere static and potential (in)stability

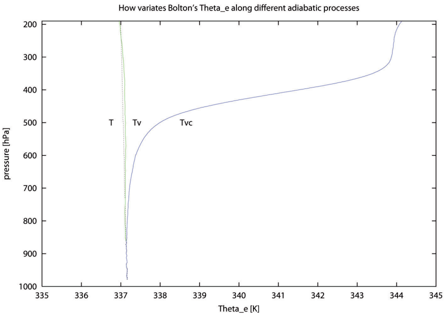

The Lifted Parcel Theory

It is based on the following assumptions:

The Lifted Parcel Theory

It is based on the following assumptions:

1. the initial parcel rises along a dry adiabat until it becomes saturated; afterward it rises along a saturated pseudo-adiabat. "Adiabatically" means *without exchange of heat* between parcel and environment;

The Lifted Parcel Theory

It is based on the following assumptions:

1. the initial parcel rises along a dry adiabat until it becomes saturated; afterward it rises along a saturated pseudo-adiabat. "Adiabatically" means *without exchange of heat* between parcel and environment;
2. the rising parcel *does not mix* with the environment (no *entrainment* and no *dilution*);

The Lifted Parcel Theory

It is based on the following assumptions:

1. the initial parcel rises along a dry adiabat until it becomes saturated; afterward it rises along a saturated pseudo-adiabat. "Adiabatically" means *without exchange of heat* between parcel and environment;
2. the rising parcel *does not mix* with the environment (no *entrainment* and no *dilution*);
3. the environment is in *hydrostatic equilibrium*, i. e. $\frac{\mathrm{d}\,\mathbf{p}}{\mathrm{d}\,\mathbf{z}} = -g\rho$ and the parcel pressure is always equal to the environment pressure at the same height (*pressure perturbations* are neglected);

The Lifted Parcel Theory

It is based on the following assumptions:

1. the initial parcel rises along a dry adiabat until it becomes saturated; afterward it rises along a saturated pseudo-adiabat. "Adiabatically" means *without exchange of heat* between parcel and environment;
2. the rising parcel *does not mix* with the environment (no *entrainment* and no *dilution*);
3. the environment is in *hydrostatic equilibrium*, i. e. $\frac{\mathrm{d}\,\mathbf{p}}{\mathrm{d}\,\mathbf{z}} = -g\rho$ and the parcel pressure is always equal to the environment pressure at the same height (*pressure perturbations* are neglected);
4. in the simplest version (conserving Θ_e), during the saturated pseudo-adiabat the condensed water falls out (so there is no condensate load and *no latent heath of freezing*).

P.S. Otherwise one could parametrize the liquid water–to–ice transition and consider the load of condensed water (which reduce buoyancy) and the latent heat of freezing (which increase buoyancy). In such a case Θ_e is not conserved and buoyancy is computed using the *virtual-cloud temperature* of the parcel, T_{vc} (see Manzato and Morgan 2003).

Parcel buoyancy

During its inviscid (no *friction*) lifting the parcel will experience the following vertical acceleration (called Archimedes buoyancy):

$$\mathbf{B}(\mathbf{z}) = \frac{\mathrm{d}w}{\mathrm{d}t} = -\frac{1}{\rho_p} \cdot \frac{\mathrm{d}p}{\mathrm{d}z} - g = -\frac{1}{\rho_p} \cdot (-g\rho_e) - g = g\frac{\rho_{\mathbf{e}}(\mathbf{z}) - \rho_{\mathbf{p}}(\mathbf{z})}{\rho_{\mathbf{p}}(\mathbf{z})} \quad (11)$$

where $w(z)$ is the parcel vertical velocity, ρ_p and ρ_e are the parcel and environment density respectively. The parcel will continue to rise if it is *less dense* than the surrounding environment.

Parcel buoyancy

During its inviscid (no *friction*) lifting the parcel will experience the following vertical acceleration (called Archimedes buoyancy):

$$\mathbf{B}(\mathbf{z}) = \frac{\mathrm{d}w}{\mathrm{d}t} = -\frac{1}{\rho_p} \cdot \frac{\mathrm{d}p}{\mathrm{d}z} - g = -\frac{1}{\rho_p} \cdot (-g\rho_e) - g = g\frac{\rho_{\mathbf{e}}(\mathbf{z}) - \rho_{\mathbf{p}}(\mathbf{z})}{\rho_{\mathbf{p}}(\mathbf{z})} \quad (11)$$

where $w(z)$ is the parcel vertical velocity, ρ_p and ρ_e are the parcel and environment density respectively. The parcel will continue to rise if it is *less dense* than the surrounding environment. Approximating the air as *dry*, then $\rho_p \cong \rho_{pd} = p/(R_d \cdot T_p)$ and $\rho_e \cong \rho_{ed} = p/(R_d \cdot T_e)$, so that:

$$\mathbf{B}(\mathbf{z}) \cong \mathbf{g} \cdot \frac{\mathbf{T_p}(\mathbf{z}) - \mathbf{T_e}(\mathbf{z})}{\mathbf{T_e}(\mathbf{z})} \quad (12)$$

In this *approximation* the parcel will continue to rise if it is *warmer* than environmental air and B(z) does not depend on environmental RH above.

Parcel buoyancy

During its inviscid (no *friction*) lifting the parcel will experience the following vertical acceleration (called Archimedes buoyancy):

$$\mathbf{B}(\mathbf{z}) = \frac{\mathrm{d}w}{\mathrm{d}t} = -\frac{1}{\rho_p} \cdot \frac{\mathrm{d}p}{\mathrm{d}z} - g = -\frac{1}{\rho_p} \cdot (-g\rho_e) - g = g\frac{\rho_{\mathbf{e}}(\mathbf{z}) - \rho_{\mathbf{p}}(\mathbf{z})}{\rho_{\mathbf{p}}(\mathbf{z})} \quad (11)$$

where $w(z)$ is the parcel vertical velocity, ρ_p and ρ_e are the parcel and environment density respectively. The parcel will continue to rise if it is *less dense* than the surrounding environment. Approximating the air as *dry*, then $\rho_p \cong \rho_{pd} = p/(R_d \cdot T_p)$ and $\rho_e \cong \rho_{ed} = p/(R_d \cdot T_e)$, so that:

$$\mathbf{B}(\mathbf{z}) \cong \mathbf{g} \cdot \frac{\mathbf{T_p}(\mathbf{z}) - \mathbf{T_e}(\mathbf{z})}{\mathbf{T_e}(\mathbf{z})} \quad (12)$$

In this *approximation* the parcel will continue to rise if it is *warmer* than environmental air and B(z) does not depend on environmental RH above.

Instead, if one would consider also the vapor contribution, then he can replace the normal temperatures with the virtual temperatures (called the *"virtual correction"*), but then he should also conserve Θ_{Paluch} instead of the simpler potential temperature Θ during the "moist" adiabat... In both cases, during the saturated pseudo-adiabat Θ_e is conserved.

The vertical profile of the buoyancy and its integral

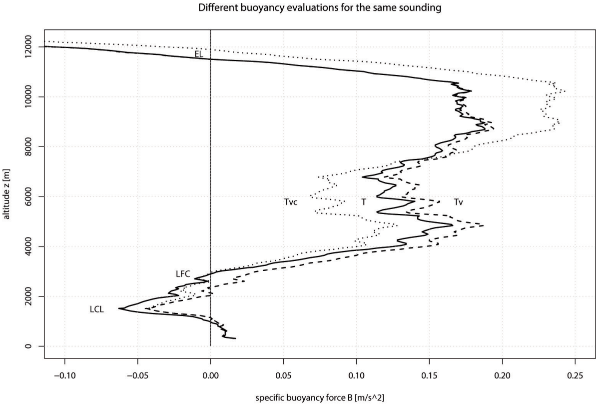

Taking a small part of environment as *"initial parcel"* and applying the Lifted Parcel Theory, it may happen that the parcel will become *buoyant* [i. e. $B(z) > 0$], from its *Level of Free Convection*, LFC, to its *Equilibrium Level*, EL.

The vertical profile of the buoyancy and its integral

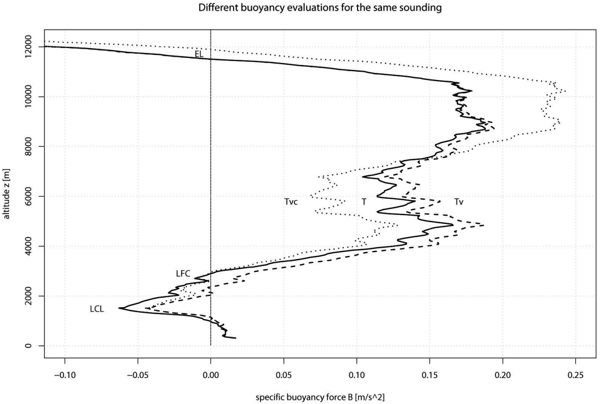

Taking a small part of environment as *"initial parcel"* and applying the Lifted Parcel Theory, it may happen that the parcel will become *buoyant* [i. e. $B(z) > 0$], from its *Level of Free Convection*, LFC, to its *Equilibrium Level*, EL.

Since $B(z) = \frac{\mathrm{d}w}{\mathrm{d}t} = w \cdot \frac{\mathrm{d}w}{\mathrm{d}z}$, integrating $B(z)$ along the vertical profile one obtains a squared vertical velocity, i. e. a kinetic energy. The *Convective Available Potential Energy*, CAPE, is obtained integrating the buoyancy from LFC to EL:

$$\mathbf{CAPE} = \int_{\mathbf{z_{LFC}}}^{\mathbf{z_{EL}}} \mathbf{B(z)} \cdot \mathrm{d}\mathbf{z} = 1/2\mathbf{w^2} \quad (13)$$

Instability Inhibition and trigger mechanisms

Starting from an initial level z_0 of an atmospheric profile, in case that the lifted air becomes more dense than the environment, one can think that an external agent will provide the energy (*forcing*) needed to –eventually– reach its LFC. This energy is the *Convective Inhibition*, CIN:

$$\mathbf{CIN} = \int_{\mathbf{z_0}}^{\mathbf{z_{LFC}}} \mathbf{B}(\mathbf{z}) \cdot \mathrm{d}\mathbf{z} < 0 \tag{14}$$

Instability Inhibition and trigger mechanisms

Starting from an initial level z_0 of an atmospheric profile, in case that the lifted air becomes more dense than the environment, one can think that an external agent will provide the energy (*forcing*) needed to –eventually– reach its LFC. This energy is the *Convective Inhibition*, CIN:

$$\mathbf{CIN} = \int_{\mathbf{z_0}}^{\mathbf{z_{LFC}}} \mathbf{B}(\mathbf{z}) \cdot \mathrm{d}\mathbf{z} < 0 \tag{14}$$

The integral of the negative buoyancy in the low levels could be quite large (e.g. CIN$\cong 100 \div 300$ J/kg) in comparison with the integral of the positive buoyancy above LFC (e.g. CAPE $\cong 1000$ J/kg). Hence, the occurrence of a trigger mechanism that lifts the low-level air to its LFC to start Convective Initiation is a *key factor* of thunderstorms forecasting.

Instability Inhibition and trigger mechanisms

Starting from an initial level z_0 of an atmospheric profile, in case that the lifted air becomes more dense than the environment, one can think that an external agent will provide the energy (*forcing*) needed to –eventually– reach its LFC. This energy is the *Convective Inhibition*, CIN:

$$\mathbf{CIN} = \int_{\mathbf{z_0}}^{\mathbf{z_{LFC}}} \mathbf{B(z)} \cdot \mathrm{d}\mathbf{z} < 0 \qquad (14)$$

The integral of the negative buoyancy in the low levels could be quite large (e.g. CIN$\cong 100 \div 300$ J/kg) in comparison with the integral of the positive buoyancy above LFC (e.g. CAPE $\cong 1000$ J/kg). Hence, the occurrence of a trigger mechanism that lifts the low-level air to its LFC to start Convective Initiation is a *key factor* of thunderstorms forecasting. Phenomena that can act as CI *trigger* include: cold fronts, orographic lifting, convergence flows and breezes, low-level jets, thermic boundaries (e.g. sunset boundary advection, sea/land PBL gradients, cold pools of previous convection, bores,. . .), drylines advection, lake/lagoons evaporation, any vertically-developed roll having sufficient w. . .

Operational definition of *potential* instability

If an atmospheric profile has at least a parcel in the low levels for which it is possible to find a LFC then the profile is said to be *potentially unstable*.

Operational definition of *potential* instability

If an atmospheric profile has at least a parcel in the low levels for which it is possible to find a LFC then the profile is said to be *potentially unstable*. Hence potential instability is a property inherently related to the Lifted Parcel Theory, applied to a level (initial parcel) of the atmospheric profile and comparing its ascent with the *temperature* profile above it.

Operational definition of *potential* instability

If an atmospheric profile has at least a parcel in the low levels for which it is possible to find a LFC then the profile is said to be *potentially unstable*. Hence potential instability is a property inherently related to the Lifted Parcel Theory, applied to a level (initial parcel) of the atmospheric profile and comparing its ascent with the *temperature* profile above it.
Potential instability is a characteristic of the *whole* profile, with respect to *very large* displacement Δz of one of his low levels, because LFC could be much higher than the initial level z_0 (e.g. $z_0 \cong 200\,\mathrm{m}$ and LFC$\cong 2200\,\mathrm{m}$, hence $\Delta z = 2000\,\mathrm{m}$).

Operational definition of *potential* instability

If an atmospheric profile has at least a parcel in the low levels for which it is possible to find a LFC then the profile is said to be *potentially unstable*. Hence potential instability is a property inherently related to the Lifted Parcel Theory, applied to a level (initial parcel) of the atmospheric profile and comparing its ascent with the *temperature* profile above it.
Potential instability is a characteristic of the *whole* profile, with respect to *very large* displacement Δz of one of his low levels, because LFC could be much higher than the initial level z_0 (e.g. $z_0 \cong 200$ m and LFC$\cong 2200$ m, hence $\Delta z = 2000$ m).
The condition that there is at least one atmospheric level for which it is possible to find a LFC is *equivalent* to say that that level (chosen as initial parcel) has CAPE> 0. As we will see on the Thetaplot diagram, that is *equivalent* to say that the atmospheric profile has a low-level Θ_e, $\Theta_e|_{low} = \Theta_e(z_0)$, which is higher then a mid-level Θ_{es}, $\Theta_{es}|_{mid}$, i.e.

$$\mathbf{MaxBuoyancy} = \boldsymbol{\Theta_e|_{low}} - \boldsymbol{\Theta_{es}|_{mid}} > \mathbf{0}. \tag{15}$$

Classic *static* instability definition

A layer of an atmospheric profile is said to be *absolutely stable* if its lapse rate decreases less than that of the saturated pseudo-adiabat, i. e. $\Gamma = -\frac{\mathrm{d}\,T}{\mathrm{d}\,z} < \Gamma_s \cong 5\,\mathrm{K/km}$.

Classic *static* instability definition

A layer of an atmospheric profile is said to be *absolutely stable* if its lapse rate decreases less than that of the saturated pseudo-adiabat, i. e. $\Gamma = -\frac{\mathrm{d}\,T}{\mathrm{d}\,z} < \Gamma_s \cong 5\,\mathrm{K/km}$. A layer of an atmospheric profile is said to be *absolutely unstable* (or superadiabatic) if its lapse rate decreases more than that of the dry adiabat, i. e. $\Gamma = -\frac{\mathrm{d}\,T}{\mathrm{d}\,z} > \Gamma_d \cong 9.8\,\mathrm{K/km}$.

Classic *static* instability definition

A layer of an atmospheric profile is said to be *absolutely stable* if its lapse rate decreases less than that of the saturated pseudo-adiabat, i. e. $\Gamma = -\frac{\mathrm{d}\,T}{\mathrm{d}\,z} < \Gamma_s \cong 5\,\mathrm{K/km}$. A layer of an atmospheric profile is said to be *absolutely unstable* (or superadiabatic) if its lapse rate decreases more than that of the dry adiabat, i. e. $\Gamma = -\frac{\mathrm{d}\,T}{\mathrm{d}\,z} > \Gamma_d \cong 9.8\,\mathrm{K/km}$.

A layer of an atmospheric profile is said to be *conditionally stable* if its lapse rate is in between the dry and saturated adiabat, i. e. $\Gamma_s < \Gamma < \Gamma_d$. Lifting the bottom of the layer it will become unstable if it is saturated, but will remain stable if it follows a dry adiabat.

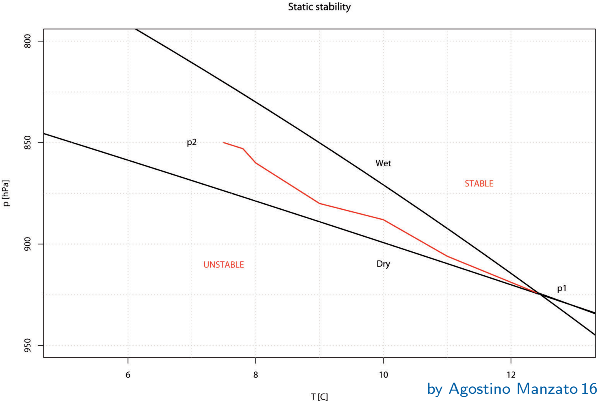

Potential vs. static instability

Static instability is a characteristic of part (a layer) of an atmospheric profile, with respect to small displacements of its bottom, in that sense it is very different from the potential instability of the entire profile, that could need a large displacement of one of its low levels.

Potential vs. static instability

Static instability is a characteristic of part (a layer) of an atmospheric profile, with respect to small displacements of its bottom, in that sense it is very different from the potential instability of the entire profile, that could need a large displacement of one of its low levels.
When a layer is absolutely stable, $\Gamma < \Gamma_s$, it means that $\frac{\mathrm{d}\,\Theta_e}{\mathrm{d}\,z} > 0$. It is even more true that $\frac{\mathrm{d}\,\Theta}{\mathrm{d}\,z} > 0$, hence it is possible to define the *Brunt-Väisälä frequency* **N**$= \sqrt{\frac{\mathbf{g}}{\mathbf{\Theta}}\frac{\mathrm{d}\,\mathbf{\Theta}}{\mathrm{d}\,\mathbf{z}}}$, that is very useful to study PBL, gravity waves. . .

Potential vs. static instability

Static instability is a characteristic of part (a layer) of an atmospheric profile, with respect to small displacements of its bottom, in that sense it is very different from the potential instability of the entire profile, that could need a large displacement of one of its low levels.
When a layer is absolutely stable, $\Gamma < \Gamma_s$, it means that $\frac{\mathrm{d}\,\Theta_e}{\mathrm{d}\,z} > 0$. It is even more true that $\frac{\mathrm{d}\,\Theta}{\mathrm{d}\,z} > 0$, hence it is possible to define the *Brunt-Väisälä frequency* $\mathbf{N} = \sqrt{\frac{\mathbf{g}}{\mathbf{\Theta}} \frac{\mathrm{d}\,\mathbf{\Theta}}{\mathrm{d}\,\mathbf{z}}}$, that is very useful to study PBL, gravity waves...
When a layer is conditionally unstable, $\Gamma_s < \Gamma < \Gamma_d$, it means that $\frac{\mathrm{d}\,\Theta_e}{\mathrm{d}\,z} < 0$ but $\frac{\mathrm{d}\,\Theta}{\mathrm{d}\,z} > 0$, hence it is still possible to define the Brunt-Väisälä frequency. The conditional instability (i.e. $\frac{\mathrm{d}\,\Theta_e}{\mathrm{d}\,z} < 0$) does not guarantee the bottom of the layer will have a LFC, but that depends on its moisture.

Potential vs. static instability

Static instability is a characteristic of part (a layer) of an atmospheric profile, with respect to small displacements of its bottom, in that sense it is very different from the potential instability of the entire profile, that could need a large displacement of one of its low levels.
When a layer is absolutely stable, $\Gamma < \Gamma_s$, it means that $\frac{\mathrm{d}\,\Theta_e}{\mathrm{d}\,z} > 0$. It is even more true that $\frac{\mathrm{d}\,\Theta}{\mathrm{d}\,z} > 0$, hence it is possible to define the *Brunt-Väisälä frequency* $\mathbf{N} = \sqrt{\frac{\mathbf{g}}{\mathbf{\Theta}} \frac{\mathrm{d}\,\mathbf{\Theta}}{\mathrm{d}\,\mathbf{z}}}$, that is very useful to study PBL, gravity waves...
When a layer is conditionally unstable, $\Gamma_s < \Gamma < \Gamma_d$, it means that $\frac{\mathrm{d}\,\Theta_e}{\mathrm{d}\,z} < 0$ but $\frac{\mathrm{d}\,\Theta}{\mathrm{d}\,z} > 0$, hence it is still possible to define the Brunt-Väisälä frequency. The conditional instability (i.e. $\frac{\mathrm{d}\,\Theta_e}{\mathrm{d}\,z} < 0$) does not guarantee the bottom of the layer will have a LFC, but that depends on its moisture.
When a layer is absolutely unstable it will be lifted even by a very small perturbation (without needs of any external forcing), so that it is the kind of instability usually defined in physics. $\Gamma > \Gamma_d$ means $\frac{\mathrm{d}\,\Theta}{\mathrm{d}\,z} < 0$ and it is *no more* possible to define the Brunt-Väisälä frequency.

Section 3

Sounding diagrams: skew-T and Thetaplot

Global homologation of thermodynamic diagrams. . .

The atmospheric profiles are usually not shown on a normal p vs. T (or z vs. T) diagram as seen until now, but are shown on specific thermodynamic diagrams. In the past many different diagrams were proposed: Neuhoff (1900), Tephigram (Shaw, 1922), Stüve (1927), Aerogram (Refsdal, 1935), Pastagram (Bellamy, 1945), skew–T (Herlofson, 1947). . . Today, in 99.999% of cases it is used the skew–T diagram, but I will show you also the Theta–Plot diagram (Morgan, 1992), which I personally believe to be the most useful.

Global homologation of thermodynamic diagrams. . .

The atmospheric profiles are usually not shown on a normal p vs. T (or z vs. T) diagram as seen until now, but are shown on specific thermodynamic diagrams. In the past many different diagrams were proposed: Neuhoff (1900), Tephigram (Shaw, 1922), Stüve (1927), Aerogram (Refsdal, 1935), Pastagram (Bellamy, 1945), skew–T (Herlofson, 1947). . . Today, in 99.999% of cases it is used the skew–T diagram, but I will show you also the Theta–Plot diagram (Morgan, 1992), which I personally believe to be the most useful.

In the approximation of *dry* air and *hydrostatic equilibrium* it is easy to derive the *hypsometric* or *thickness* eq. of a layer with $\overline{T(z)}$ mean temp.:

$$\ln \frac{\mathbf{p_2}}{\mathbf{p_1}} = -\frac{\mathbf{g}}{\mathbf{R_d}\,\overline{\mathbf{T(z)}}} \cdot (\mathbf{z_2} - \mathbf{z_1}) \tag{16}$$

Global homologation of thermodynamic diagrams. . .

The atmospheric profiles are usually not shown on a normal p vs. T (or z vs. T) diagram as seen until now, but are shown on specific thermodynamic diagrams. In the past many different diagrams were proposed: Neuhoff (1900), Tephigram (Shaw, 1922), Stüve (1927), Aerogram (Refsdal, 1935), Pastagram (Bellamy, 1945), skew–T (Herlofson, 1947). . . Today, in 99.999% of cases it is used the skew–T diagram, but I will show you also the Theta–Plot diagram (Morgan, 1992), which I personally believe to be the most useful.

In the approximation of *dry* air and *hydrostatic equilibrium* it is easy to derive the *hypsometric* or *thickness* eq. of a layer with $\overline{T(z)}$ mean temp.:

$$\ln \frac{\mathbf{p_2}}{\mathbf{p_1}} = -\frac{\mathbf{g}}{\mathbf{R_d}\,\overline{\overline{\mathbf{T(z)}}}} \cdot (\mathbf{z_2} - \mathbf{z_1}) \qquad (16)$$

From this equation it is possible to see that the height z is approximately proportional to the opposite of the natural logarithm of pressure p. Hence, on the ordinate it will be shown $-\ln(p/1000)$.

A Skew-T chart

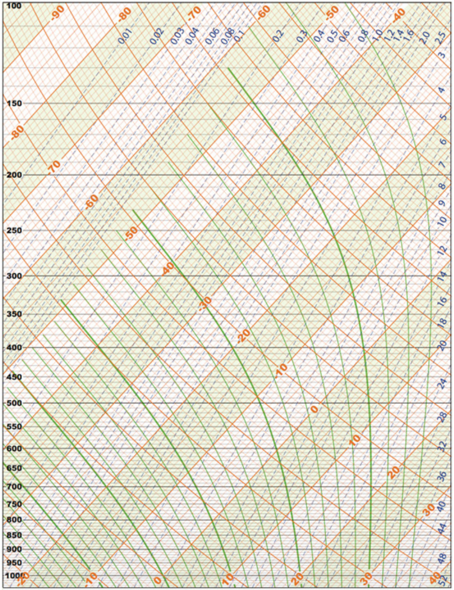

- On the skew-T diagram the abscissa is turned 45^{o}, so that isotherms are no more vertical lines, but are skewed of 45 degree to the *right*.

A Skew-T chart

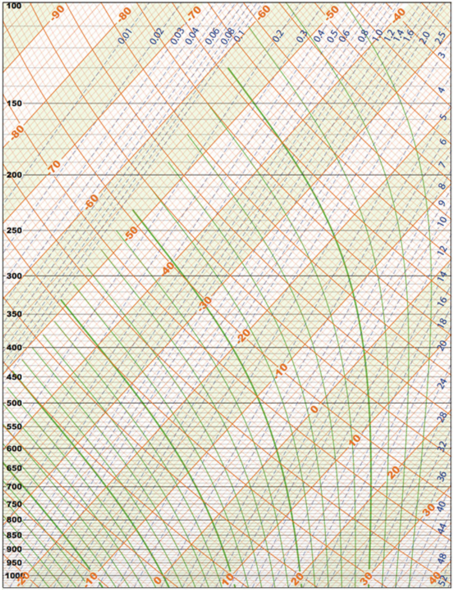

- On the skew-T diagram the abscissa is turned 45^{o}, so that isotherms are no more vertical lines, but are skewed of 45 degree to the *right*.
- The dry adiabats (iso-Θ lines) here are the orange lines, slanted to the *left* from surface upward. In the low levels they are almost straight.

A Skew-T chart

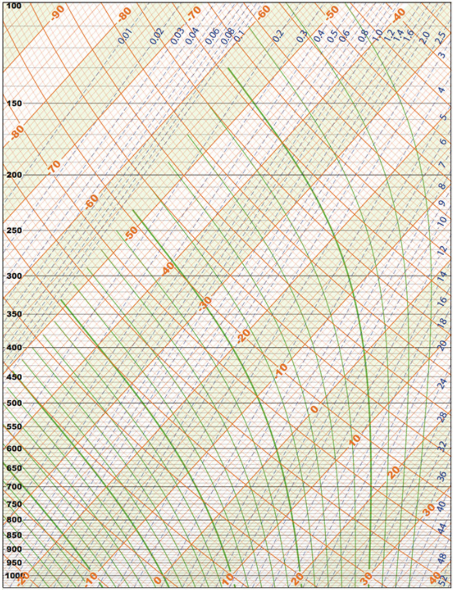

- On the skew-T diagram the abscissa is turned 45^{o}, so that isotherms are no more vertical lines, but are skewed of 45 degree to the *right*.
- The dry adiabats (iso-Θ lines) here are the orange lines, slanted to the *left* from surface upward. In the low levels they are almost straight.
- The saturated pseudo-adiabats (iso-Θ_e lines) are shown here as the green curves, going toward left from surface upward.

A Skew-T chart

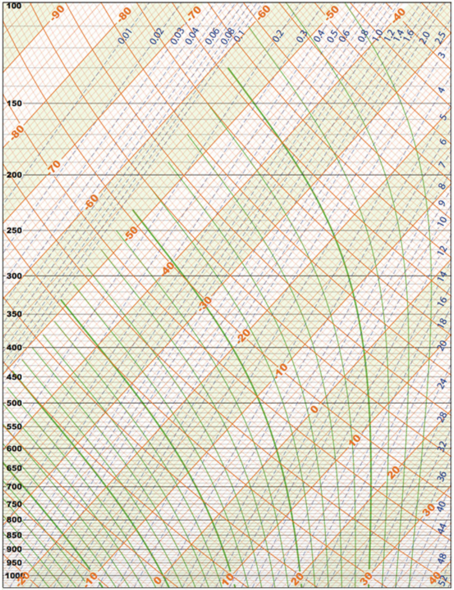

- On the skew-T diagram the abscissa is turned 45^o, so that isotherms are no more vertical lines, but are skewed of 45 degree to the *right*.
- The dry adiabats (iso-Θ lines) here are the orange lines, slanted to the *left* from surface upward. In the low levels they are almost straight.
- The saturated pseudo-adiabats (iso-Θ_e lines) are shown here as the green curves, going toward left from surface upward.
- The iso-q lines are the dashed blue lines, going toward right from surface upward.

Skew-T graphical explanation

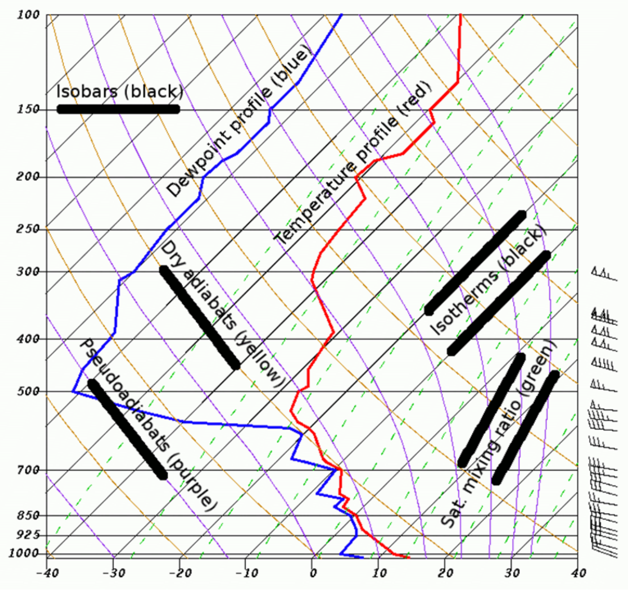

The atmosphere profile is drawn reporting at each pressure level **T**(p) and $\mathbf{T_d}$(p).

Usually also the horizontal–wind profile is shown on the right side.

A potentially unstable sounding shown on a Skew-T

28–jun–1998,12:00:00 Skew–t plot for rds16044 (28–Jun–1998,11:00:00).

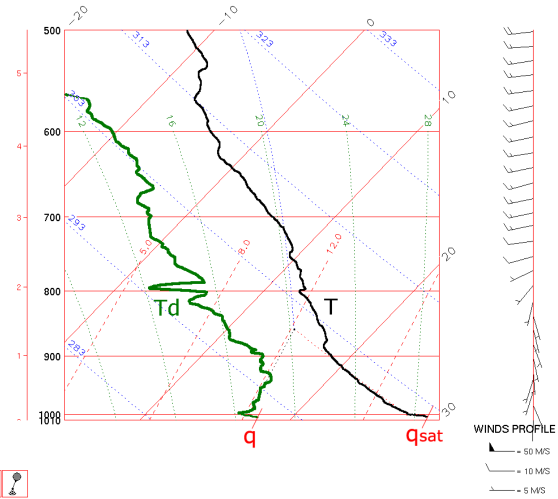

A potentially unstable sounding shown on a Skew-T

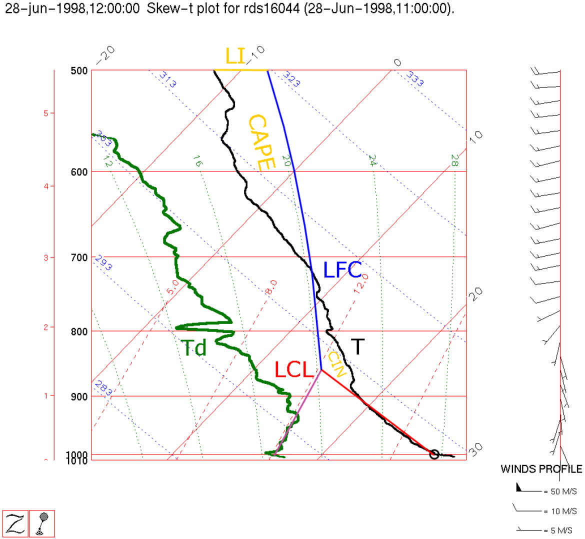

If the mean air in the lowest levels (note the superadiabatic surface) is lifted along a dry adiabat until LCL and then along a saturated pseudo-adiabat, a LFC can be found, hence CAPE>0. Note that it is needed some forcing to overtake the CIN area.

A potentially unstable sounding shown on a Skew-T

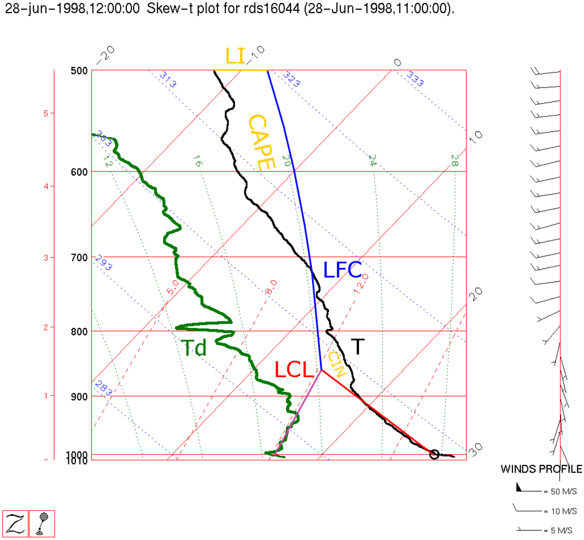

If the mean air in the lowest levels (note the superadiabatic surface) is lifted along a dry adiabat until LCL and then along a saturated pseudo-adiabat, a LFC can be found, hence CAPE> 0. Note that it is needed some forcing to overtake the CIN area. The temperature difference between the lifted parcel and the environment at $p = 500\,\text{hPa}$ is the *Lifted Index* (Galway 1956).

A Theta–plot chart (made by the NCAR “Zebra” software)

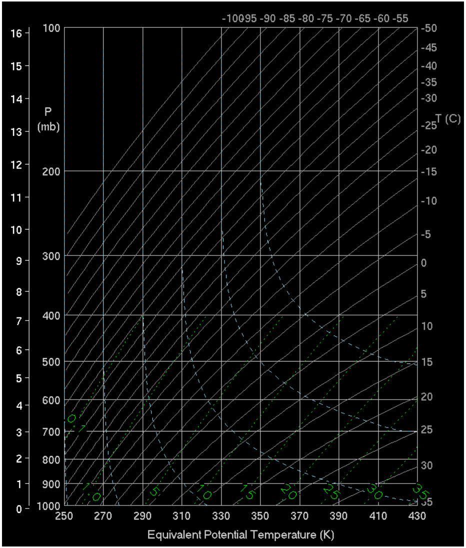

- On the Thetaplot diagram the abscissa is Θ_e, so that saturated pseudo-adiabats (iso-Θ_e) are vertical lines.

A Theta–plot chart (made by the NCAR “Zebra” software)

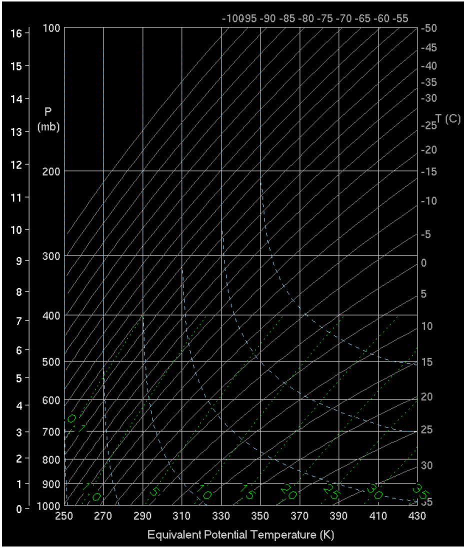

- On the Thetaplot diagram the abscissa is Θ_e, so that saturated pseudo-adiabats (iso-Θ_e) are vertical lines.
- The isotherms are no more straight lines, but are curves (white in this example) going to the right from surface upward.

A Theta–plot chart (made by the NCAR "Zebra" software)

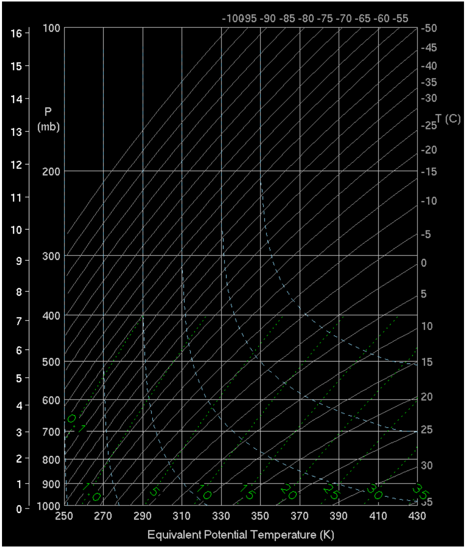

- On the Thetaplot diagram the abscissa is Θ_e, so that saturated pseudo-adiabats (iso-Θ_e) are vertical lines.
- The isotherms are no more straight lines, but are curves (white in this example) going to the right from surface upward.
- The dry adiabats (iso-Θ lines) are the blue curves, going toward left from surface upward. At low temperatures they are almost vertical.

A Theta–plot chart (made by the NCAR "Zebra" software)

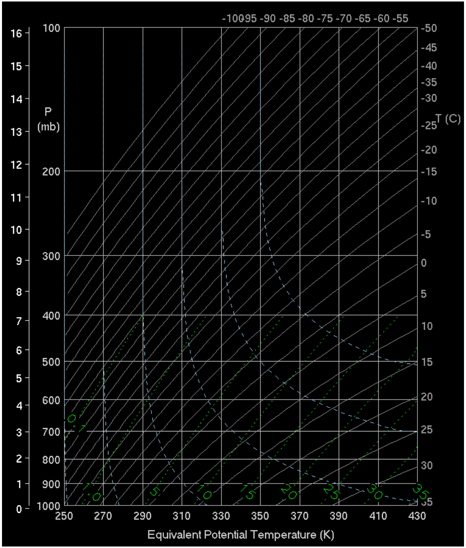

- On the Thetaplot diagram the abscissa is Θ_e, so that saturated pseudo-adiabats (iso-Θ_e) are vertical lines.
- The isotherms are no more straight lines, but are curves (white in this example) going to the right from surface upward.
- The dry adiabats (iso-Θ lines) are the blue curves, going toward left from surface upward. At low temperatures they are almost vertical.
- The iso-q lines are the dashed green lines, going toward right from surface upward.

Theta-plot graphical explanation

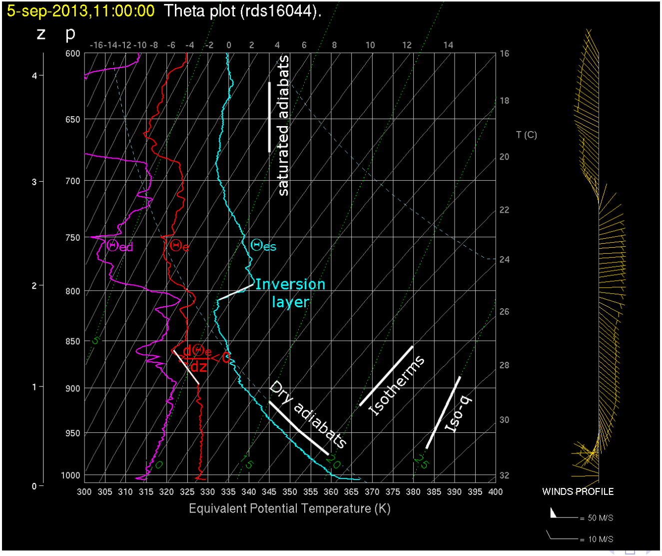

On each level of a Theta-plot these 3 values are drawn: Θ_{ed}, Θ_e and Θ_{es}.

Theta-plot graphical explanation

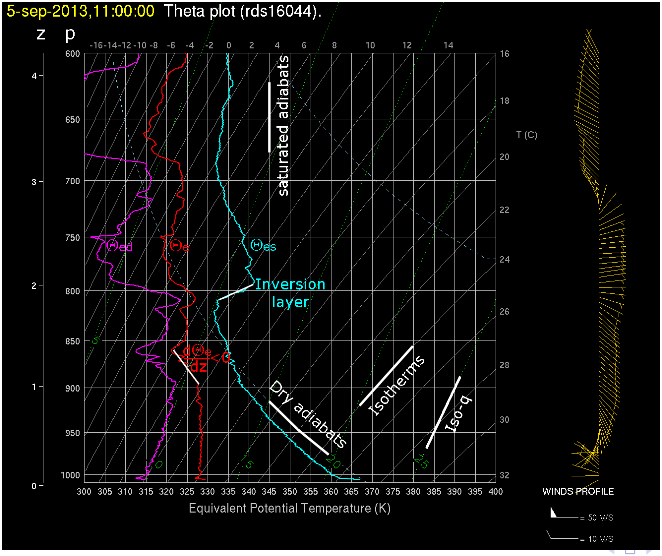

On each level of a Theta-plot these 3 values are drawn: Θ_{ed}, Θ_e and Θ_{es}. This Udine sounding, launched at 11:00 UTC of 05/09/2013, has an *inversion* layer ($\mathrm{d}T/\mathrm{d}z < 0$) at 800 hPa and also a layer where $\mathrm{d}\Theta_e/\mathrm{d}z < 0$ (between 900 and 850 hPa), but it is not *potentially unstable* (no LFC).

On Theta-plot is easy to identify constant Θ_e layers

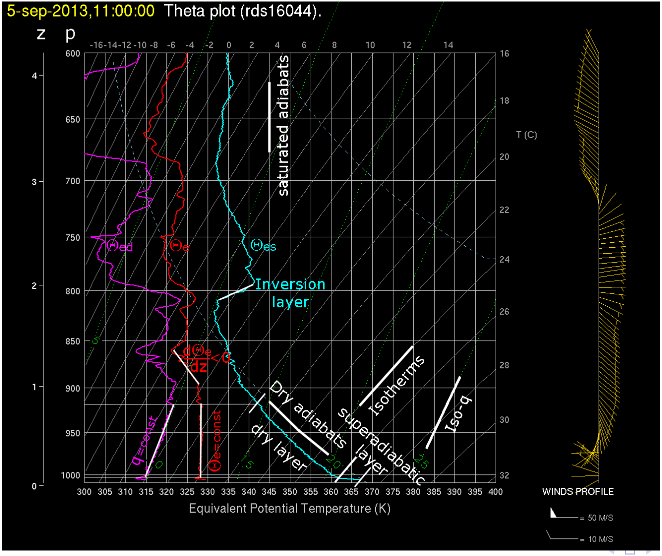

The "third" line of the Thetaplot shows $\mathbf{\Theta_e}$, that is one of the most *conserved* variables in atmosphere, since it is conserved even in *"dry layers"*, like that between 1000 and 925 hPa (q=10g/kg!).

On Theta-plot is easy to identify constant Θ_e layers

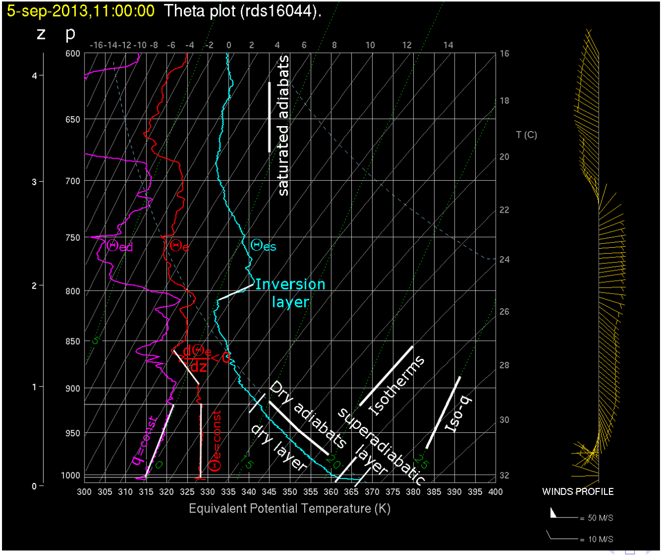

The "third" line of the Thetaplot shows $\mathbf{\Theta_e}$, that is one of the most *conserved* variables in atmosphere, since it is conserved even in *"dry layers"*, like that between 1000 and 925 hPa (q=10g/kg!). The small *superadiabatic* layer near surface can lead to overestimation of instability, if surface is taken as initial parcel.

Vertical time-series of Θ_e observed by RDS every 6h

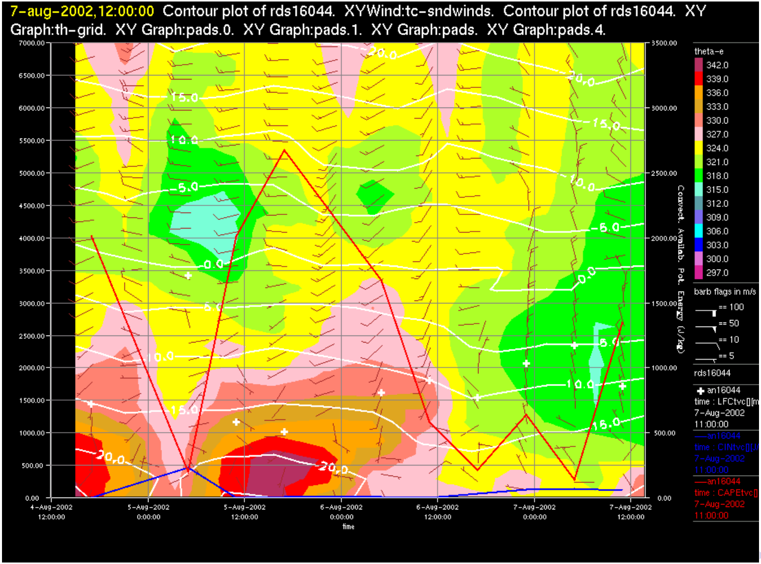

Θ_e (filled) gradients track very well the air mass changes, e.g. fronts. Note CAPE, CIN and LFC (+).

Vertical time-series of Θ_e observed by RDS every 6h

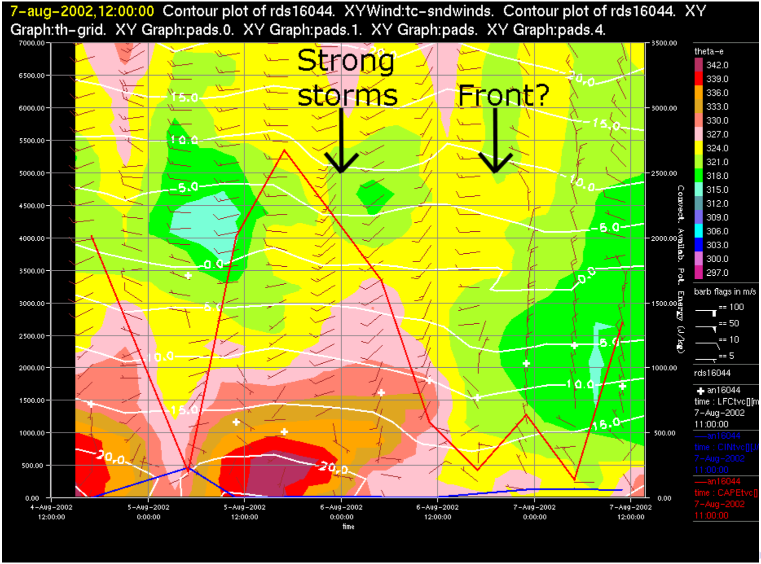

Θ_e (filled) gradients track very well the air mass changes, e.g. fronts. Note CAPE, CIN and LFC (+). Observed very strong storms around 00 UTC of 06/08/2002.

RDS vertical time series every 12 h for widespread hailfall

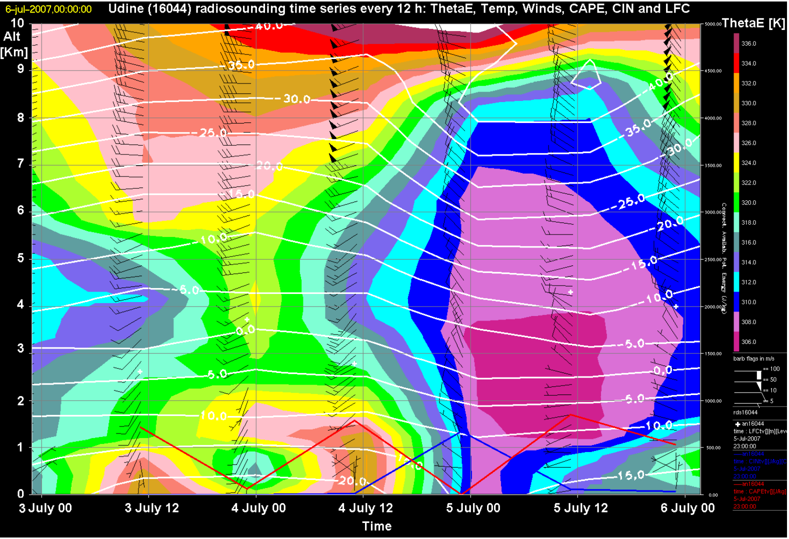

RDS vertical time series every 12 h for widespread hailfall

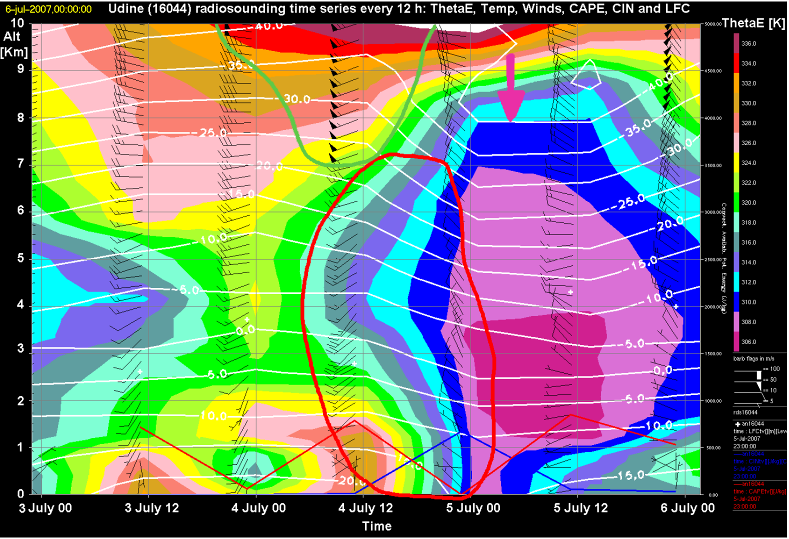

Note the strong Θ_e gradient in the afternoon of 04/07/07 and the wind jet above 7 km associated with the cold front.

At 5 July 00 UTC the tropopause sinks at only 8.2 km.

Equivalent Potential Temperatures on a Theta-plot

28−jun−1998,12:00:00 Theta plot (rds16044).

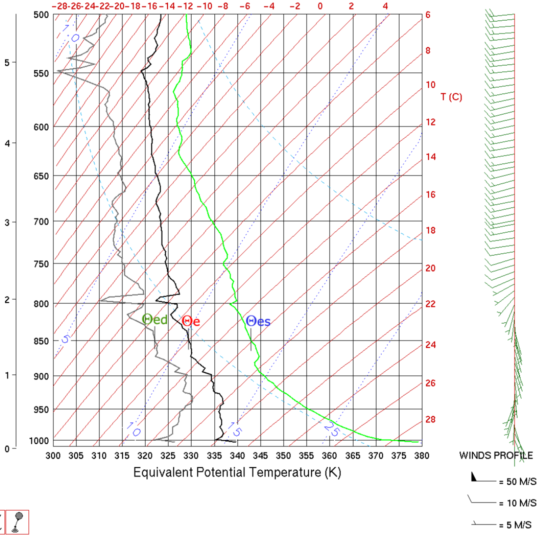

Operatively, the Theta-plot diagram is computed observing at different levels p, T and T_d, then deriving $q(p, T, T_d)$ and $q_{sat}(p, T)$ and lastly computing and drawing at each level $\Theta_{ed} = \Theta_e(p, T_d, q)$, $\Theta_e = \Theta_e(p, T, q)$ and $\Theta_{es} = \Theta_e(p, T, q_{sat})$.

Equivalent Potential Temperatures on a Theta-plot

28−jun−1998,12:00:00 Theta plot (rds16044).

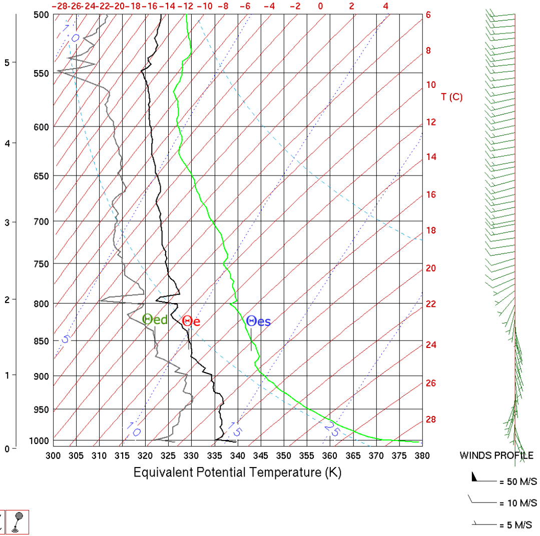

Operatively, the Theta-plot diagram is computed observing at different levels p, T and T_d, then deriving $q(p, T, T_d)$ and $q_{sat}(p, T)$ and lastly computing and drawing at each level $\Theta_{ed} = \Theta_e(p, T_d, q)$, $\Theta_e = \Theta_e(p, T, q)$ and $\Theta_{es} = \Theta_e(p, T, q_{sat})$. Note that, for any given pressure level p, Θ_{es} depends only from $T(p)$.

Temperatures on a Theta-plot

28-jun-1998,12:00:00 Theta plot (rds16044).

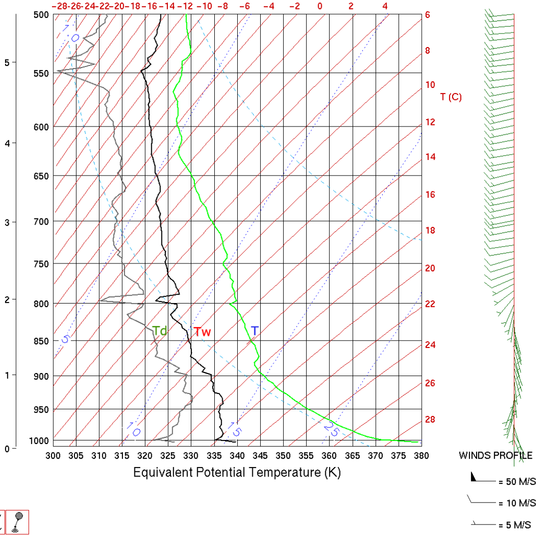

The vertical profiles of Θ_{ed}, Θ_e and Θ_{es} intersect on the isotherms T_d, T_w and T respectively, because of the correspondences seen before. Example shows temperatures at 850 hPa. $(\Theta_{es} - \Theta_{ed})$ resembles the dew-point depressure $(T - T_d)$: the more distant are these two lines, the more dry is that level.

Temperatures on a Theta-plot

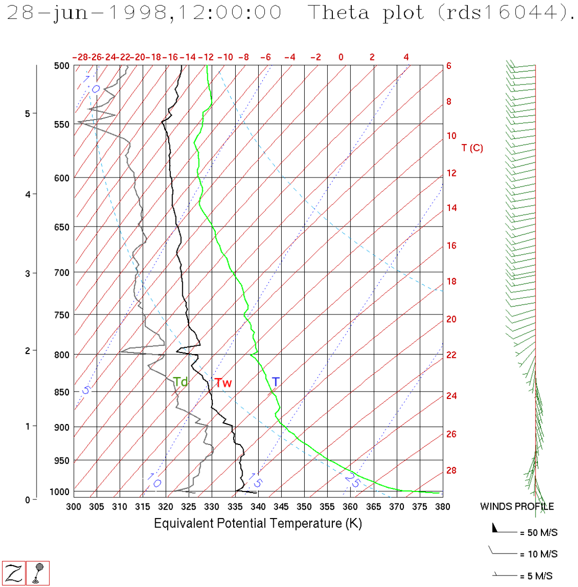

The vertical profiles of Θ_{ed}, Θ_e and Θ_{es} intersect on the isotherms $\mathbf{T_d}$, $\mathbf{T_w}$ and $\mathbf{T}$ respectively, because of the correspondences seen before. Example shows temperatures at 850 hPa. $(\Theta_{es} - \Theta_{ed})$ resembles the dew-point depressure $(T - T_d)$: the more distant are these two lines, the more dry is that level. Note that on the skew-T it is not possible to read the value of T_w.

Mixing ratios on a Theta-plot

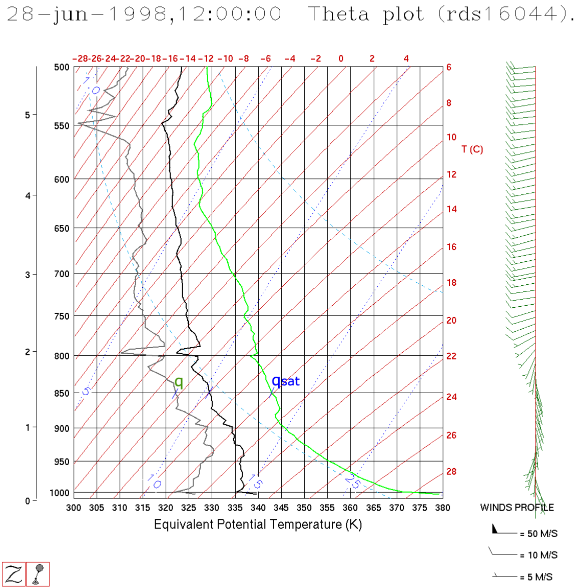

The vertical profiles of Θ_{ed} and Θ_{es} intersect on the iso-mixing ratio lines ($q = const$) **q** and $\mathbf{q_{sat}}$, respectively.

Mixing ratios on a Theta-plot

28-jun-1998,12:00:00 Theta plot (rds16044).

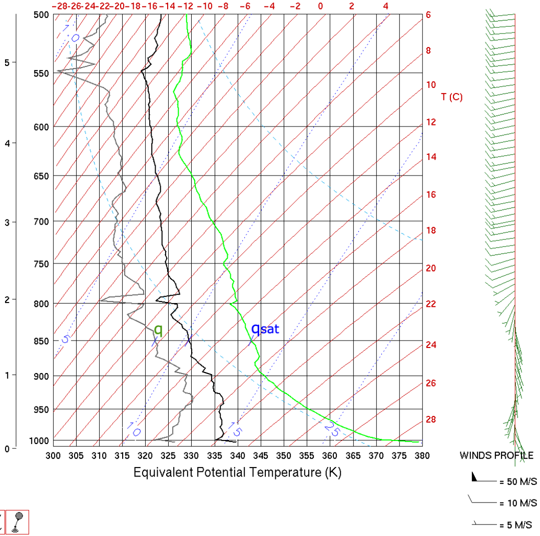

The vertical profiles of Θ_{ed} and Θ_{es} intersect on the iso-mixing ratio lines ($q = const$) **q** and **q_{sat}**, respectively.

The sounding shown is the Udine RDS launched at 11:00 UTC of 28/06/1998. Note that soundings are launched before their nominal "time" because the ascension to tropopause takes about 45 minutes.

A potentially unstable sounding shown on a Theta-plot

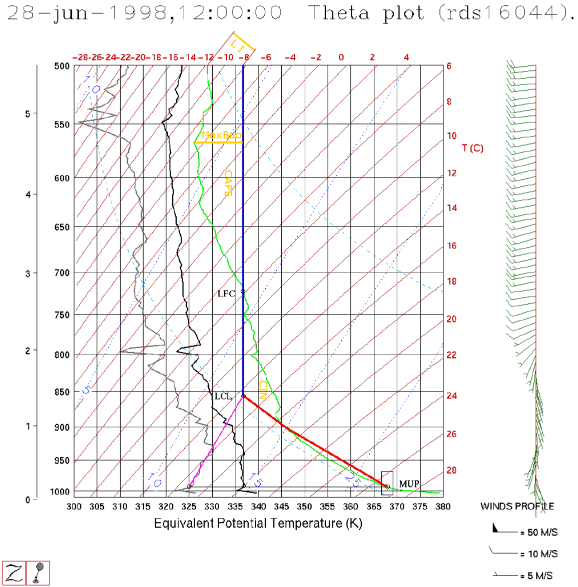

If the mean air in the lowest levels (avoiding the surface superadiabatic thin layer) is lifted along a dry adiabat until LCL and then along a vertical saturated pseudo-adiabat, a LFC can be found, hence CAPE>0.

A potentially unstable sounding shown on a Theta-plot

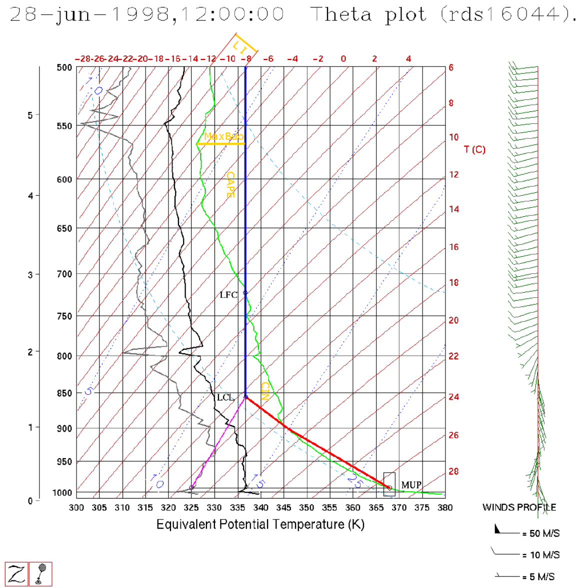

If the mean air in the lowest levels (avoiding the surface superadiabatic thin layer) is lifted along a dry adiabat until LCL and then along a vertical saturated pseudo-adiabat, a LFC can be found, hence CAPE>0. Since Θ_e is conserved along the whole process, the **LFC exists** *if and only if* Θ_e of the initial parcel is *larger* then the lowest Θ_{es} in the mid-levels, i. e. **MaxBuo**>0.

The Lifted Parcel Theory on a Theta-plot

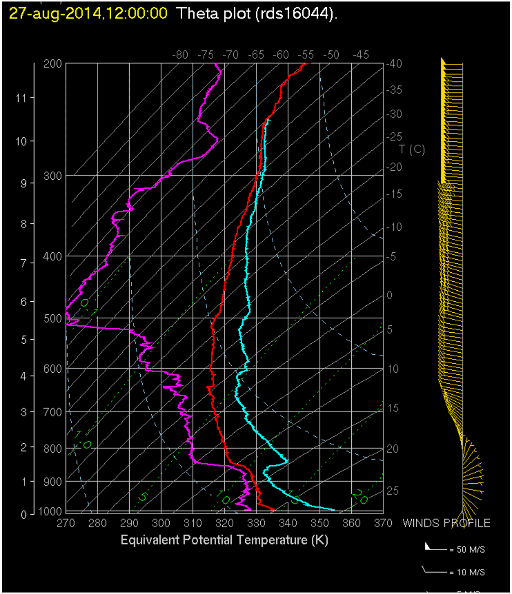

Since Θ_e is conserved along the whole process, the Lifted Parcel Theory on a Thetaplot means simply to draw a vertical line starting from the initial parcel Θ_e, that fixes everything else.

The Lifted Parcel Theory on a Theta-plot

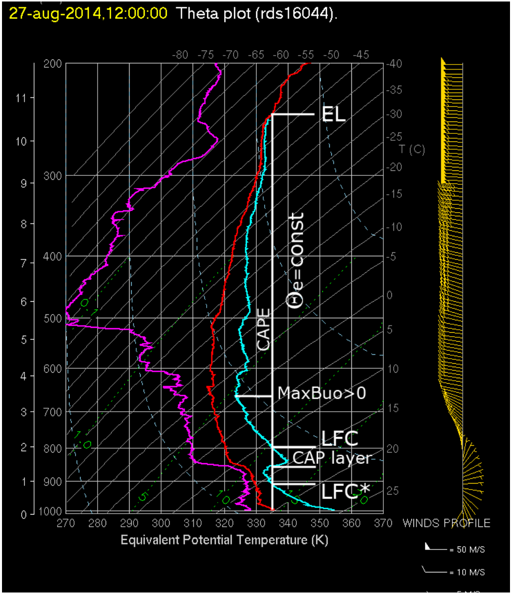

Since Θ_e is conserved along the whole process, the Lifted Parcel Theory on a Thetaplot means simply to draw a vertical line starting from the initial parcel Θ_e, that fixes everything else.

In this case there is a first LFC*, followed by a *capping layer*, **CAP**. In this case, it is an *inversion*, but in general it is sufficient to have a layer where $\mathrm{d}\boldsymbol{\Theta}_{\mathbf{es}}/\mathrm{d}\mathbf{z} > \mathbf{0}$ and not also $\mathrm{d}T/\mathrm{d}z > 0$, because an increase of Θ_{es} with z can already stop the rising parcel.

The Lifted Parcel Theory on a Theta-plot

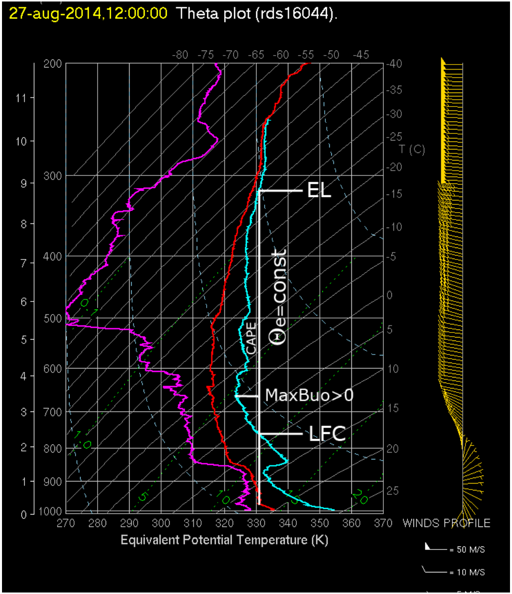

Choosing another *initial parcel* means simply to start from a different Θ_e and to draw another vertical line. It is immediate to see how LFC and EL change and how much are reduced the CAPE energy and the MaxBuo.

The Lifted Parcel Theory on a Theta-plot

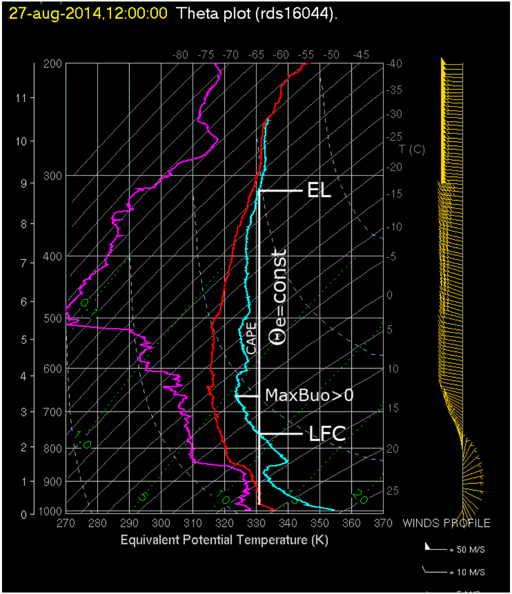

Choosing another *initial parcel* means simply to start from a different Θ_e and to draw another vertical line. It is immediate to see how LFC and EL change and how much are reduced the CAPE energy and the MaxBuo.

On the Thetaplot the *Most Unstable Parcel* (MUP) is simply identified as the level (or thin *layer*) having the maximum Θ_e in the low levels. The choice of the initial parcel determines everything in the adiabatic lifting.

A potentially *stable* sounding having $d\Theta_e/dz < 0$

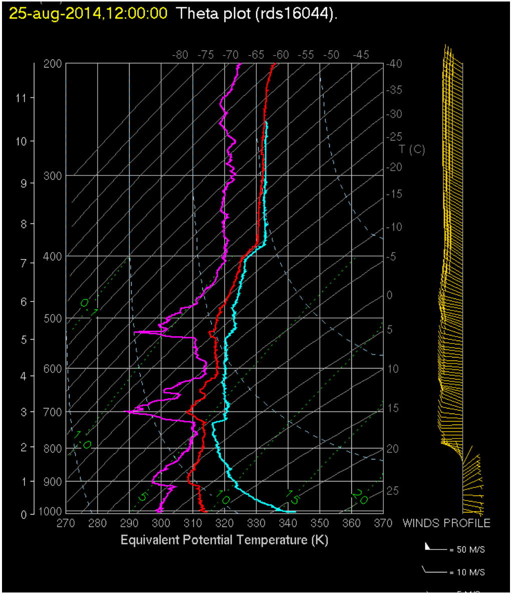

If Θ_e is always lower than Θ_{es} then it is not possible to find a LFC, hence CAPE $= 0$ and MaxBuo< 0. It is better to have a variable defined even for stable soundings (like MaxBuo or LI) than a *bounded* variable like CAPE.

A potentially *stable* sounding having $\mathrm{d}\Theta_e/\mathrm{d}z < 0$

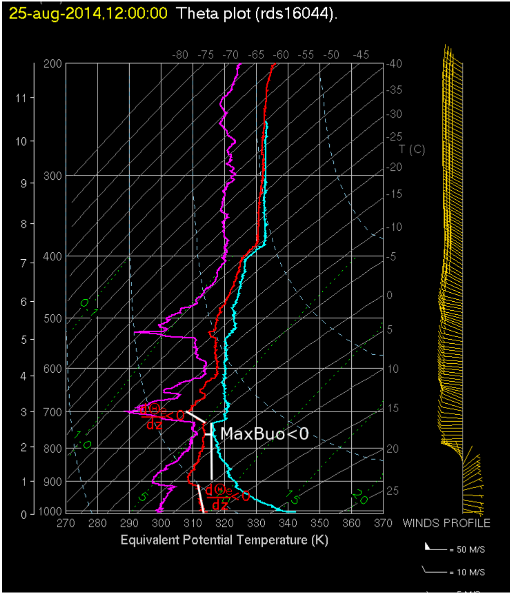

If Θ_e is always lower than Θ_{es} above, then it is not possible to find a LFC, hence CAPE $= 0$ and MaxBuo< 0.
It is better to have a variable defined even for stable soundings (like MaxBuo or LI) than a *bounded* variable like CAPE.
Note that the fact that in this example there are two layers with $\mathrm{d}\Theta_e/\mathrm{d}z < 0$ have no influences on the *potential* instability.

Importance of low-levels Θ_e and of initial parcel choice

- The fact that the identification of the initial parcel fixes its Θ_e value means that all the rest of the pseudo-adiabatic lifting is determined by that single value.

Importance of low-levels Θ_e and of initial parcel choice

- The fact that the identification of the initial parcel fixes its Θ_e value means that all the rest of the pseudo-adiabatic lifting is determined by that single value.
- After that the –conserved– Θ_e value of the initial parcel is chosen, all its buoyancy and derived indices (LFC, EL, CAPE, CIN, MaxBuo, LI,. . .) will *depend only by the Θ_{es} profile above it*, hence by the environmental *temperature* alone, not by its *humidity* profile.

Importance of low-levels Θ_e and of initial parcel choice

- The fact that the identification of the initial parcel fixes its Θ_e value means that all the rest of the pseudo-adiabatic lifting is determined by that single value.
- After that the –conserved– Θ_e value of the initial parcel is chosen, all its buoyancy and derived indices (LFC, EL, CAPE, CIN, MaxBuo, LI,...) will *depend only by the* Θ_{es} *profile above it*, hence by the environmental *temperature* alone, not by its *humidity* profile.
- The environmental humidity is particularly important in the *lowest levels*, where the initial parcel is chosen, because the initial Θ_e value strongly depends on it, but it is not important (from the point of view of the parcel buoyancy) above the level where the initial parcel is taken.

Importance of low-levels Θ_e and of initial parcel choice

- The fact that the identification of the initial parcel fixes its Θ_e value means that all the rest of the pseudo-adiabatic lifting is determined by that single value.
- After that the –conserved– Θ_e value of the initial parcel is chosen, all its buoyancy and derived indices (LFC, EL, CAPE, CIN, MaxBuo, LI,. . .) will *depend only by the* Θ_{es} *profile above it*, hence by the environmental *temperature* alone, not by its *humidity* profile.
- The environmental humidity is particularly important in the *lowest levels*, where the initial parcel is chosen, because the initial Θ_e value strongly depends on it, but it is not important (from the point of view of the parcel buoyancy) above the level where the initial parcel is taken.
- All that is true when buoyancy is computed using the normal temperature. If the virtual correction is used, then there is a –*very small*– influence of the environmental humidity profile even above the initial parcel level.

Skew-T vs. Theta-plot

1. The skew-T is widely used, so there are many software to compute it.

Skew-T vs. Theta-plot

1. The skew-T is widely used, so there are many software to compute it.
2. The area in the skew-T are proportional to the real energy, so the CAPE/CIN "areas" are perfectly proportional to their values. That is not true on the Theta-plot, but presently these values are computed via software's.

Skew-T vs. Theta-plot

1. The skew-T is widely used, so there are many software to compute it.
2. The area in the skew-T are proportional to the real energy, so the CAPE/CIN "areas" are perfectly proportional to their values. That is not true on the Theta-plot, but presently these values are computed via software's.
3. The Theta-plot show also Θ_e, that is probably the single most useful variable in meteorology, because it is conserved under many processes.

Skew-T vs. Theta-plot

1. The skew-T is widely used, so there are many software to compute it.
2. The area in the skew-T are proportional to the real energy, so the CAPE/CIN "areas" are perfectly proportional to their values. That is not true on the Theta-plot, but presently these values are computed via software's.
3. The Theta-plot show also Θ_e, that is probably the single most useful variable in meteorology, because it is conserved under many processes.
4. On the Theta-plot it is very easy to identify if an initial parcel has a LFC (unstable sounding) or not, just lifting it along a vertical line.

Skew-T vs. Theta-plot

1. The skew-T is widely used, so there are many software to compute it.
2. The area in the skew-T are proportional to the real energy, so the CAPE/CIN "areas" are perfectly proportional to their values. That is not true on the Theta-plot, but presently these values are computed via software's.
3. The Theta-plot show also Θ_e, that is probably the single most useful variable in meteorology, because it is conserved under many processes.
4. On the Theta-plot it is very easy to identify if an initial parcel has a LFC (unstable sounding) or not, just lifting it along a vertical line.
5. For this reason on the Theta-plot it is obvious to identify the Most Unstable Parcel, i. e. that having the maximum Θ_e in the low levels. Instead, on the skew-T one have to apply the curved adiabat processes to many initial parcels and find the one that produces the maximum CAPE.

Skew-T vs. Theta-plot

1. The skew-T is widely used, so there are many software to compute it.
2. The area in the skew-T are proportional to the real energy, so the CAPE/CIN "areas" are perfectly proportional to their values. That is not true on the Theta-plot, but presently these values are computed via software's.
3. The Theta-plot show also Θ_e, that is probably the single most useful variable in meteorology, because it is conserved under many processes.
4. On the Theta-plot it is very easy to identify if an initial parcel has a LFC (unstable sounding) or not, just lifting it along a vertical line.
5. For this reason on the Theta-plot it is obvious to identify the Most Unstable Parcel, i. e. that having the maximum Θ_e in the low levels. Instead, on the skew-T one have to apply the curved adiabat processes to many initial parcels and find the one that produces the maximum CAPE.
6. The Theta-plot show also T_w and not only T and T_d.

Make your choice!

Section 4

Some sounding-derived indices and their properties

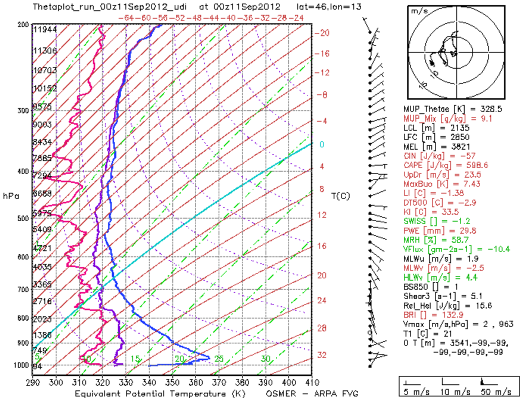

Data-mining: the human effort to simplify Nature

- A radiosounding is a very complex set of data describing the detailed thermodynamical and horizontal-wind structure of the atmospheric profile. For example, the Vaisala RS-92 sonde provides one observed level every one second. The nominal ascension velocity is about 4.4 m/s, so the troposphere is sampled in about 45 minutes (more than 2500 measured levels!), during which the horizontal winds can shift the sounding location of about 10-50 km.

Data-mining: the human effort to simplify Nature

- A radiosounding is a very complex set of data describing the detailed thermodynamical and horizontal-wind structure of the atmospheric profile. For example, the Vaisala RS-92 sonde provides one observed level every one second. The nominal ascension velocity is about 4.4 m/s, so the troposphere is sampled in about 45 minutes (more than 2500 measured levels!), during which the horizontal winds can shift the sounding location of about 10-50 km.
- All this information is condensed into the WMO TEMP format, that provides only *mandatory* levels (TTAA) and *significant* levels (TTBB) reducing the *vertical resolution* in troposphere to only $\sim$ 50 levels.

Data-mining: the human effort to simplify Nature

- A radiosounding is a very complex set of data describing the detailed thermodynamical and horizontal-wind structure of the atmospheric profile. For example, the Vaisala RS-92 sonde provides one observed level every one second. The nominal ascension velocity is about 4.4 m/s, so the troposphere is sampled in about 45 minutes (more than 2500 measured levels!), during which the horizontal winds can shift the sounding location of about 10-50 km.
- All this information is condensed into the WMO TEMP format, that provides only *mandatory* levels (TTAA) and *significant* levels (TTBB) reducing the *vertical resolution* in troposphere to only ~ 50 levels.
- Since the information is still "too large", people have invented many "indices" to reduce even more this "redundancy". Each of this indices try to investigate a particular characteristic of the sounding.

Data-mining: the human effort to simplify Nature

- A radiosounding is a very complex set of data describing the detailed thermodynamical and horizontal-wind structure of the atmospheric profile. For example, the Vaisala RS-92 sonde provides one observed level every one second. The nominal ascension velocity is about 4.4 m/s, so the troposphere is sampled in about 45 minutes (more than 2500 measured levels!), during which the horizontal winds can shift the sounding location of about 10-50 km.
- All this information is condensed into the WMO TEMP format, that provides only *mandatory* levels (TTAA) and *significant* levels (TTBB) reducing the *vertical resolution* in troposphere to only $\sim$ 50 levels.
- Since the information is still "too large", people have invented many "indices" to reduce even more this "redundancy". Each of this indices try to investigate a particular characteristic of the sounding.
- Manzato and Morgan (2003) and Manzato (2003) have presented the SOUND_ANALYS.PY software to compute $\sim$ 50 indices from a high-vertical resolution sounding.

Comparing the raw data with the GTS-TEMP format 1/3

20150704_12_Udine_original.txt - Blocco note

File Modifica Formato Visualizza ?

616 44 4604 1319 93 2015 0704 1100 J2923862 RS92-SGP

TIME	HEIGHT	PRESS	T	RH	Td	Wdir	Wspd	Code
0	93	10110	310	44	174	179	38	TUDFV
1	103	10099	304	45	172	178	38	TI
2	111	10090	300	46	171	178	39	TI
3	117	10084	297	46	168	177	39	TI
4	122	10077	294	45	164	177	39	100
5	128	10071	291	45	160	176	40	100
6	133	10065	289	45	159	175	40	100
7	138	10060	288	46	159	175	41	100
8	142	10055	287	46	161	174	41	T
9	147	10050	287	47	162	174	41	100
10	151	10045	286	47	163	173	41	100
11	155	10040	286	48	164	172	42	100
12	160	10034	286	48	165	172	42	100
13	165	10028	285	48	166	171	42	100
14	171	10023	284	49	166	171	42	100
15	175	10017	284	49	166	170	42	100
16	181	10011	283	49	166	169	42	100
17	187	10004	283	49	166	169	42	100
18	194	9996	282	49	166	168	42	100
19	202	9987	281	50	167	168	41	100
20	209	9979	281	50	167	167	41	100
21	216	9971	280	50	168	167	41	100
22	223	9964	280	51	168	167	40	100
23	229	9957	279	51	169	166	40	100
24	235	9950	279	51	169	166	39	100
25	241	9943	278	51	169	165	39	100
26	247	9936	278	51	169	165	39	200
27	253	9930	277	52	169	165	38	200
28	259	9923	276	52	168	164	38	200
29	266	9916	276	52	168	164	37	200
30	273	9908	275	52	169	164	36	200
31	280	9900	275	52	169	163	36	200
32	286	9893	274	53	169	163	35	200
33	292	9887	274	53	169	163	35	200
34	297	9880	273	53	169	162	34	200
35	303	9874	273	53	169	162	34	200
36	309	9867	272	53	169	161	33	200
37	315	9860	272	53	168	161	33	200
38	321	9854	271	53	168	160	32	200
39	327	9848	271	53	168	160	32	200
40	333	9841	270	54	169	159	31	200
41	338	9835	270	54	170	158	31	200
42	344	9829	270	54	171	158	30	200
43	349	9823	270	55	172	157	30	200
44	355	9817	270	55	172	156	29	200
45	361	9810	269	55	172	155	29	200
46	367	9803	269	55	171	154	28	200
47	373	9796	268	55	170	153	28	200
48	379	9790	267	55	170	151	27	200
49	385	9783	266	55	168	150	27	200
50	390	9777	265	55	166	149	26	200
51	395	9772	264	55	165	148	26	200
52	400	9767	263	55	165	147	25	200
53	405	9761	263	55	165	146	25	200

405 m

weather.uwyo.edu/cgi-bin/sounding?region=europe&TYPE=TEXT%3ALIST&YEAR=2015&MON

16044 LIPD Udine Observations at 12Z 04 Jul 2015

PRES hPa	HGHT m	TEMP C	DWPT C	RELH %	MIXR g/kg	DRCT deg	SKNT knot	THTA K	THTE K	THTV K
1011.0	94	31.0	17.0	43	12.20	180	7	303.2	339.7	305.4
1005.0	147	28.6	15.6	45	11.21	175	8	301.3	334.6	303.4
1000.0	191	28.2	16.2	48	11.71	170	8	301.4	336.1	303.5
925.0	876	21.6	15.6	69	12.19	165	8	301.4	337.5	303.6
868.0	1425	17.2	12.3	73	10.46	297	3	302.3	333.6	304.2
865.0	1454	17.6	11.6	68	10.01	304	2	303.1	333.1	304.9
850.0	1604	16.8	9.8	63	9.02	340	1	303.7	331.0	305.4
837.0	1735	16.2	8.2	59	8.21	344	3	304.4	329.4	305.9
809.0	2025	17.2	2.2	37	5.57	352	7	308.5	326.0	309.5
781.0	2323	15.2	-0.2	35	4.84	0	12	309.4	324.8	310.3
744.0	2734	12.4	-3.6	33	3.96	4	16	310.7	323.5	311.5
700.0	3241	8.6	-15.4	17	1.66	10	22	312.0	317.6	312.3
681.0	3463	6.8	-17.6	16	1.42	10	24	312.5	317.4	312.8
659.0	3728	4.8	-20.1	14	1.18	15	22	313.1	317.2	313.3
624.0	4168	1.3	-24.4	13	0.85	0	14	314.1	317.1	314.2
595.0	4552	-1.7	-28.1	11	0.64	15	18	314.9	317.1	315.0
573.0	4856	-4.1	-31.1	10	0.50	3	20	315.4	317.3	315.6
558.0	5064	-4.9	-40.5	4	0.20	355	22	316.9	317.7	316.9
547.0	5220	-5.5	-47.6	2	0.10	10	23	318.0	318.4	318.0
537.0	5365	-6.1	-54.1	1	0.05	7	22	319.0	319.2	319.0
509.0	5781	-8.5	-55.8	1	0.04	0	20	321.0	321.1	321.0
500.0	5920	-9.3	-56.3	1	0.04	5	19	321.6	321.8	321.6
498.0	5951	-9.3	-53.3	1	0.05	7	19	322.0	322.2	322.0
485.0	6152	-11.1	-50.2	2	0.08	20	19	322.2	322.6	322.3
432.0	7031	-18.9	-36.9	19	0.38	1	22	323.1	324.6	323.2
418.0	7275	-20.8	-33.0	33	0.57	355	23	323.8	325.9	323.9
406.0	7491	-22.5	-29.5	53	0.82	358	22	324.3	327.3	324.4
400.0	7600	-23.1	-32.1	44	0.65	0	21	324.9	327.3	325.0
397.0	7655	-23.5	-38.5	24	0.35	0	21	325.1	326.4	325.1
384.0	7897	-25.3	-40.3	23	0.30	0	21	325.8	327.0	325.9
333.0	8909	-33.9	-42.9	40	0.26	0	21	327.6	328.6	327.6
326.0	9057	-34.9	-47.9	25	0.15	0	21	328.2	328.8	328.2
317.0	9251	-36.3	-43.3	48	0.26	0	21	328.9	329.9	328.9
308.0	9450	-37.5	-53.5	17	0.09	0	21	329.9	330.3	329.9
300.0	9630	-38.9	-53.9	19	0.08	0	21	330.4	330.8	330.4
293.0	9792	-40.3	-58.3	13	0.05	2	23	330.7	330.9	330.7
281.0	10077	-42.5	-67.5	5	0.02	5	26	331.5	331.6	331.5
280.0	10101	-42.7	-67.2	5	0.02	5	26	331.6	331.6	331.6
252.0	10807	-48.3	-59.3	27	0.05	10	14	333.4	333.6	333.4
250.0	10860	-48.7	-58.7	30	0.06	10	14	333.5	333.8	333.5
247.0	10939	-49.1	-59.1	30	0.05	7	14	334.1	334.3	334.1
227.0	11486	-52.9	-66.9	17	0.02	343	12	336.4	336.5	336.4
217.0	11774	-55.5	-63.5	36	0.03	330	11	336.8	336.9	336.8

11774 m

The first ∼ 50 levels in a RAW sounding (left) or TEMP format (right).

Comparing the raw data with the GTS-TEMP format 2/3

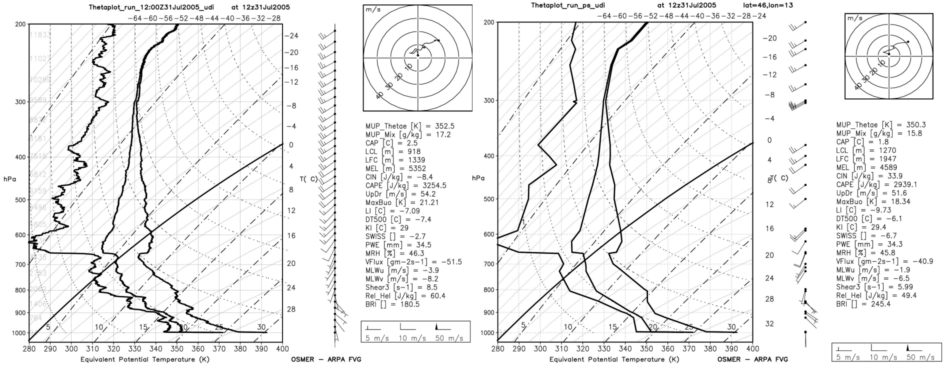

Thetaplot diagram from a RAW sounding (left) or TEMP format (right). The main features are preserved but many high resolution details, in particular in the low–levels, are smoothed away and that change the value of sounding–derived indices.

Comparing the raw data with the GTS-TEMP format 3/3

Manzato (2008) have done a comparison among 40 sounding–derived indices computed from RAW and TEMP formats (and also ECMWF pseudo–sounding forecasted indices), finding R^2 between 0.6 and 1.0, but for the Shear in the lowest 3 km, which had a very low correlation.

TABLE 2. As in Table 1 but comparing observed soundings in raw and TEMP formats at 1200 UTC. Examples with $R^2 \geq 0.5$ are highlighted in boldface.

Rank	Index	R^2	a	b	Bias	RMSE	RAE	No. of cases
1	PWE (mm)	**0.99**	1.00	0.1	−0.1	0.7	0.03	550
2	KI (°C)	**0.99**	0.98	0.3	−0.1	1.2	0.07	547
3	Thetae (K)	**0.99**	0.99	4.2	−1	1.6	0.08	546
4	MRH (%)	**0.99**	0.99	−0.06	0.6	1.8	0.09	540
5	LRH (%)	**0.98**	0.98	0.5	0.4	2.6	0.12	546
6	MLWv (m s^{-1})	**0.97**	1.09	0.06	−0.08	1.0	0.18	546
7	MLWu (m s^{-1})	**0.96**	1.04	−0.1	0.2	1.0	0.17	546
8	Mix (g kg^{-1})	**0.96**	1.06	−0.2	−0.2	0.8	0.16	546
9	WBZ (m)	**0.96**	0.92	−22	210	319	0.23	550
10	PWC (mm)	**0.96**	1.08	0.6	−1.3	3.6	0.13	546
11	CAPE (J kg^{-1})	**0.95**	1.13	16	−34	105	0.17	550
12	DT500 (°C)	**0.95**	0.93	−0.3	0.5	1.2	0.20	545
13	SWEAT	**0.95**	0.96	2.5	−0.2	12.7	0.13	546
14	HD (cm)	**0.94**	1.11	0.09	−0.19	0.6	0.17	546
15	VFlux (kg s^{-1} m^{-2})	**0.94**	1.00	0.0001	−0.0001	0.004	0.22	545
16	UpDr (m s^{-1})	**0.94**	1.05	0.7	−1	3.1	0.15	546
17	EL (m)	**0.93**	1.00	295	−265	891	0.15	255
18	Tbase (°C)	**0.93**	1.04	0.1	−0.2	3.4	0.20	546
19	MaxBuo (K)	**0.92**	0.88	1.3	−1.6	2.4	0.37	546
20	DTC (°C)	**0.92**	0.94	−0.2	0.3	1	0.26	456
21	LLWu (m s^{-1})	**0.92**	1.08	0.3	−0.4	1	0.31	442
22	|VFlux| (kg s^{-1} m^{-2})	**0.91**	0.99	0.0003	−0.0001	0.004	0.29	545
23	b_PBL (cm s^{-2})	**0.90**	1.03	0.02	−0.02	0.1	0.27	546
24	MLWspd (m s^{-1})	**0.90**	1.09	−0.09	−0.44	1.25	0.31	546
25	SWISS	**0.87**	0.85	−0.9	1.5	2.7	0.43	392
26	LLWspd (m s^{-1})	**0.87**	1.06	0.4	−0.6	1.1	0.43	442
27	Rel_Hel (m^2 s^{-2})	**0.87**	1.16	4.5	−10.6	29.7	0.37	545
28	LI (°C)	**0.86**	0.82	0.5	−0.1	1.7	0.36	546
29	LLWv (m s^{-1})	**0.84**	1.09	−0.05	0.11	0.99	0.42	442
30	ShowI (°C)	**0.81**	0.83	0.8	0.2	1.7	0.36	546
31	MEL (m)	**0.80**	0.87	711	−380	585	0.53	546
32	Hel (J kg^{-1})	**0.80**	1.06	2.3	−3.4	30.2	0.41	546
33	LCL (m)	**0.77**	1.03	−31	−28	549	0.36	546
34	BRI	**0.74**	1.11	0.04	−1.4	24.2	0.26	501
35	CAP (°C)	**0.74**	0.65	1.2	1	3.3	0.60	510
36	EHI	**0.71**	0.91	0.02	−0.02	0.09	0.27	549
37	CIN (J kg^{-1})	**0.70**	0.82	−63	−29	300	0.33	550
38	h_MUP (m)	**0.65**	1.06	−164	95	564	0.46	546
39	LFC (m)	**0.59**	0.70	43	815	1030	1.24	255
40	Shear3 (s^{-1})	0.15	0.48	0.008	−0.005	0.006	1.42	546

Different type of sounding-derived indices

From a sounding it is possible to derive three types of information:

Different type of sounding-derived indices

From a sounding it is possible to derive three types of information:

1. *Environmental indices* (that do not need to apply the Lifted Parcel Theory). Very commonly used are: K-index, Precipitable Water (PWE), mean relative humidity of a layer, mean wind of a layer, Shear, Helicity…

Different type of sounding-derived indices

From a sounding it is possible to derive three types of information:

1. *Environmental indices* (that do not need to apply the Lifted Parcel Theory). Very commonly used are: K-index, Precipitable Water (PWE), mean relative humidity of a layer, mean wind of a layer, Shear, Helicity...
2. Indices that are computed based on the Lifted Parcel Theory and hence strongly depends on the choice of the initial parcel (initial Θ_e) and on the details observed in the low-levels. Very commonly used *instability indices* are: LCL height or temperature, Showalter or Lifted Index, CAPE, CIN, updraft velocity, MaxBuo...

Different type of sounding-derived indices

From a sounding it is possible to derive three types of information:

1. *Environmental indices* (that do not need to apply the Lifted Parcel Theory). Very commonly used are: K-index, Precipitable Water (PWE), mean relative humidity of a layer, mean wind of a layer, Shear, Helicity...
2. Indices that are computed based on the Lifted Parcel Theory and hence strongly depends on the choice of the initial parcel (initial Θ_e) and on the details observed in the low-levels. Very commonly used *instability indices* are: LCL height or temperature, Showalter or Lifted Index, CAPE, CIN, updraft velocity, MaxBuo...
3. *Mixed indices*, which typically uses instability indices together with wind information. Very commonly used are: Energy-Helicity Index (EHI), SWEAT, SWISS...

We will see only a few of them!

K–Index and its 1995-2002 distribution above Udine

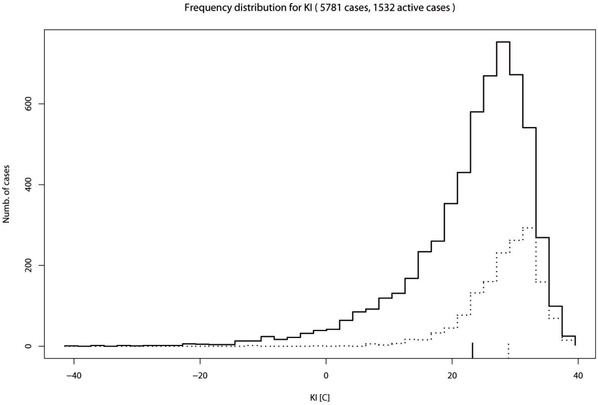

One of the oldest indices is the K–Index (George, 1960). The dot line is the sub-sample for soundings associated with convective activity in the FVG plain in the 6 hours after launch (1995-2002). Values above 25 are often associated with lightning occurrences.

K–Index and its 1995-2002 distribution above Udine

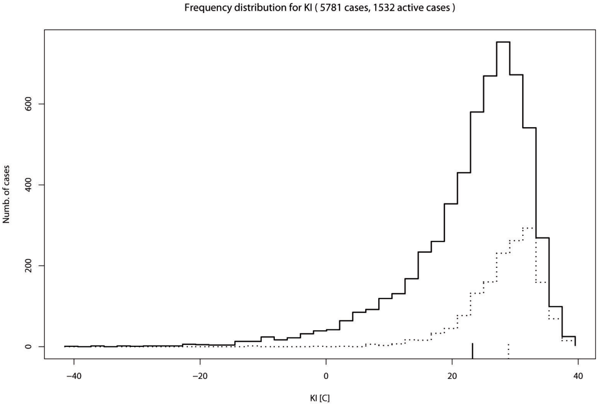

One of the oldest indices is the K–Index (George, 1960). The dot line is the sub-sample for soundings associated with convective activity in the FVG plain in the 6 hours after launch (1995-2002). Values above 25 are often associated with lightning occurrences.

$$\mathrm{KI} = T_{@850} - T_{@500} + T_{d\,@850} - (T_{@700} - T_{d\,@700}). \qquad (17)$$

KI is defined using only environmental temperature and dew-point depressure on three mandatory levels. Even if very simple, it is also correlated to rainfall intensity.

"Two-levels" potential instability family

- *Showalter* (1953) was the first to use the difference of temperature between the lifted parcel and the environmental air at 500 hPa:

$$\mathrm{ShowI} = T_{e\,@500} - T_{p\,@500} \qquad [K] \tag{18}$$

Showalter used as initial parcel the mean air at 850 hPa.

"Two-levels" potential instability family

- *Showalter* (1953) was the first to use the difference of temperature between the lifted parcel and the environmental air at 500 hPa:

$$\mathrm{ShowI} = T_{e\,@500} - T_{p\,@500} \qquad [K] \tag{18}$$

  Showalter used as initial parcel the mean air at 850 hPa.

- Galway (1956) defined the *Lifted Index* (LI) in the same way, but using as initial parcel the mean air of the lowest 500 m.

"Two-levels" potential instability family

- *Showalter* (1953) was the first to use the difference of temperature between the lifted parcel and the environmental air at 500 hPa:

$$\mathrm{ShowI} = T_{e\,@500} - T_{p\,@500} \qquad [K] \tag{18}$$

  Showalter used as initial parcel the mean air at 850 hPa.
- Galway (1956) defined the *Lifted Index* (LI) in the same way, but using as initial parcel the mean air of the lowest 500 m.
- Nowadays the most used "lifted index" is the one using as initial parcel the Most Unstable Parcel ($\max \Theta_e$), called DT500 in Manzato (2003) or MULI by many authors.

"Two-levels" potential instability family

- *Showalter* (1953) was the first to use the difference of temperature between the lifted parcel and the environmental air at 500 hPa:

$$\mathrm{ShowI} = T_{e\,@500} - T_{p\,@500} \qquad [K] \tag{18}$$

  Showalter used as initial parcel the mean air at 850 hPa.
- Galway (1956) defined the *Lifted Index* (LI) in the same way, but using as initial parcel the mean air of the lowest 500 m.
- Nowadays the most used "lifted index" is the one using as initial parcel the Most Unstable Parcel ($\max \Theta_e$), called DT500 in Manzato (2003) or MULI by many authors.
- Manzato (2003) introduced also the temperature difference between environment and lifted parcel evaluated at a fixed *parcel temperature* (chosen at -15°C) instead than to a fixed pressure level (500 hPa). It was called Difference of Temperature at the Core Level (DTC).

1995-2002 distribution of the Udine MULI (called DT500)

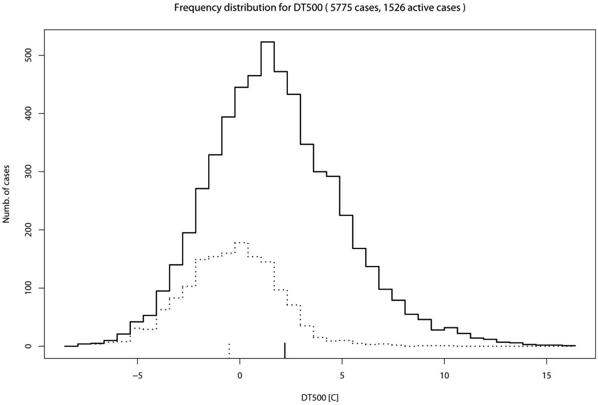

The dot distribution is the sub-sample for soundings associated with convective activity in the FVG plain in the 6 hours after launch (1995-2002). *Low* ($< +2^oC$) or *negative* values are associated with lightning occurrences.

1995-2002 distribution of the Udine MULI (called DT500)

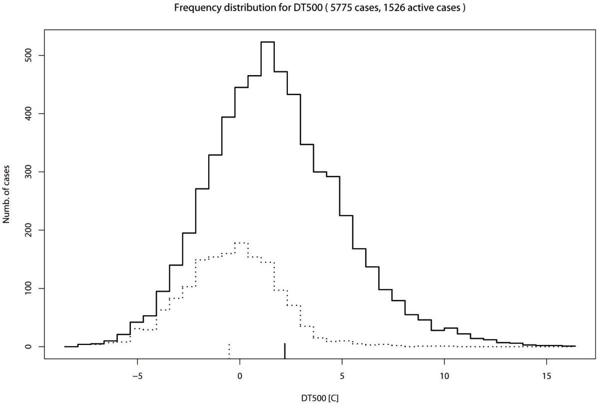

The dot distribution is the sub-sample for soundings associated with convective activity in the FVG plain in the 6 hours after launch (1995-2002). *Low* ($< +2^{o}$C) or *negative* values are associated with lightning occurrences.

At least in Europe, there are a number of evidences where the Most Unstable Lifted Index gives better *statistical performances* when forecasting convection (lightnings or hail or storm occurrences) than CAPE, which is a bounded variable. References includes Manzato (2003), Groenemeijer & van Delden (2007), Kunz (2007), Ukkonen et al. (2017), ...

1995-2002 distribution of the Udine CAPE and CIN

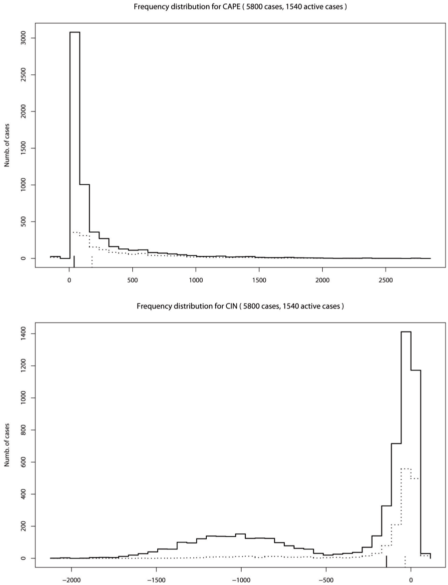

Differently from the "two-level" instability indices (which includes also MaxBuo), CAPE and CIN are *integrated* measures of buoyancy (positive for CAPE and negative for CIN). Note that SOUND_ANALYS.PY computes the maximum UpDr velocity using CAPE integrated only up to the parcel level of -15°C, instead than up to EL.

1995-2002 distribution of the Udine CAPE and CIN

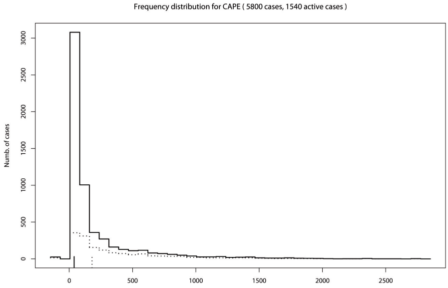

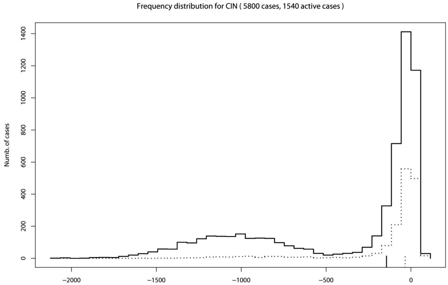

Differently from the “two-level” instability indices (which includes also MaxBuo), CAPE and CIN are *integrated* measures of buoyancy (positive for CAPE and negative for CIN). Note that SOUND_ANALYS.PY computes the maximum UpDr velocity using CAPE integrated only up to the parcel level of -15^{o}C, instead than up to EL. CAPE distribution is not much discriminating the convective cases...
Convective events in the FVG plain can have also CIN< -100 J/kg.

Maximum Buoyancy and Downdraft Potential

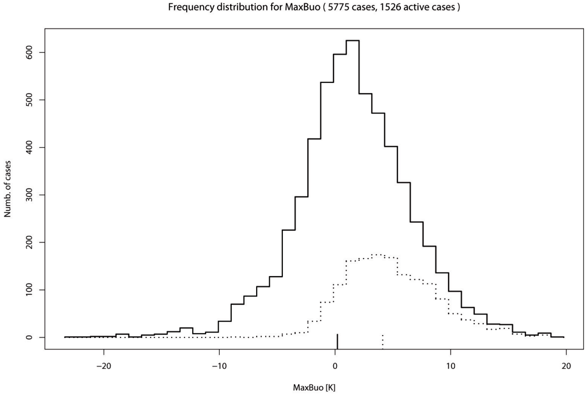

Storms are more likely when MaxBuo> -2K. Morgan and Tuttle (1984) defined MaxBuo but also other indices, like the difference between the maximum Θ_{es} in the low levels and the minimum Θ_e in the mid levels, called *Downdraft Potential*. **DownPot**$=$ $Max(\Theta_{es}|_{low}) - Min(\Theta_e|_{mid})$.

Maximum Buoyancy and Downdraft Potential

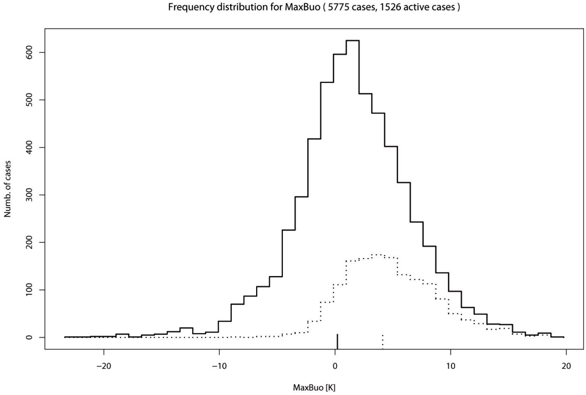

Storms are more likely when MaxBuo> -2K. Morgan and Tuttle (1984) defined MaxBuo but also other indices, like the difference between the maximum Θ_{es} in the low levels and the minimum Θ_e in the mid levels, called *Downdraft Potential*. **DownPot**$=$ $Max(\Theta_{es}|_{low}) - Min(\Theta_e|_{mid})$.

Physical meaning: the coolest and more dry air in the middle troposphere $[Min(\Theta_e|_{mid})]$ is supposed to saturate by rainfall evaporation and hence is brought down along a saturated pseudo-adiabat (Θ_e is conserved). The maximum thermal contrast (generating the outflow wind) will happen at the low level where Θ_{es} is maxima. It tries to estimate the *downdraft negative buoyancy*.

Wind hodograph and shear

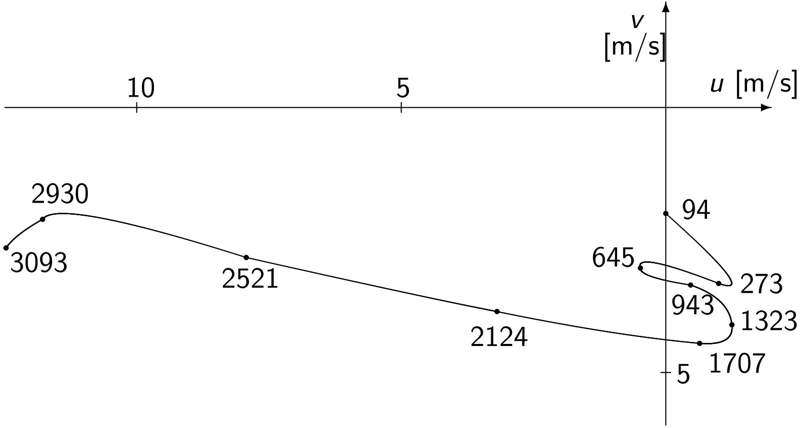

Wind hodograph and shear

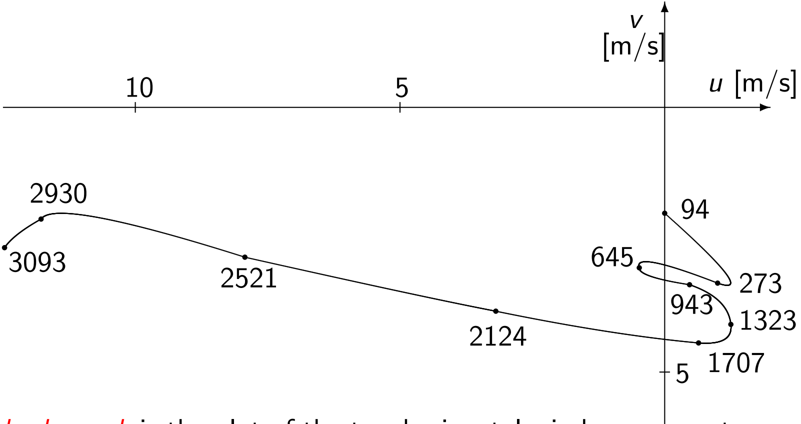

The *hodograph* is the plot of the two horizontal wind components u and v. Low level *veering* favors uplift. The hodograph path length is called Shear.

$$\textbf{Shear} = \frac{\int_{z_0}^{z_N} \left\| \frac{\partial \vec{W}}{\partial z} \right\| \cdot \mathrm{d}z}{z_N - z_0} \cong \frac{\sum_1^N \sqrt{(u_n - u_{n-1})^2 + (v_n - v_{n-1})^2}}{z_N - z_0} \tag{19}$$

Bulk shear

- Shear is usually computed from surface up to 6 or from surface up to troposphere (about 12 km).

Bulk shear

- Shear is usually computed from surface up to 6 or from surface up to troposphere (about 12 km).
- Very often the shear is confused with the Bulk Shear, that is simply the magnitude of the vectorial difference between two winds at two different levels: BS$=\sqrt{(u_2-u_1)^2+(v_2-v_1)^2}$.

Bulk shear

- Shear is usually computed from surface up to 6 or from surface up to troposphere (about 12 km).
- Very often the shear is confused with the Bulk Shear, that is simply the magnitude of the vectorial difference between two winds at two different levels: BS= $\sqrt{(u_2 - u_1)^2 + (v_2 - v_1)^2}$.
- The most used levels for the BS are: sfc vs. 1 km, sfc vs. 850 hPa, sfc. vs. 3 km, sfc. vs. 5 km, 1 km vs. 3 km, 1 km vs. 6 km...

Bulk shear

- Shear is usually computed from surface up to 6 or from surface up to troposphere (about 12 km).
- Very often the shear is confused with the Bulk Shear, that is simply the magnitude of the vectorial difference between two winds at two different levels: BS$=\sqrt{(u_2-u_1)^2+(v_2-v_1)^2}$.
- The most used levels for the BS are: sfc vs. 1 km, sfc vs. 850 hPa, sfc. vs. 3 km, sfc. vs. 5 km, 1 km vs. 3 km, 1 km vs. 6 km...
- For example, the Bulk Richardson Number is defined as 2 times CAPE divided by the square of the bulk shear between 6 km and 500 m: **BRN**$=2\frac{\mathrm{CAPE}}{BS_{BRI}{}^2}$.

Bulk shear

- Shear is usually computed from surface up to 6 or from surface up to troposphere (about 12 km).
- Very often the shear is confused with the Bulk Shear, that is simply the magnitude of the vectorial difference between two winds at two different levels: BS$=\sqrt{(u_2-u_1)^2+(v_2-v_1)^2}$.
- The most used levels for the BS are: sfc vs. 1 km, sfc vs. 850 hPa, sfc. vs. 3 km, sfc. vs. 5 km, 1 km vs. 3 km, 1 km vs. 6 km...
- For example, the Bulk Richardson Number is defined as 2 times CAPE divided by the square of the bulk shear between 6 km and 500 m: **BRN**$= 2\frac{\mathrm{CAPE}}{{BS_{BRI}}^2}$.
- In very complex orography terrains, like northern Italy, it is not obvious that shear will have the same importance in governing storm organization (single cell, multicell, squall lines) as it has been found in the US's plains, because of representativeness of RDS-derived shear compared with the real interaction between winds and complex orography...

Storm–Relative Helicity

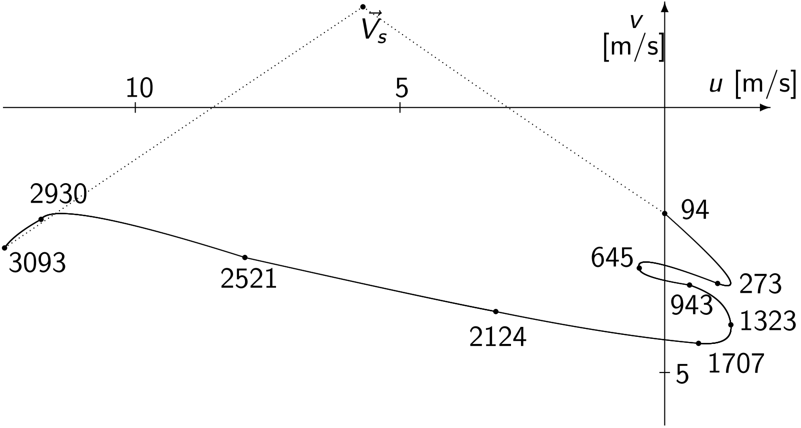

Storm–Relative Helicity

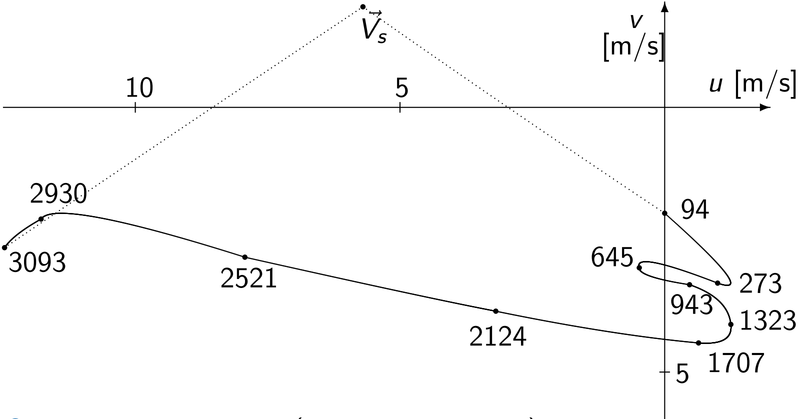

The *Storm-Relative Helicity* (Davies-Jones 1990) is the area between the *storm-velocity vector*, V_s, and the hodograph. Usually integrated up to 3 km.

$$\mathbf{SRH} = -\int_{z_0}^{z_N} \vec{k}\cdot(\vec{W}-\vec{V_s})\times\frac{\partial\vec{W}}{\partial z}\cdot \mathrm{d}z \cong -\sum_{1}^{N}(u_n-u_s)(v_n-v_{n-1})-(u_n-u_{n-1})(v_n-v_s) \qquad (20)$$

Should be useful for supercells and tornadogenesis.

Water Vapor Flux in the lowest 3 km

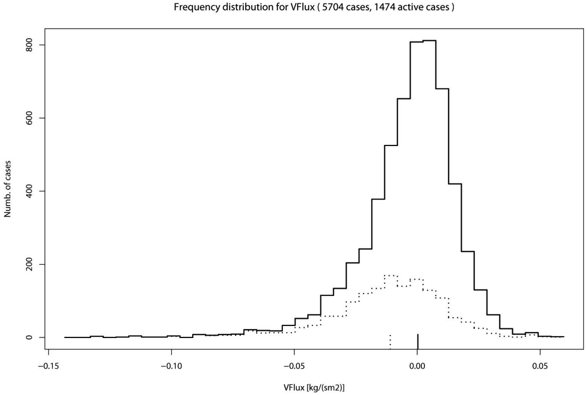

In FVG (Adriatic Sea on the South and Alps on the North) we have found to be very useful the *water vapor flux* in the lowest 3 km:

$$\mathbf{VFlux} = \frac{1}{N} \cdot \sum_{z_0}^{z_N} \rho_{v\,n} \cdot v_n \tag{21}$$

where v is the meridional wind component.

Water Vapor Flux in the lowest 3 km

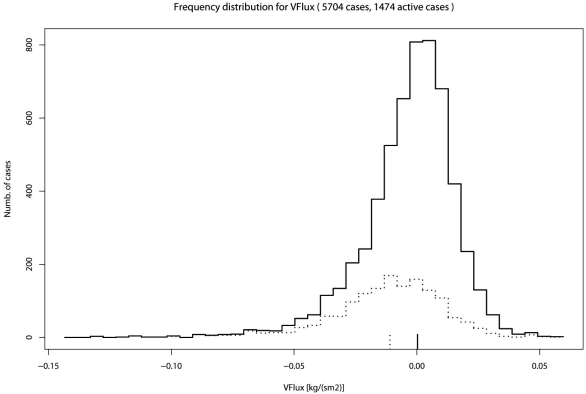

In FVG (Adriatic Sea on the South and Alps on the North) we have found to be very useful the *water vapor flux* in the lowest 3 km:

$$\mathbf{VFlux} = \frac{1}{N} \cdot \sum_{z_0}^{z_N} \rho_{v\,n} \cdot v_n \tag{21}$$

where v is the meridional wind component.

Physical meaning: strong moist winds blowing from South (VFlux< 0) brings the “convective fuel” against the orographic barrier, producing convection triggered by orographic lifting or strong precipitating systems (especially in autumn). Useful in particular for heavy rainfall forecast.

Example of SOUND_ANALYS.PY output in a HTML page

SOUND_ANALYSIS RESULTS:

Year	Month	Day	Hour
1998	06	28	12

Udine Sounding (WMO code 16044, managed by the Italian Aeronautica Militare)

Index [5 : 95 percentils unit on all cases April-November 1995-2007]	T	Tv	Tvc
MUP ThetaE [296:336 K] Thetae	337.2	337.2	337.2
MUP Mixing Ratio [2.2:12.5 g/kg] Mix	12.4	12.4	12.4
MUP height [228:2434 m] h_MUP	271	271	271
Convective Available Potential Energy [0:923 J/kg] CAPE	1124.2	1243.1	1220.4
Convective Inhibition [-1385:-0.4 J/kg] CIN	-46.4	-14.7	-25.0
Tropopause height [9298:13611 m] Trop	12514	12514	12514
Cloud top [2279:11687 m] EL	11506	11464	11857
Lev. of Free Convection [925:4136 m] LFC	2932	2080	2608
Cloud base height [648:3553 m] LCL	1469	1469	1469
Cloud base temperature [-12.2:15.3 C] Tbase	14.5	14.4	14.4
Boundary Layer Top [313:4297m] PBL	752	752	752
Melting level [1720:4338 m] MEL	4402	4587	4312
Wet Bulb Zero [921:3590 m] WBZ	3421	3421	3421
Max Updraft velocity [0:29.3 m/s] UpDr	29.7	32.6	26.0
Max Hail diameter [0:4.8 cm] HD	5.0	6.0	3.8
Precip. Wat. Env. [9.1:36.4 mm] PWE	34.5	34.2	34.2
Precip. Wat. Cloud [0:44.5 mm] PWC	44.3	44.1	44.4
sfc-250hPa Low Rel. Humidity [38:91 %] LRH	64.1	64.1	64.1
sfc-500hPa Medium Rel. Humidity [31:88 %] MRH	58.7	58.7	58.7
500-300hPa High Rel. Humidity [11:71 %] HRH	22.5	22.5	22.5
CAP diff. theta_es [1.3:17.8 C] CAP	1.4	1.4	1.4
Low buo. accel. [-44:31cm/s2] b_PBL	-47.0	-47.0	-47.0
Downdraft Potential [3.5:52.4 K] DownPot	47.6	47.6	47.6
Maximum Buoyancy [-9.8:9.6 K] MaxBuo	10.33	10.33	10.33

Index	T	Tv	Tvc
Lifted Index 500m [-2.57:13.0 C] LI	-3.22	-3.74	-2.01
Diff. Temp. 500hPa [-3.3:9.4 C] DT500	-3.3	-3.81	-2.11
Diff. Temp. at -15 [-3.5:7.0 C] DTC	-2.89	-3.27	-2.76
Showalter Index [-1.0:11.7 C] ShowI	0.06	-0.28	0.8
Stabil. Wind Shear Index Switz.) [-4.3:15.9] SWISS	-3.2	-3.7	-2.0
Severe WEAth. Threat [7.4:186] SWEAT	129.5	129.5	129.5
K Index [-4.9:33.4 C] KI	28.7	28.7	28.7
Boyden Index [91.6:98.9] BOY	95.4	95.4	95.4
Vapour Flux [-41:20 gm-2s-1] VFlux	-31.7	-31.7	-31.7
U Low Lev. Wind [-2.7:7.6 m/s] LLWu	0.5	0.5	0.5
V Low Lev. Wind [-4.0:3.9 m/s] LLWv	-3.1	-3.1	-3.1
U Med. Lev. Wind [-10.3:5.7 m/s] MLWu	-7.6	-7.6	-7.6
V Med. Lev. Wind [-13.2:4.3 m/s] MLWv	-3.1	-3.1	-3.1
U High Lev. Wind [-31.3:9.9 m/s] HLWu	-23.9	-23.9	-23.9
V High Lev. Wind [-18.6:24.4 m/s] HLWv	-4.2	-4.2	-4.2
Low Level Jet (>15m/s) Depth [0:2776 m] LLJD	387	387	387
High Level Jet (>30m/s) Depth [0:4781 m] HLJD	0	0	0
Bulk Richardson Numb. [0:86] BRI	34.1	37.5	36.8
Bulk Shear sfc-850hPa [1.2:11.5 m/s] BS850	1.7	1.7	1.7
Shear * E-3 [4.0:14 s-1] Shear	4.6	4.6	4.6
Shear * E-3 [5.0:17 s-1] Shear3	0.0	0.0	0.0
Helicity [-55:127 J/kg] Hel	50.1	50.1	50.1
Storm Rel. Helicity [-18:187 J/kg] Rel_Hel	65.2	65.3	65.3
Energy-Hel. [-0.004:0.298 m4/s4] EHI	0.46	0.51	0.5
Radiosonde vertical vel. [3.78:5.53 m/s] VV	4.46	4.46	4.46
Stand. dev. vertical vel. [0.25:0.97 m/s] VVstd	0.39	0.39	0.39

Sounding Analysis results

Kelvin = Celsius + 273.15

See Thetaplot example for some variable definitions

See Sound_Analys.PY Handbook for more details

Developed by agostino.manzato@osmer.fvg.it

Another sounding

HOME

Just an example of the many indices computed by SOUND_ANALYS.PY (*freely* available upon request) for the Udine 1998/06/28 12 UTC sounding.

The three methods "T", "T_v" and T_{vc} are explained in Manzato and Morgan (2003).

Matrix of inter-correlations among sounding-derived indices

Manzato JAMC (2012) has studied the correlations among 52 indices derived from 1992–2009 00, 06, 12 and 18 UTC Udine soundings.

RDS-derived indices can be seen as a non-linear reduction of 3D observed atmosphere variables (p, T, RH, Θ_e, wind at many levels) into a set of highly intercorrelated parameters.

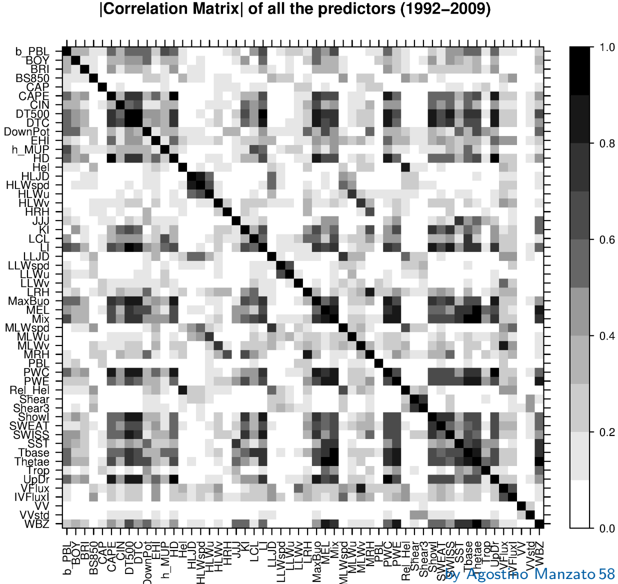

Results: 3 groups of indices inter-correlated (R$\geq$ 0.80)

1. Indices related to the most unstable parcel, like its equivalent potential temperature (Θ_e), its mixing ratio (Mix) and the height where its ascent temperature becomes 0 ^{o}C (MEL), or related to other environmental characteristics, like the height where the atmospheric wet bulb temperature becomes 0 ^{o}C (WBZ) and the precipitable water integrated along the entire atmospheric column (PWE).

Results: 3 groups of indices inter-correlated (R$\geq$ 0.80)

1. Indices related to the most unstable parcel, like its equivalent potential temperature (Θ_e), its mixing ratio (Mix) and the height where its ascent temperature becomes 0 ^{o}C (MEL), or related to other environmental characteristics, like the height where the atmospheric wet bulb temperature becomes 0 ^{o}C (WBZ) and the precipitable water integrated along the entire atmospheric column (PWE).
2. Indices of "two–levels" potential instability such as Lifted Index (Galway 1956), Showalter Index (Showalter 1953), DT500 and DTC (Manzato 2003), i. e. the "lifted index family". Also the Maximum Buoyancy (Morgan and Tuttle 1984, Manzato and Morgan 2003,) is very well related to three of these indices.

Results: 3 groups of indices inter-correlated (R$\geq$ 0.80)

1. Indices related to the most unstable parcel, like its equivalent potential temperature (Θ_e), its mixing ratio (Mix) and the height where its ascent temperature becomes 0 °C (MEL), or related to other environmental characteristics, like the height where the atmospheric wet bulb temperature becomes 0 °C (WBZ) and the precipitable water integrated along the entire atmospheric column (PWE).
2. Indices of "two–levels" potential instability such as Lifted Index (Galway 1956), Showalter Index (Showalter 1953), DT500 and DTC (Manzato 2003), i. e. the "lifted index family". Also the Maximum Buoyancy (Morgan and Tuttle 1984, Manzato and Morgan 2003,) is very well related to three of these indices.
3. Indices of "integrated" potential instability, i. e. maximum updraft velocity (UpDr), hail diameter (HD), CAPE and precipitable water integrated between LFC and the equilibrium level (PWC). MaxBuo is also well correlated with three of these indices.

High spatio-temporal variability of sounding-derived indices

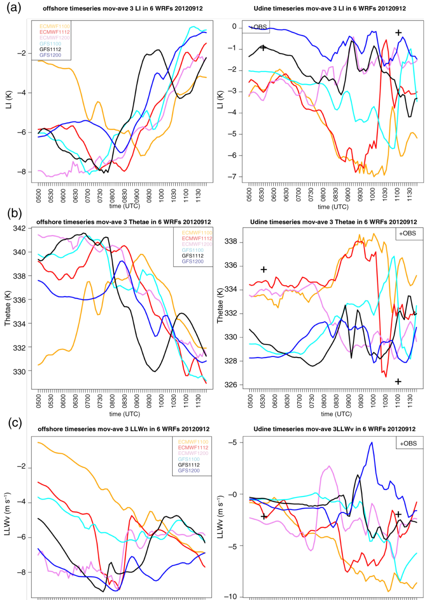

Miglietta et al. (2016) have shown how fast some instability indices can vary, using WRF simulations on the HyMeX case of 12 September 2012. Shown are the time-series of WRF-derived LI, MUP Θ_e and meridional component of Low-Level Wind (LLWv) above Udine (inland, on the right) and offshore (70 km southerly, on the left) every 5', but smoothed with 10'-moving average, for 6 different initial conditions.

High spatio-temporal variability of sounding-derived indices

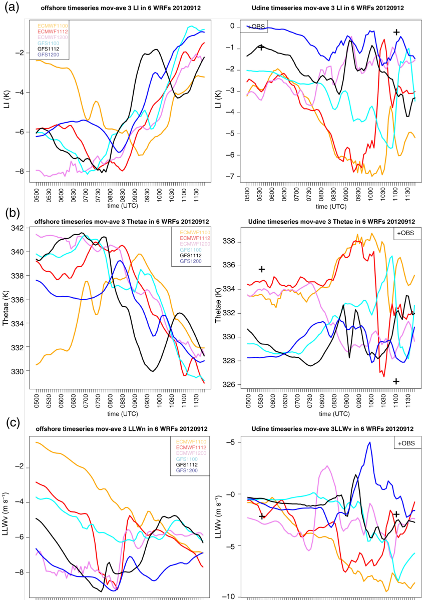

Miglietta et al. (2016) have shown how fast some instability indices can vary, using WRF simulations on the HyMeX case of 12 September 2012. Shown are the time-series of WRF-derived LI, MUP Θ_e and meridional component of Low-Level Wind (LLWv) above Udine (inland, on the right) and offshore (70 km southerly, on the left) every 5’, but smoothed with 10’-moving average, for 6 different initial conditions.
Note that the indices derived from real RDS (black crosses “+”) every 6 h can be quite far from simulations, e.g. Θ_e inland.

Obs. & WRF sim. convergence line for 12/09/12 supercell

A. Manzato et al. / Atmospheric Research 153 (2014) 98–118

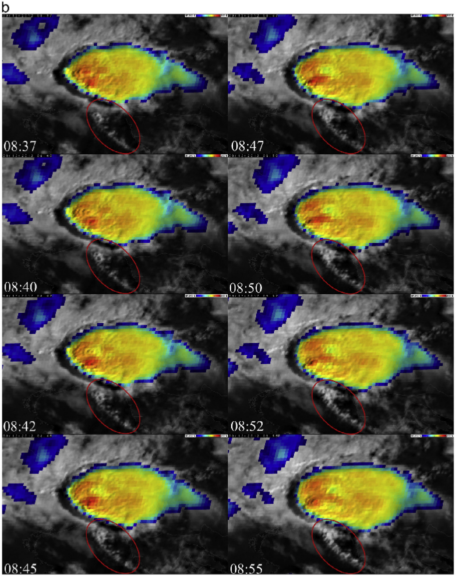

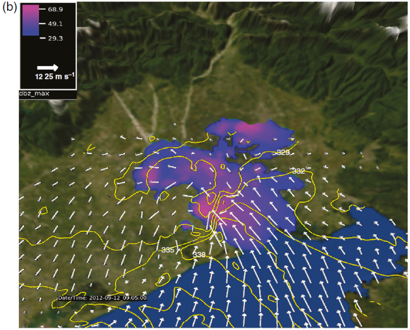

Figure 12. (b) Maximum reflectivity (shading; values below 30 dBZ are not shown), θ_e (contour interval 3 K; contours) and wind vectors at 100 m, simulated by the WRF model inner grid (GFS1112 run) at 0905 UTC 12 Septe

Miglietta et al. (2016) simulated the convergence line feeding supercell that was seen by MSG Super Rapid Scan (Manzato et al. 2015).

High spatiotemporal change MULI map (court. A. Pucillo)

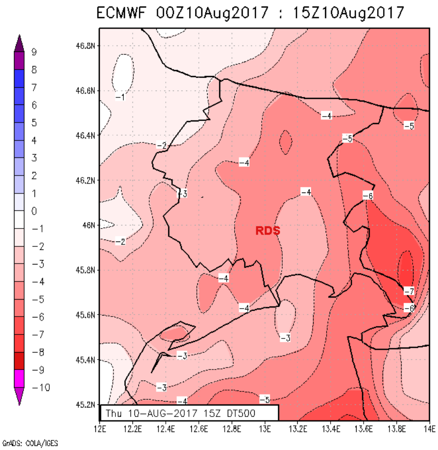

Ex. of MULI spatial variability derived by ECMWF pseudo-RDS: from -1 to -7 °C 100 km apart.

High spatiotemporal change MULI map (court. A. Pucillo)

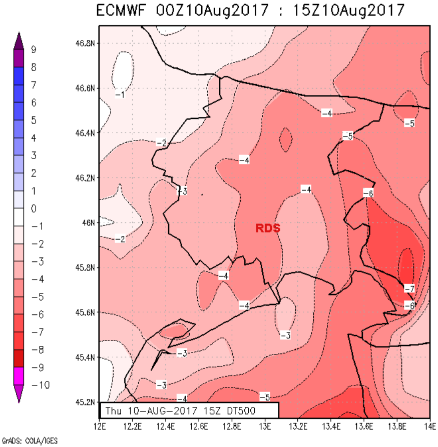

Ex. of MULI spatial variability derived by ECMWF pseudo-RDS: from -1 to -7 °C 100 km apart.

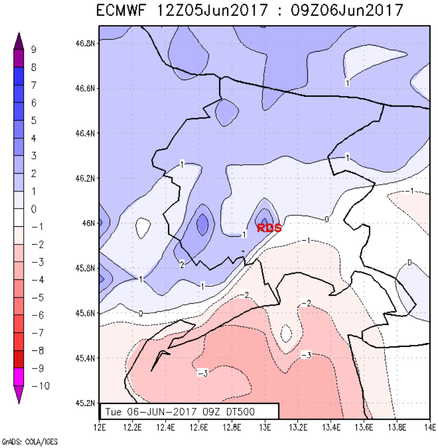

If the sounding is located near to a minimum of potential instability then the forecast can be underestimated.

Section 5

Forecasting with sounding-derived indices: examples & problems

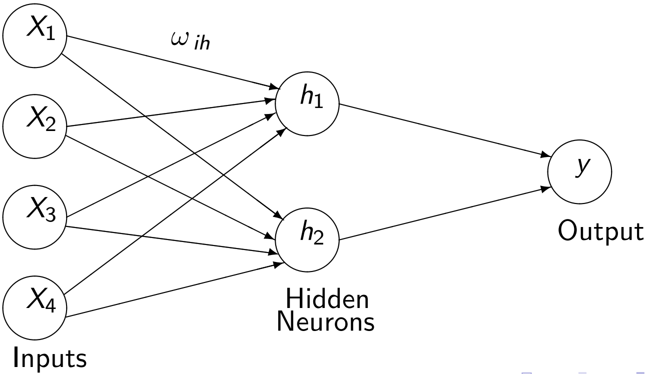

The simplest way to use indices is setting a threshold. . .

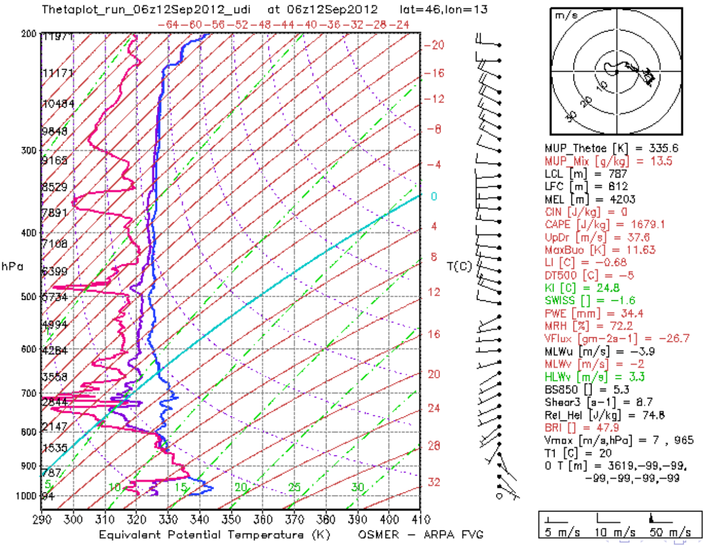

Here you can see a Thetaplot + hodograph (note veering) + index table made by Arturo Pucillo (OSMER) in GrADS.

The simplest way to use indices is setting a threshold. . .

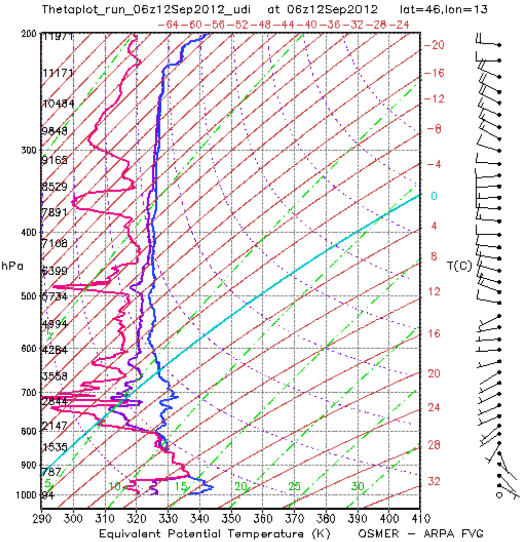

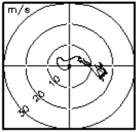

MUP_Thetae [K] = 335.6
MUP_Mix [g/kg] = 13.5
LCL [m] = 787
LFC [m] = 812
MEL [m] = 4203
CIN [J/kg] = 0
CAPE [J/kg] = 1679.1
UpDr [m/s] = 37.6
MaxBuo [K] = 11.63
LI [C] = −0.68
DT500 [C] = −5
KI [C] = 24.8
SWISS [] = −1.6
PWE [mm] = 34.4
MRH [%] = 72.2
VFlux [gm−2s−1] = −26.7
MLWu [m/s] = −3.9
MLWv [m/s] = −2
HLWv [m/s] = 3.3
BS850 [] = 5.3
Shear3 [s−1] = 8.7
Rel_Hel [J/kg] = 74.8
BRI [] = 47.9
Vmax [m/s,hPa] = 7 , 965
T1 [C] = 20
0 T [m] = 3619,−99,−99,
−99,−99,−99,−99

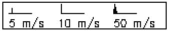

Here you can see a Thetaplot + hodograph (note veering) + index table made by Arturo Pucillo (OSMER) in GrADS.

Note the red–green colors when a statistical threshold (found maximizing the Pierce Skill Score) is exceeded.

. . . but multivariate analysis is much better then univariate

- Instead of using one or more indices dichotomized with a *"magic"* threshold, it is much more useful to apply a multivariate analysis, in the multispace of more indices (*joint* probability).

. . . but multivariate analysis is much better then univariate

- Instead of using one or more indices dichotomized with a *"magic"* threshold, it is much more useful to apply a multivariate analysis, in the multispace of more indices (*joint* probability).
- The simplest way to do it is to apply a Linear Discriminant Analysis (LDA), finding a condition like $a_1 X_1 + a_2 X_2 + ... + a_N X_N \lesseqgtr const$.

... but multivariate analysis is much better then univariate

- Instead of using one or more indices dichotomized with a *"magic"* threshold, it is much more useful to apply a multivariate analysis, in the multispace of more indices (*joint* probability).
- The simplest way to do it is to apply a Linear Discriminant Analysis (LDA), finding a condition like $a_1 X_1 + a_2 X_2 + ... + a_N X_N \lesseqgtr const$.
- Since the instability indices (candidate predictors) are usually too many and since they are often correlated among them, it is mandatory to implement a input selection algorithm, like a *stepwise selection* (forward or backward) or a brute-force exhaustive search of a limited subset of inputs (as the LEAPS algorithm in linear regression problems), in order to reduce noise in the statistical model.

. . . but multivariate analysis is much better then univariate

- Instead of using one or more indices dichotomized with a *"magic"* threshold, it is much more useful to apply a multivariate analysis, in the multispace of more indices (*joint* probability).
- The simplest way to do it is to apply a Linear Discriminant Analysis (LDA), finding a condition like $a_1X_1 + a_2X_2 + ... + a_NX_N \lesseqgtr const$.
- Since the instability indices (candidate predictors) are usually too many and since they are often correlated among them, it is mandatory to implement a input selection algorithm, like a *stepwise selection* (forward or backward) or a brute-force exhaustive search of a limited subset of inputs (as the LEAPS algorithm in linear regression problems), in order to reduce noise in the statistical model.
- When a complex statistical method is applied, like one with many predictors or non–linear models (neural networks), it is mandatory to avoid the *overfitting*. A good way is to develop the model fitting a *trainig* set and choosing the model that optimize the *validation* set. Lastly, an independent *test* sample should be used.

Pre-processing the input data

- For any forecasting problem it should be clarified if it is a classification problem (categorical forecast among a few classes, e.g. binary events) or a regression problem (forecasting the value of a continuous variable), because the statistical techniques used are different and also the verification methods are different (e.g. Cross-Entropy Error, ROC and indices of contingency table vs. MSE and Taylor diagram).

Pre-processing the input data

- For any forecasting problem it should be clarified if it is a classification problem (categorical forecast among a few classes, e.g. binary events) or a regression problem (forecasting the value of a continuous variable), because the statistical techniques used are different and also the verification methods are different (e.g. Cross-Entropy Error, ROC and indices of contingency table vs. MSE and Taylor diagram).
- When simple linear methods are used, a pre-processing of inputs is not always needed, but when non-linear methods are applied (maybe using a random initial choice of parameters) it is much better to *pre-process* the candidate predictors to make their domains more similar.

Pre-processing the input data

- For any forecasting problem it should be clarified if it is a classification problem (categorical forecast among a few classes, e.g. binary events) or a regression problem (forecasting the value of a continuous variable), because the statistical techniques used are different and also the verification methods are different (e.g. Cross-Entropy Error, ROC and indices of contingency table vs. MSE and Taylor diagram).
- When simple linear methods are used, a pre-processing of inputs is not always needed, but when non-linear methods are applied (maybe using a random initial choice of parameters) it is much better to *pre-process* the candidate predictors to make their domains more similar.
- For example, for regression problems, it is a commonly to standardize each variable, subtracting the mean value and dividing for the standard deviation.

Pre-processing the input data

- For any forecasting problem it should be clarified if it is a classification problem (categorical forecast among a few classes, e.g. binary events) or a regression problem (forecasting the value of a continuous variable), because the statistical techniques used are different and also the verification methods are different (e.g. Cross-Entropy Error, ROC and indices of contingency table vs. MSE and Taylor diagram).
- When simple linear methods are used, a pre-processing of inputs is not always needed, but when non-linear methods are applied (maybe using a random initial choice of parameters) it is much better to *pre-process* the candidate predictors to make their domains more similar.
- For example, for regression problems, it is a commonly to standardize each variable, subtracting the mean value and dividing for the standard deviation.
- For the classification problem, we suggest to transform each variable in its empirical posterior probability of event occurrence, as explained in Manzato (2005).

From conditional distrib. to Event Posterior Probability

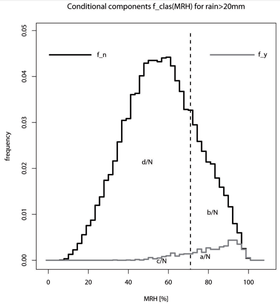

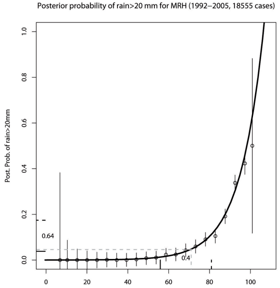

An example, from Manzato (2007c), of transforming the Mean Relative Humidity in the lowest 500 hPa (MRH) into its Empirical Posterior Probability of having at least 20 mm of rain in the 6 hours after the sounding release.

From conditional distrib. to Event Posterior Probability

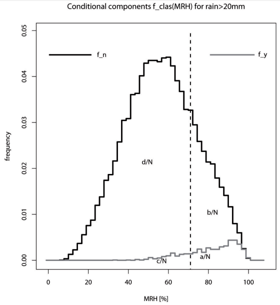

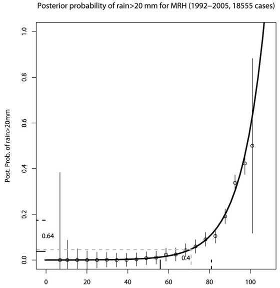

An example, from Manzato (2007c), of transforming the Mean Relative Humidity in the lowest 500 hPa (MRH) into its Empirical Posterior Probability of having at least 20 mm of rain in the 6 hours after the sounding release.

The histograms above (derived from the *active* and *non-active* empirical distributions) are proportional to the 4 entries of the contingency table (a, b, c and d divided by the total number of cases N), while the event posterior probability (Bayes theorem), shown below, becomes an effective pre-processing technique, when all variables are converted into functions fitting their empirical probabilities.

38-year hi-res climo of annual RAIN (Isotta et al. IJC 2013)

CLIMATE OF DAILY PRECIPITATION IN THE ALPS

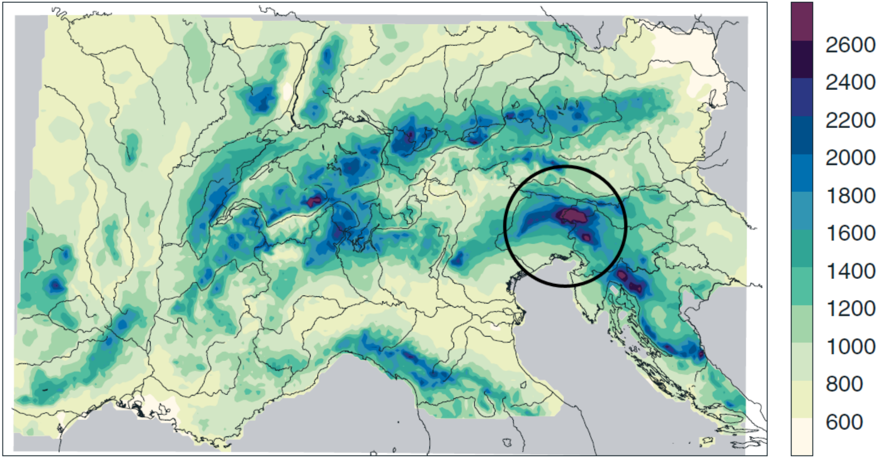

Figure 6. Mean annual precipitation (mm per year) for the period 1971–2008.

Annual climo Udine daily rain and FVG MaxRain every 6h

Frequency of the 20089 Rain/24h cases in UDI per 31–days moving average of Julian day (1960–2014)

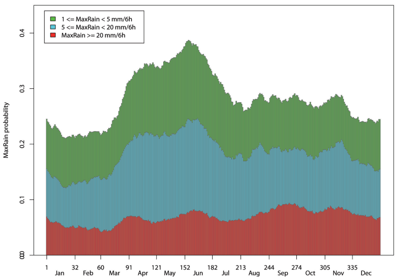

Mean value and SD of the 13131 MaxRain 6h cases per 30–days moving average of Julian day (20060215–20150215)

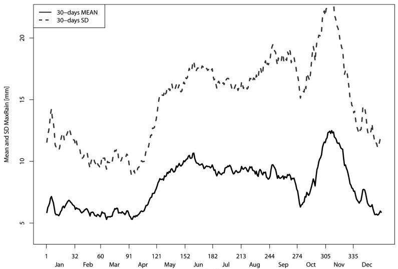

The annual cycle of 3–classes of daily rain in Udine (FVG plain), derived from 55 years, shows that weak rain are more likely in Spring, while rain$>$ 20 mm probability is maximum in Sep-Nov.

Annual climo Udine daily rain and FVG MaxRain every 6h

Frequency of the 20089 Rain/24h cases in UDI per 31–days moving average of Julian day (1960–2014)

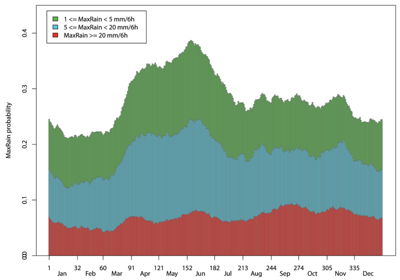

Mean value and SD of the 13131 MaxRain 6h cases per 30–days moving average of Julian day (20060215–20150215)

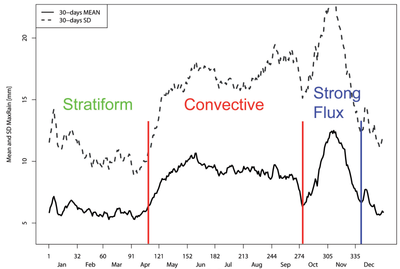

The annual cycle of 3–classes of daily rain in Udine (FVG plain), derived from 55 years, shows that weak rain are more likely in Spring, while rain $>$ 20 mm probability is maximum in Sep-Nov.

The annual cycle of the Maximum Rain in 6h in all the FVG region (derived by 10 years series of 104 raingauge stations) has a peak at the beginning of November, when strong flux precipitation (see Davolio et al., QJ 2016) falls on the Prealps, eventually with embedded convection. One can identify 3 different regimes.

Climatological forecast with indices is relatively "easy"

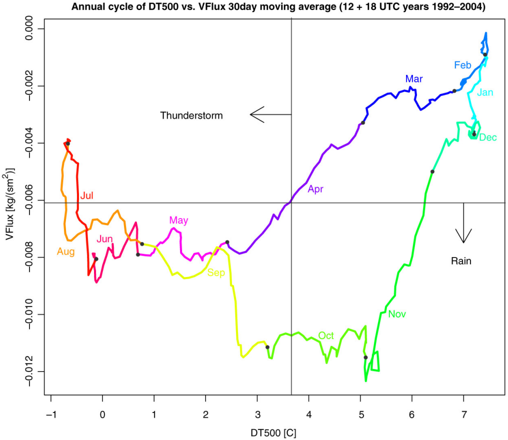

Fig. 7. The annual cycle of the 30-day moving average DT500 vs. the 30-day moving average VFlux. On the top-right corner are the months with low North–South water vapour flux and high stability, while the left-bottom corner means soundings close to instability and with high VFlux. The labels are written near the "middle of the month" points. The two gray lines used to divide in quarters correspond to the mean values of the DT500 and VFlux, only the 12 and 18 UTC soundings have been used.

The composite annual cycle of MULI and VFlux (from Manzato 2007b) has an high correlation with the annual cycle of FVG rain, and also for the mean-Adriatic SST from satellite has a good R.

Climatological forecast with indices is relatively "easy"

346 A. Manzato / Atmospheric Research 83 (2007) 336–348

3 regimes

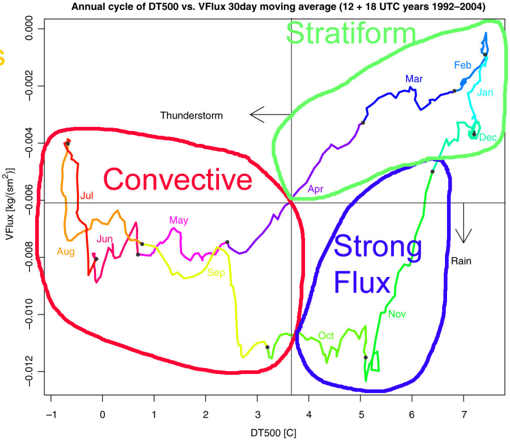

The composite annual cycle of MULI and VFlux (from Manzato 2007b) has an high correlation with the annual cycle of FVG rain, and also for the mean-Adriatic SST from satellite has a good R.

Fig. 7. The annual cycle of the 30-day moving average DT500 vs. the 30-day moving average VFlux. On the top-right corner are the months with low North–South water vapour flux and high stability, while the left-bottom corner means soundings close to instability and with high VFlux. The labels are written near the "middle of the month" points. The two gray lines used to divide in quarters correspond to the mean values of the DT500 and VFlux, only the 12 and 18 UTC soundings have been used.

18-year EUCLID CG-LIGHTNING climo in "NE" Italy

DECEMBER 2014 FEUDALE AND MANZATO 2655

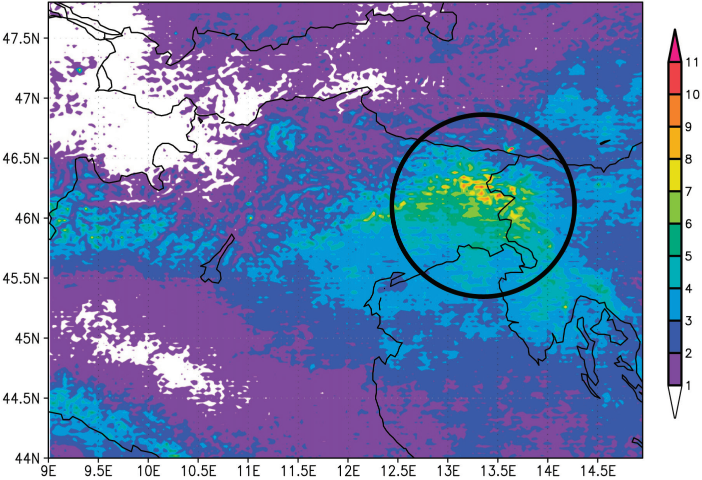

Feudale and Manzato (JAMC 2014) found a maximum in the Carnic and Julian Prealps (on the border between Italy and Slovenia)

FIG. 2. Spatial distribution of lightning density defined as the average number of CG flashes h^{-1} km^{-2} during the period 1995–2012 (18 yr) on a $0.03° \times 0.02°$ grid. The scale is multiplied by a factor of 10^4 for convenience.

Defining an objective Convective Activity variable

Manzato (2003) introduced an objective measure of 6-h storm "intensity":

$$CalCA\,6h = \begin{cases} \dfrac{\frac{1}{8}\cdot \ln\left(1+num\_light\right)+\frac{1}{6}\cdot \ln\left(1+rain\right)+\frac{1}{3}\cdot \ln\left(1+wind\right)}{2.9} & \text{if} \quad num\_light \geq 3, \\ 0 & \text{if} \quad num\_light < 3. \end{cases} \tag{22}$$

Defining an objective Convective Activity variable

Manzato (2003) introduced an objective measure of 6-h storm "intensity":

$$CalCA6h = \begin{cases} \frac{\frac{1}{8}\cdot \ln(1+num\_light)+\frac{1}{6}\cdot \ln(1+rain)+\frac{1}{3}\cdot \ln(1+wind)}{2.9} & \text{if } num\_light \geq 3, \\ 0 & \text{if } num\_light < 3. \end{cases} \tag{22}$$

It is a weighted sum of rain, C2G lightnings and gust. The distribution of thunderstorm "intensity" is bell shaped:

340 A. Manzato / Atmospheric Research 83 (2007) 336–348

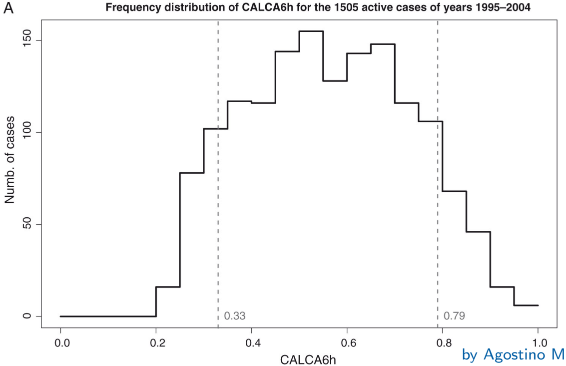

Trying to forecast thunderstorms in FVG plain with ANN

Manzato (2007) fitted the CaICA6h database with neural networks, using *a selection of Udine sounding–derived indices* as predictors. The same statistical model has been applied (via a linear fit) to ECMWF run12 pseudo–soundings.

Trying to forecast thunderstorms in FVG plain with ANN

Manzato (2007) fitted the CaICA6h database with neural networks, using *a selection of Udine sounding–derived indices* as predictors. The same statistical model has been applied (via a linear fit) to ECMWF run12 pseudo–soundings.

When the forecast ANN (ForCA6h) is above ≅ 0.5 we expect strong storms, but in this case they are too strong: OBS= CaICA6h> 0.8! Weather forecast are more difficult than climate for.!

Time Series of PseudoForCA6h and CalCA6h in the current period, run 12UTC.

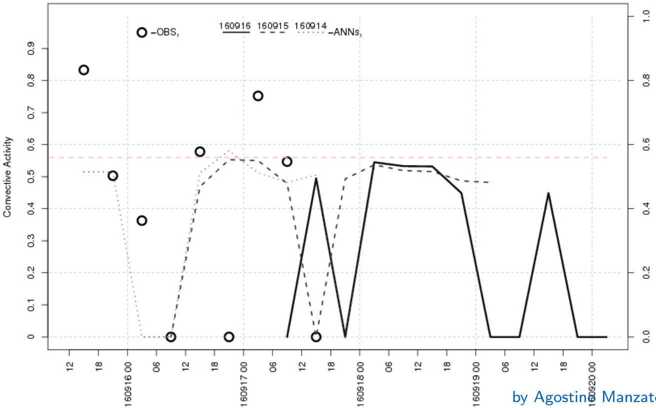

The case of 20170810: Thetaplot of 12 UTC Udine RDS

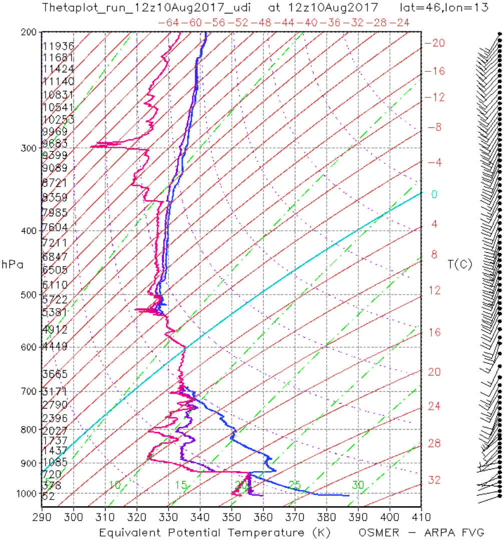

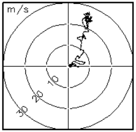

MUP_Thetae [K] = 355.9
MUP_Mix [g/kg] = 18.7
LCL [m] = 682
LFC [m] = 714
MEL [m] = 5590
CIN [J/kg] = 0.9
CAPE [J/kg] = 3870
UpDr [m/s] = 62.1
MaxBuo [K] = 28.21
LI [C] = −10.99
DT500 [C] = −11
KI [C] = 40.6
SWISS [] = −15.3
PWE [mm] = 52.5
MRH [%] = 84.7
VFlux [gm−2s−1] = −51.8
MLWu [m/s] = −6
MLWv [m/s] = −10
HLWv [m/s] = −19.9
BS850 [] = 3.9
Shear3 [s−1] = 14.24
Rel_Hel [J/kg] = 37.2
BRI [] = 77.8
Vmax [m/s,hPa] = 5 , 977
T1 [C] = 30
0 T [m] = 4334,−99,−99,
−99,−99,−99,−99

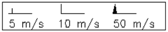

Theta-plot shows the historical (in the last 26 years) maximum of potential instability in NE Italy: CAPE= 4352 J/kg, MULI= -12 °C and MaxBuo= +28 K, when using the virtual correction.

No directional shear at all!

All indices computed by SOUND_ANALYS.PY in 3 ways

Index [5 : 95 percentils unit on all cases April-November 1995-2007]	T	Tv	Tvc
MUP ThetaE [296:336 K] **Thetae**	355.9	355.9	355.9
MUP Mixing Ratio [2.2:12.5 g/kg] **Mix**	18.7	18.7	18.7
MUP height [228:2434 m] **h_MUP**	189	189	189
Convective Available Potential Energy [0:923 J/kg] **CAPE**	3872.6	4351.6	4158.3
Convective Inhibition [-1385:-0.4 J/kg] **CIN**	0.8	1.1	1.1
Tropopause height [9298:13611 m] **Trop**	12580	12580	12580
Cloud top [2279:11687 m] **EL**	13146	13207	13561
Lev. of Free Convection [925:4136 m] **LFC**	714	699	714
Cloud base height [648:3553 m] **LCL**	681	681	681
Cloud base temperature [-12.2:15.3 C] **Tbase**	22.2	22.2	22.2
Boundary Layer Top [313:4297m] **PBL**	670	670	670
Melting level [1720:4338 m] **MEL**	5596	5863	5397
Wet Bulb Zero [921:3590 m] **WBZ**	4334	4334	4334
Max Updraft velocity [0:29.3 m/s] **UpDr**	62.1	66.8	61.9
Max Hail diameter [0:4.8 cm] **HD**	21.8	25.3	21.7
Precip. Wat. Env. [9.1:36.4 mm] **PWE**	52.5	51.9	51.9
Precip. Wat. Cloud [0:44.5 mm] **PWC**	75.2	73.9	73.2
sfc-250hPa Low Rel. Humidity [38:91 %] **LRH**	73.2	73.2	73.2
sfc-500hPa Medium Rel. Humidity [31:88 %] **MRH**	84.7	84.7	84.7
500-300hPa High Rel. Humidity [11:71 %] **HRH**	72.9	72.9	72.9
CAP diff. theta_es [1.3:17.8 C] **CAP**	2.8	2.8	2.8
Low buo. accel. [-44:31cm/s2] **b_PBL**	-78.5	-78.5	-78.5
Downdraft Potential [3.5:52.4 K] **DownPot**	44.4	44.4	44.4
Maximum Buoyancy [-9.8:9.6 K] **MaxBuo**	28.22	28.22	28.22
Lifted Index 500m [-2.57:13.0 C] **LI**	-11.0	-12.06	-9.31
Diff. Temp. 500hPa [-3.3:9.4 C] **DT500**	-11.04	-12.11	-9.35
Diff. Temp. at -15 [-3.5:7.0 C] **DTC**	-12.3	-13.24	-12.05

All indices computed by SOUND_ANALYS.PY in 3 ways

Index [5 : 95 percentils unit on all cases April-November 1995-2007]	T	Tv	Tvc
MUP ThetaE [296:336 K] **Thetae**	355.9	355.9	355.9
MUP Mixing Ratio [2.2:12.5 g/kg] **Mix**	18.7	18.7	18.7
MUP height [228:2434 m] **h_MUP**	189	189	189
Convective Available Potential Energy [0:923 J/kg] **CAPE**	3872.6	4351.6	4158.3
Convective Inhibition [-1385:-0.4 J/kg] **CIN**	0.8	1.1	1.1
Tropopause height [9298:13611 m] **Trop**	12580	12580	12580
Cloud top [2279:11687 m] **EL**	13146	13207	13561
Lev. of Free Convection [925:4136 m] **LFC**	714	699	714
Cloud base height [648:3553 m] **LCL**	681	681	681
Cloud base temperature [-12.2:15.3 C] **Tbase**	22.2	22.2	22.2
Boundary Layer Top [313:4297m] **PBL**	670	670	670
Melting level [1720:4338 m] **MEL**	5596	5863	5397
Wet Bulb Zero [921:3590 m] **WBZ**	4334	4334	4334
Max Updraft velocity [0:29.3 m/s] **UpDr**	62.1	66.8	61.9
Max Hail diameter [0:4.8 cm] **HD**	21.8	25.3	21.7
Precip. Wat. Env. [9.1:36.4 mm] **PWE**	52.5	51.9	51.9
Precip. Wat. Cloud [0:44.5 mm] **PWC**	75.2	73.9	73.2
sfc-250hPa Low Rel. Humidity [38:91 %] **LRH**	73.2	73.2	73.2
sfc-500hPa Medium Rel. Humidity [31:88 %] **MRH**	84.7	84.7	84.7
500-300hPa High Rel. Humidity [11:71 %] **HRH**	72.9	72.9	72.9
CAP diff. theta_es [1.3:17.8 C] **CAP**	2.8	2.8	2.8
Low buo. accel. [-44:31cm/s2] **b_PBL**	-78.5	-78.5	-78.5
Downdraft Potential [3.5:52.4 K] **DownPot**	44.4	44.4	44.4
Maximum Buoyancy [-9.8:9.6 K] **MaxBuo**	28.22	28.22	28.22
Lifted Index 500m [-2.57:13.0 C] **LI**	-11.0	-12.06	-9.31
Diff. Temp. 500hPa [-3.3:9.4 C] **DT500**	-11.04	-12.11	-9.35
Diff. Temp. at -15 [-3.5:7.0 C] **DTC**	-12.3	-13.24	-12.05

Showalter Index [-1.0:11.7 C] **Showl**	-3.2	-3.52	-2.25
Stabil. Wind Shear Index Switz.) [-4.3:15.9] **SWISS**	-15.3	-16.3	-13.6
Severe WEAth. Threat [7.4:186] **SWEAT**	248.9	248.9	248.9
K Index [-4.9:33.4 C] **KI**	40.6	40.6	40.6
Boyden Index [91.6:98.9] **BOY**	98.8	98.8	98.8
Vapour Flux [-41:20 gm-2s-1] **VFlux**	-51.9	-51.9	-51.9
U Low Lev. Wind [-2.7:7.6 m/s] **LLWu**	-3.1	-3.1	-3.1
V Low Lev. Wind [-4.0:3.9 m/s] **LLWv**	-0.4	-0.4	-0.4
U Med. Lev. Wind [-10.3:5.7 m/s] **MLWu**	-6.0	-6.0	-6.0
V Med. Lev. Wind [-13.2:4.3 m/s] **MLWv**	-10.0	-10.0	-10.0
U High Lev. Wind [-31.3:9.9 m/s] **HLWu**	-11.0	-11.0	-11.0
V High Lev. Wind [-18.6:24.4 m/s] **HLWv**	-19.9	-19.9	-19.9
Low Level Jet (>15m/s) Depth [0:2776 m] **LLJD**	2233	2233	2233
High Level Jet (>30m/s) Depth [0:4781 m] **HLJD**	0	0	0
Bulk Richardson Numb. [0:86] **BRI**	77.9	87.2	83.3
Bulk Shear sfc-850hPa [1.2:11.5 m/s] **BS850**	3.9	3.9	3.9
Shear * E-3 [4.0:14 s-1] **Shear**	11.3	11.3	11.3
Shear * E-3 [5.0:17 s-1] **Shear3**	0.0	0.0	0.0
Helicity [-55:127 J/kg] **Hel**	-43.6	-43.6	-43.6
Storm Rel. Helicity [-18:187 J/kg] **Rel_Hel**	37.2	37.3	37.3
Energy-Hel. [-0.004:0.298 m4/s4] **EHI**	0.9	1.01	0.97
Radiosonde vertical vel. [3.78:5.53 m/s] **VV**	4.93	4.93	4.93
Stand. dev. vertical vel. [0.25:0.97 m/s] **VVstd**	0.92	0.92	0.92

Sounding Analysis results

For differences in the 3 adiabatic process methods see Manzato & Morgan (2003).

ECMWF-derived maps of MUP Θ_e and MULI at 12 UTC

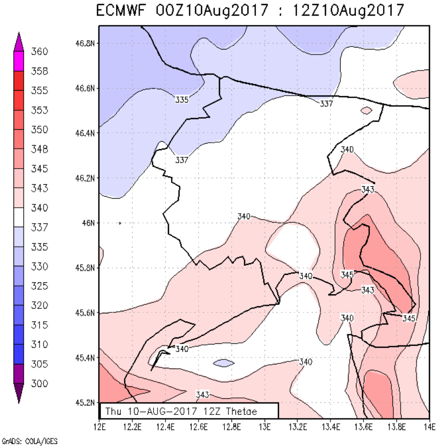

Θ_e of the Most Unstable Parcel.

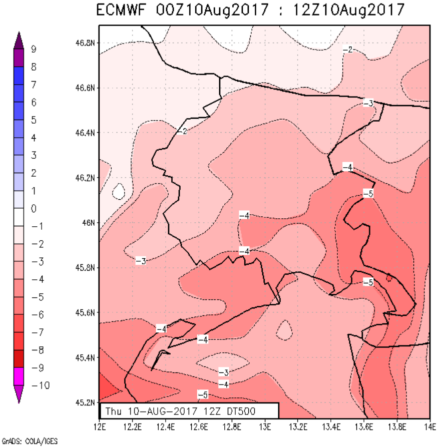

Most Unstable Lifted Index.

ECMWF-derived maps of MUP Θ_e and MULI at 15 UTC

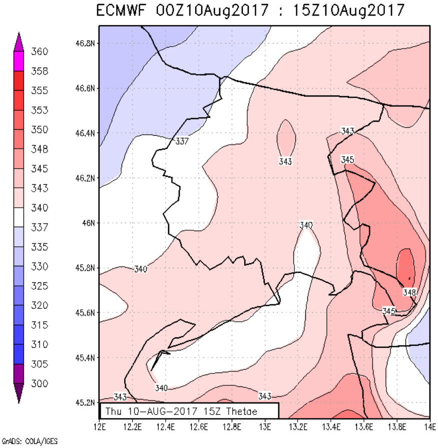

Θ_e of the Most Unstable Parcel.

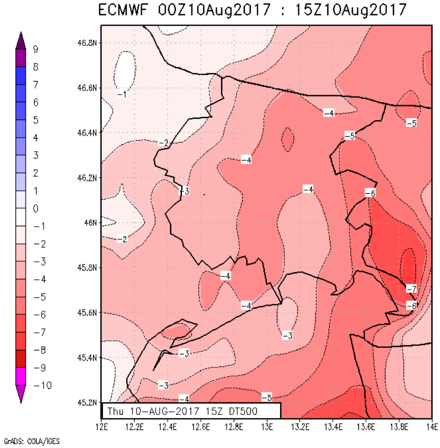

Most Unstable Lifted Index.

ECMWF-derived maps of MUP Θ_e and MULI at 18 UTC

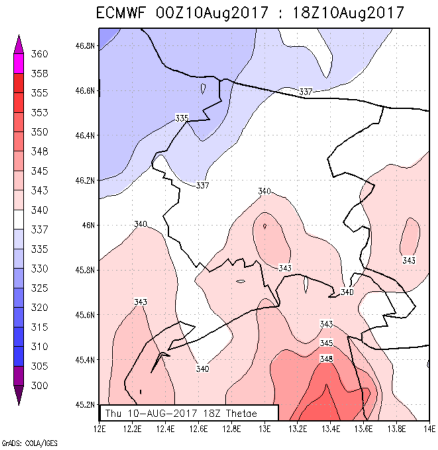

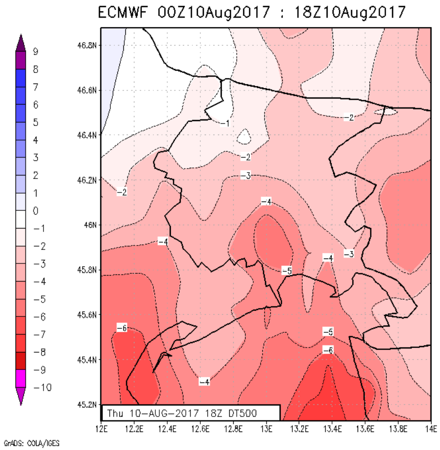

Θ_e of the Most Unstable Parcel.

Most Unstable Lifted Index.

The shape of initial parcel Θ_e and potential instability are very similar!

Max Θ_e is much lower than observed (356 K).

ECMWF-derived maps of CAPE and CIN at 12 UTC

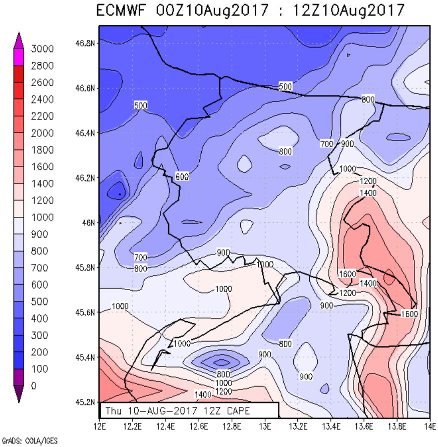

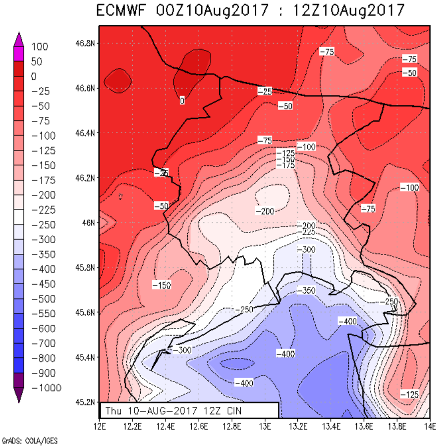

CAPE was largerly underestimated.

CIN was largerly overestimated.

ECMWF-derived maps of CAPE and CIN at 15 UTC

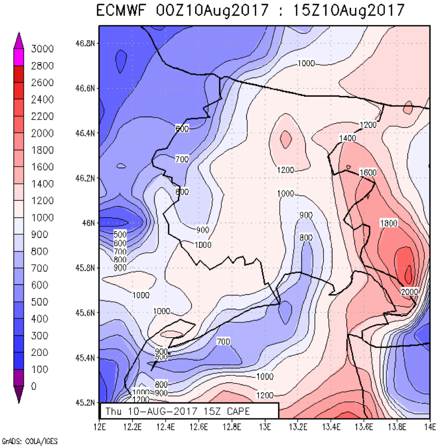

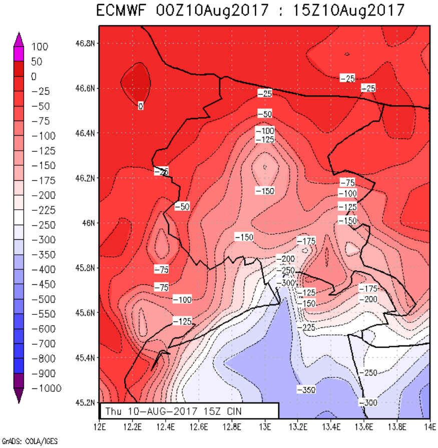

CAPE was largerly underestimated.

CIN was largerly overestimated.

ECMWF-derived maps of CAPE and CIN at 18 UTC

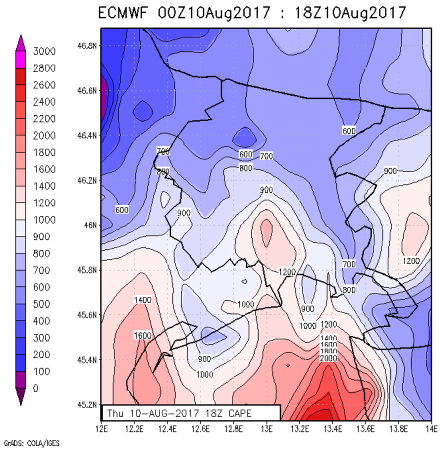

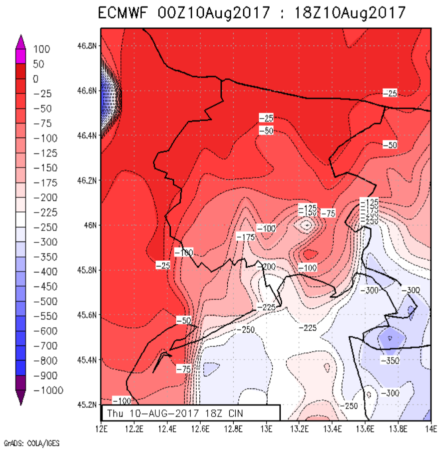

CAPE was largerly underestimated.

CIN was largerly overestimated.

Only at 18 UTC ECMWF saw some more unstable air above Adriatic sea, in front of Istria.

ECMWF-derived maps of PWE and DownPot at 12 UTC

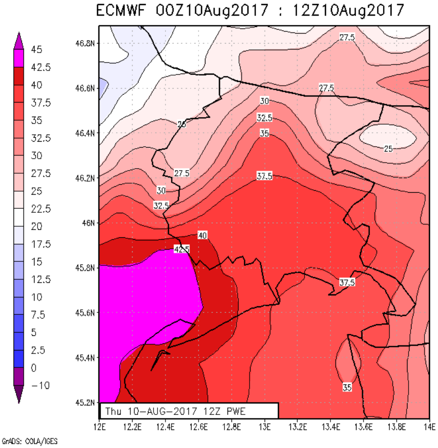

Environmental precipitable water.

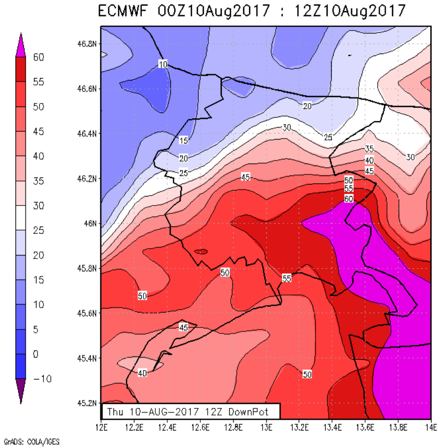

Downdraft Pot. $Max(\Theta_{es}|_{low}) - Min(\Theta_e|_{mid})$.

ECMWF-derived maps of PWE and DownPot at 15 UTC

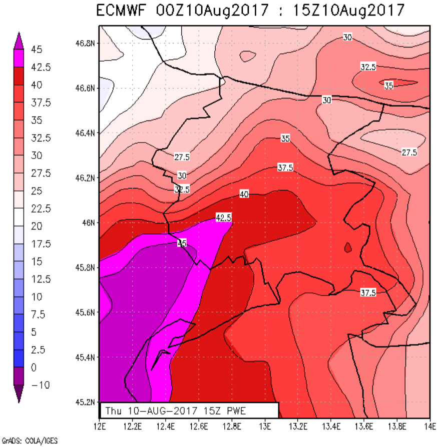

Environmental precipitable water.

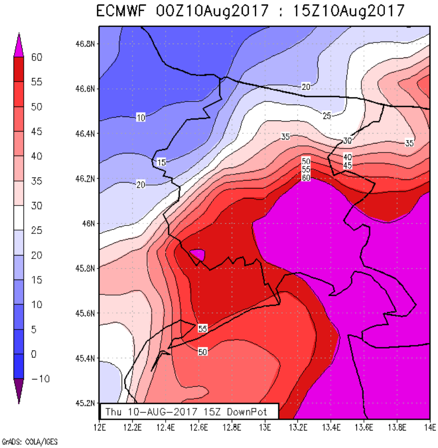

Downdraft Pot. $Max(\Theta_{es}|_{low}) - Min(\Theta_{e}|_{mid})$.

ECMWF-derived maps of PWE and DownPot at 18 UTC

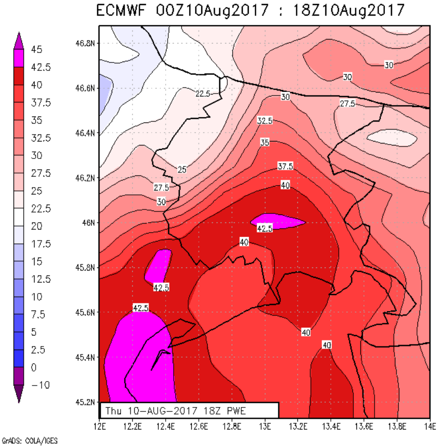

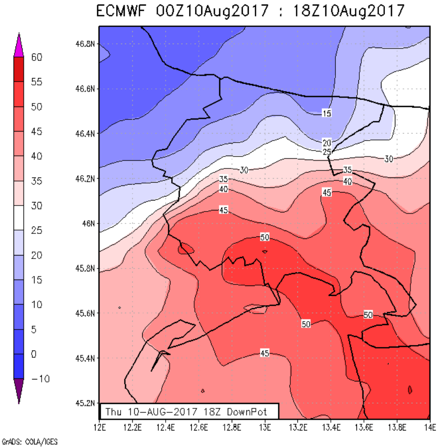

Environmental precipitable water.

Downdraft Pot. $Max(\Theta_{es}|_{low}) - Min(\Theta_e|_{mid})$.

Only PWE and some wind fields like Downdraft Potential seems to get closer to the area really hit by MCS.

MSG 10.8 μm BT plus CESI lightnings 1200-1600 UTC

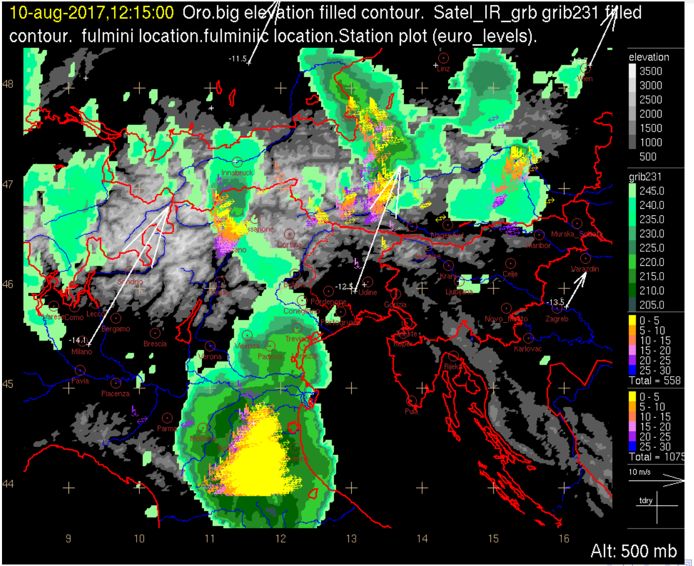

The Mesoscale Convective System started on the Apennines and developed strongly along the Adriatic coast.

VMI radar, 5’ stations and CESI lightnings 1400-1520 UTC

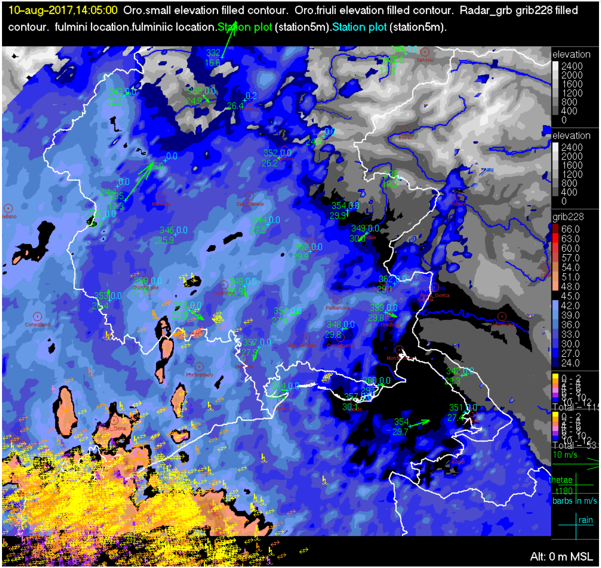

Only in Friuli Venezia Giulia region it produced more that 300 M€ of damages (mostly by wind).

Conclusions

"Pazzo è bene da catene,
Chi fastidio mai si dà
Per saper quel che sarà..."

He is a raving madman
who ever takes the trouble
to know what the future holds...

from the first act of "Sant'Alessio" (1631) by Stefano Landi (1587–1639), text by Giulio Rospigliosi (1600–1669, also known as Pope Clemente IX).

Conclusions

- Think in terms of equivalent potential temperature, Θ_e, that is quite *conserved* and -if possible- look at the Thetaplot diagram.

Conclusions

- Think in terms of equivalent potential temperature, Θ_e, that is quite *conserved* and -if possible- look at the Thetaplot diagram.
- Remember that *potential* instability is a characteristic of an atmosphere profile with respect to large displacements, while *static* (and conditional) instability is a characteristic of an atmosphere layer with respect to relatively small displacements.

Conclusions

- Think in terms of equivalent potential temperature, Θ_e, that is quite *conserved* and -if possible- look at the Thetaplot diagram.
- Remember that *potential* instability is a characteristic of an atmosphere profile with respect to large displacements, while *static* (and conditional) instability is a characteristic of an atmosphere layer with respect to relatively small displacements.
- Reflect on the importance of the choice if the initial parcel, that determine the full adiabatic process (initial parcel Θ_e) and in particular on the importance of moisture in the low levels.

Conclusions

- Think in terms of equivalent potential temperature, Θ_e, that is quite *conserved* and -if possible- look at the Thetaplot diagram.
- Remember that *potential* instability is a characteristic of an atmosphere profile with respect to large displacements, while *static* (and conditional) instability is a characteristic of an atmosphere layer with respect to relatively small displacements.
- Reflect on the importance of the choice if the initial parcel, that determine the full adiabatic process (initial parcel Θ_e) and in particular on the importance of moisture in the low levels.
- Consider the old Lifted Index before CAPE and check also MaxBuo.

Conclusions

- Think in terms of equivalent potential temperature, Θ_e, that is quite *conserved* and -if possible- look at the Thetaplot diagram.
- Remember that *potential* instability is a characteristic of an atmosphere profile with respect to large displacements, while *static* (and conditional) instability is a characteristic of an atmosphere layer with respect to relatively small displacements.
- Reflect on the importance of the choice if the initial parcel, that determine the full adiabatic process (initial parcel Θ_e) and in particular on the importance of moisture in the low levels.
- Consider the old Lifted Index before CAPE and check also MaxBuo.
- Consider the high spatio-temporal variation of indices, particularly those using low–levels. Try to foresee possible trigger mechanisms.

Conclusions

- Think in terms of equivalent potential temperature, Θ_e, that is quite *conserved* and -if possible- look at the Thetaplot diagram.
- Remember that *potential* instability is a characteristic of an atmosphere profile with respect to large displacements, while *static* (and conditional) instability is a characteristic of an atmosphere layer with respect to relatively small displacements.
- Reflect on the importance of the choice if the initial parcel, that determine the full adiabatic process (initial parcel Θ_e) and in particular on the importance of moisture in the low levels.
- Consider the old Lifted Index before CAPE and check also MaxBuo.
- Consider the high spatio-temporal variation of indices, particularly those using low–levels. Try to foresee possible trigger mechanisms.
- Try always a *multivariate* approach because more indices are better then 1 or 2 and be careful to avoid overfitting in your verification process. Use preprocessing. Test on a fully independent sample.

Thanks! For info: *agostino.manzato@meteo.fvg.it*

References 1/3

1. Bolton, D., 1980. The computation of equivalent potential temperature. *Mon. Wea. Rev.*, **108**, 1046–1053.
2. Corbet, J. M., Mueller, C., Burghart, C., Gould, K., and Granger, G., 1994. ZEB: Software for Integration, Display and Management of Diverse Environmental Datasets, *Bull AMS*, **75**, 783–792.
3. Davies–Jones, R., D. Burgess and M. Foster, 1990. Test of helicity as a tornado forecast parameter. Preprints, *16th Conf. on Severe Local Storms*, Kananaskis Park, Canada, AMS, 50–60.
4. Davolio, S., Volonté, A., Manzato, A., Pucillo, A., Cicogna, A. and M. E. Ferrario, 2016: Mechanisms producing different precipitation patterns over north-eastern Italy: insights from HyMeX-SOP1 and previous events, Quarterly J. RMS, **142**, 188-205.
5. Doswell, C. A., III and E. Rasmussen, 1994. The effect of Neglecting the Virtual Temperature Correction on CAPE Calculations, *Wea. Forecasting*, **9**, 625–629.
6. Emanuel, K. A., 1994: *Atmospheric Convection*, Oxford University press., 580 pp.
7. Feudale, L. and A. Manzato, 2014: Cloud-to-Ground Lightning Distribution and its Relationship with Orography and anthropogenic emissions in the Po Valley. *JAMC*, **53**, 2651–2670.
8. Galway, J.G., 1956. The lifted index as a predictor of latent instability, *Bull. AMS*, **37**, 528–529.
9. George, J.J., 1960. *Weather Forecasting for Aeronautics*. Academic Press, 673 pp.
10. Groenemeijer and van Delden, 2007: Sounding-derived parameters associated with large hail and tornadoes in the Netherlands Atmospheric research, **83**, 473-487.
11. Haklander, A. J., and A. van Delden, 2003: Thunderstorm predictors and their forecast skill for the Netherlands. *Atmos. Res.*, **67-68**, 273–299.

References 2/3

12. Huntrieser, H., Schiesser, H. H., W. Schmid, and A. Waldvogel, 1997: Comparison of Traditional and Newly Developed Thunderstorm Indices for Switzerland. *Wea. Forecasting* **12**, 108–125.
13. Kunz, M., 2007: The skill of convective parameters and indices to predict isolated and severe thunderstorms, Nat. Hazards Earth Syst. Sci., **7**, 327-342,
14. Isotta, F. A., Frei, C., et al., 2013: The climate of daily precipitation in the Alps: development and analysis of a high-resolution grid dataset from pan-Alpine rain-gauge data. *Int. J. Climatol*, **34**, 1657–1675.
15. Manzato, A., 2003: A climatology of instability indices derived from Friuli Venezia Giulia soundings, using three different methods. *Atmos. Res.*, **67–68**, 417–454.
16. ———, 2003: Considerazioni sul profilo verticale dell'atmosfera, Udine University internal report (in italian), 56 pp.
17. ———, 2005: The use of sounding derived indices for a neural network short-term thunderstorm forecast. *Wea. Forecasting*, **20**, 896–917.
18. ———, 2007 a: Sounding–derived indices for neural network based short–term thunderstorm and rainfall forecasts. *Atmos. Res.*, **83**, 349–365.
19. ———, 2007 b: The 6 Hours Climatology of Thunderstorms and Rainfalls in the Friuli Venezia Giulia Plain, *Atmos. Res.*, **83**, 336–348.
20. ———, 2007 c: A Note on the Maximum Peirce Skill Score. *Wea. Forecasting*, **22**, 1148–1154.
21. ———, 2008: A Verification of Numerical Model Forecasts for Sounding-Derived Indices above Udine, NE Italy, Weather and Forecasting, **23**, 477–495.
22. ———, 2012: Hail in NE Italy: Climatology and Bivariate Analysis with Sounding–Derived Indices. *J. Appl. Meteor. Climatol.*, **51**, 449–467.

References 3/3

23. ———, 2013: Hail in NE Italy: A neural network ensemble forecast using sounding–derived indices, *Weather and Forecasting*, **28**, 3–28.
24. ———, A., Davolio, S., Miglietta, M. M., Pucillo, A., and M. Setvák, 2015: 12 September 2012: A supercell outbreak in NE Italy?, *Atmos. Res.*, **153**, 98-118.
25. ———, and G. M. Morgan, 2003: Evaluating the sounding instability with the Lifted Parcel Theory. *Atmos. Res.*, **67–68**, 455–473.
26. Miglietta, M. M., Manzato, A., and R. Rotunno, 2016: Characteristics and Predictability of a Supercell during HyMeX SOP1, *Quarterly J. of RMS*, **142**, 2839-2853.
27. Moncrieff, M. W., and J. S. A. Green, 1972. The propagation of steady convective overturning in shear, *Quart. J. Roy. Meteor. Soc.*, **98**, 336–352.
28. Morgan, G. M. Jr, 1992. ThetaPlot, an Equivalent Potential Temperature Diagram, *Meteorol. Atmos. Phys.*, **47**, 259–265.
29. Morgan, G. M. Jr., and J. Tuttle, 1984. Some experimental techniques for the study of the evolution of atmospheric thermodynamic instability. Paper presented at the Second International Conference on Hailstorms and Hail Suppression, Sofia, Bulgaria (Proceedings), Bulgarian Hydrometeorological Service, 192–196.
30. Paluch, I. R., 1979. The Entrainment Mechanism in Colorado Cumuli, *Journ. of Atmos. Sci.*, **36**, 2467–2478.
31. Rasmussen, E. N. and D. O. Blanchard, 1998. A baseline climatology of sounding–derived supercell and tornado forecast parameters, *Wea. Forecasting*, **13**, 1148–1164.
32. Showalter, A. K., 1953. A stability index for thunderstorm forecasting, *Bull. AMS*, **34**, 250–252.
33. Ukkonen, P. Manzato, A., Mäkelä, A., 2017: Evaluation of Thunderstorm Predictors for Finland Using Reanalyses and Neural Networks, *JAMC*, **56**, 2335-2352.